School of Civil and Mechanical Engineering
Department of Civil Engineering

Structural Characteristics of Reinforced Concrete Beams and Slabs with Lightweight Blocks Infill

Ade Sri Wahyuni

This thesis is presented for the Degree of
Doctor of Philosophy
of
Curtin University

July 2012

DECLARATION

To the best of my knowledge and belief this thesis contains no material previously published by any other person except where due acknowledgment has been made.

This thesis contains no material which has been accepted for the award of any other degree or diploma in any university.

Signature:

Ade Sri Wahyuni

Date : July 2012

ABSTRACT

A Lightweight Sandwich Reinforced Concrete (LSRC) section has been developed with a novel use of prefabricated Autoclaved Aerated Concrete (AAC). This LSRC section is a reinforced concrete section in which AAC blocks are used as infill material in the section where concrete is considered ineffective under bending. This technology is suitable to be used for slab and beam.

Five beams were prepared to investigate the flexural and shear capacity of the LSRC. Based on the test results, the flexural capacity was found to be almost identical to the capacity of the equivalent solid beam, while the shear capacity was reduced. The shear strength reduction was as expected due to the reduction in the compressive strength of AAC infill material.

Furthermore, eight tests were also conducted on four slabs, one solid and three LSRC slabs. Based on the test results, all LSRC slabs exhibited similar behaviour to the equivalent solid slab and had varying shear capacities depending on the profile of AAC blocks infill. The obtained shear capacities were compared with the design values based on several major design codes and found to be within the safety predictions of the codes.

ANSYS 12.1 was employed to develop nonlinear finite element models of LSRC beams and slabs. The numerical results agree well with the experimental one. The beams modelled with ANSYS followed the same trend as the actual beam in the linear range, however after the first cracking the loss of stiffness in ANSYS model caused the bigger deflection compared to the actual beam. For slab models, ANSYS overestimates the load deflection behaviour due to the cracks that already available in slabs from the previous test. The crack propagation modelled with ANSYS for beams and slabs shows the cracks in the area of AAC blocks which associates with the brittle failure of LSRC beams and slabs.

In General ANSYS can predict the behaviour of the LSRC beams and slabs. The developed model can be used to investigate LSRC members with different structural and loading parameters.

The proposed LSRC section will be suitable for large span construction. The main benefits of this LSRC member are the cost and time savings due to the weight reduction and the less of supporting structure and foundation and the consequent ease of construction.

Keywords: *lightweight concrete; reinforced concrete; composite section; sandwich section*

ACKNOWLEDGMENT

The author wishes to express sincere thanks to the following individuals:

Prof Hamid Nikraz, Head of Department of Civil Engineering, Curtin University as supervisor and Dr Vanissorn Vimonsatit, as associate supervisor, who were extremely dedicated to the supervision of the present study. The author is particularly grateful for their encouragement, empathy and guidance throughout the period of research.

The sincere thanks is extended to Dr Ian Chandler, Mr. Rob Cutter and all of the technical staff of the Civil Engineering workshop and laboratories, for their assistance in the experimental work.

Thank you to Muhammad Al-Shaffrin Mazlan and Peter Macri for taking part in experimental work as final year project.

I would like to acknowledge Bengkulu University, my current employer in Indonesia and thank you to DIKTI for funding this research.

Finally, the author acknowledge special thanks to Jefri Marta, her husband, for his loving patience, understanding, assistance and active encouragement over the past three and a half year, and to her lovely children, M Farhan Alghifari, Tsamara Salsabila, M Nabil Alfaruq, who also give encouragement in different way.

LIST OF PUBLICATIONS

The research described in the thesis had resulted in the following publications:

Wahyuni, A.S., Vimonsatit, V, Nikraz, H (2012)" Shear Behaviour of Lightweight Sandwich Reinforced Concrete Slabs", Advances in Structural Engineering (Accepted Manuscript).

Vimonsatit, V., Wahyuni, A.S., and Nikraz, H. (2011). "Behaviour and Strength of Lightweight Sandwich Reinforced Concrete Beams", Proceedings, ISEC-6, Modern Methods and Advances in Structural Engineering and Construction, Editor: Cheung, S.O., Yazdani, S., Ghafoori, N., Singh, A, Zurich, Switzerland, June 21-26, 747-751.

Vimonsatit, V., Wahyuni, A.S., and Nikraz, H. (2011). "Shear Behaviour of Lightweight Sandwich Reinforced Concrete Slabs", Proceedings, ISEC-6, Modern Methods and Advances in Structural Engineering and Construction, Editor: Cheung, S.O., Yazdani, S., Ghafoori, N., Singh, A, Zurich, Switzerland, June 21-26, 917-921.

Vimonsatit, V., Wahyuni, A.S., Mazlan, M.A and Nikraz, H. (2010). "Use of Lightweight Concrete as Infill of Reinforced Concrete Sections", Proceedings, ACMSM 21, Editor: Fragomeni, S., Venkatesan, S.,Lam, N.T.K., Setunge, S, Melbourne, Australia, December 7-10, 245-250.

Vimonsatit, V., Wahyuni, A.S., Macri, P.J. and Nikraz, H. (2010). "Experimental Investigation of Behaviour and Shear Strength Capacity of Lightweight Sandwich Reinforced Concrete Slab", Proceedings, ACMSM 21, Editor: Fragomeni, S., Venkatesan, S.,Lam, N.T.K., Setunge, S, Melbourne, Australia, December 7-10, 251-256.

TABLE OF CONTENTS

LIST OF FIGURES

LIST OF TABLES

NOTATION

A_{st}	=	*the cross-sectional area of tension reinforcement.*
A_{sv}	=	*cross-sectional area or shear reinforcement*
A_{sc}	=	*the cross-sectional area of compressive reinforcement*
a	=	*distance between the load to the nearest support (mm).*
b	=	*width of the cross section*
b_v	=	*effective web width.*
D	=	*the overall depth of a cross-section in the plane of flexure.*
d_o	=	*distance form extreme compression fibre to the centre of the outermost layer of longitudinal reinforcement, and*
d_n	=	*depth of neutral axis from the extreme compressive fibre.*
Δ	=	*deflection at midspan (mm)*
d_{sc}	=	*the distance from the extreme compressive fibre of the concrete to the centroid of the compressive reinforcement*
E_c	=	*the modulus of elasticity of concrete*
E_s	=	*the modulus of elasticity of steel,*
f'_c	=	*the characteristic compressive cylinder strength of concrete at 28 days.*
f'_{cf}	=	*the characteristic flexural tensile strength on concrete AS 3600.*
f_{sy}	=	*the yield strength of reinforcing steel,(AS 3600)*
$f_{sy.f}$	=	*yield stress of a shear reinforcement.*
I	=	*second moment of area of the cross-section.*
I_{cr}	=	*second moment of area of cracked reinforced section*
I_{ef}	=	*effective second moment of area*
ℓ	=	*distance between the two supports*
M_{cr}	=	*bending moment causing cracking of the section.*

M^*	=	*the design bending moment*
ν	=	*poisson's ratio*
P	=	*load applied (N).*
Q	=	*the first moment about the centroidal axis of the top (or bottom) portion of the member's cross-sectional area, defined from the level at which τ is being calculated.*
s	=	*spacing of the stirrup.*
θ_v	=	*angle of inclination of the concrete compression strut*
w	=	*uniformly distributed load.*

CHAPTER 1

INTRODUCTION

1.1 Background

Concrete is one of the most common construction materials. It has been pointed out (Sumajouw and Rangan 2006) that the overall use of concrete in the world is only second to water. The main advantages of concrete material are that it is cost-effective, made from locally available material, and can be readily moulded into any required shape. A challenge for engineers when using concrete is to overcome its heavy weight with increasing demand for large span construction due to economic and aesthetic reasons (Matthew and Bennett 1990). Practitioners are facing even more challenges in providing cost effective solutions to fulfill this demand. Sustainability is another essential area in the construction industry. A way to depict sustainability is by minimizing resources used. As a result there has been a vast interest in research and development of lightweight concrete as alternatives to normal weight concrete (Ramamurthy et. al.2009, Jones & McCarthy 2005).

Lightweight concrete can either be made with lightweight aggregate, foamed technology, or autoclaved aerated technology (which will be focused on this research). Autoclaved aerated concrete (AAC) was invented in Sweden in the mid 1920s and has been used worldwide. The basic raw materials in producing AAC are Portland cement, limestone, aluminum powder, and sand. In the process aluminum powder reacts chemically to create million of tiny hydrogen gas bubbles that give AAC its light weight, which is about one fourth of the normal concrete weight (Autoclaved Cellular Concrete 2009). AAC is known to provide excellent thermal and sound insulation, and fire resistance. Current productions of AAC are in the form of blocks, wall panels, floor and roof panels, and lintels. Use of AAC as a primary structure is still very limited due to its low compressive strength compared to normal concrete.

The lightweight option, if feasible, leads to several benefits in the construction process. Clearly, the main benefits are the cost and time savings due to the weight reduction and the less of supporting structure and foundation. Basic concept in dealing with the weight is by minimizing the use of concrete while maintaining the

desired strength and stiffness of the section. There has been extensive research in the lightweight area which includes lightweight concrete (Bobrowski (1980), Horler (1980), Bungey & Madandoust (1994), Ahmad et al (1994)), hollow structure (Prestressed Hollow-core concrete Slabs (2001) ,Alnuaimi et al (2008)) or composite sandwich structures (Russo and Zuccarello (2007), Abbadi et al (2009), and Meidell (2009)) in the attempt to enhance the structural performance, and at the same time to make it lighter and cost effective

Despite many efforts of investigating the composite sandwich section to minimize the weight of the structure, there are still limited attempts in incorporating AAC with normal reinforced concrete.

1.2 Research Objectives

This research focuses on the novel use of AAC as infill of a reinforced concrete section. The section is made up of reinforced concrete filled with prefabricated AAC blocks in the region where the concrete is considered ineffective under bending. The developed LSRC section can be used either as structural or non-structural elements. LSRC members are particularly suitable for large span construction due to the weight saving benefits and the consequent ease of construction. The construction method of LSRC members can either be fully precast, semi precast, or cast in situ. In addition to the weight saving benefit of the developed LSRC section, the semi-precast construction of LSRC members has additional cost and time saving benefits.

Since AAC is used in the ineffective concrete under bending, it is of primary concern to investigate the behavior and strength of LSRC members when the failure is likely to be under shear.

The objectives of this research project are:

1. To perform test for determining the behavior of LSRC under bending and shear.
2. To develop an analytical 3D finite element model with ANSYS.
3. To investigate the strength and serviceability of LSRC section.

1.3 Scope of the Work

1. The experimental work involved the casting of 5 beams and 4 slabs.

Three beams are appointed for flexural test (1 control and 2 LSRC beams) while another two beams are for shear test (1 control and one LSRC with full amount of AAC blocks).

Four slabs comprising: 1 control, 1 slab with full amount of AAC blocks, 1 slab with half amount of AAC blocks and, and 1 slab with curve AAC blocks.

2. Conducting the experimental work in laboratory to determine the behavior as well as the ultimate load and displacement relation of solid and LSRC beams under shear and flexure.
3. Investigate the behavior and load displacement behavior of solid and LSRC slabs under shear.
4. Develop the Finite Element Analysis of solid and LSRC beams and slabs with ANSYS to predict the load deflection behaviour of solid and sandwich section.
5. Study the crack propagation of each specimen with ANSYS to ensure serviceability of LSRC beams and slabs.
6. Study the stiffness of solid and LSRC beams
7. Compare the shear capacity from the experimental results with those predicted by different design codes of practice.

1.4 Organization Of Thesis

This thesis consists of 8 chapters.

The first chapter indentifies the aims and scope of this research.

Chapter 2 describes previous research work related to lightweight concrete, hollow structure, composite sandwich concrete and utilizing ANSYS to simulate the reinforced concrete behaviour.

The design provision for flexure and shear based on AS 3600 and some previous research regarding the shear capacity are discussed in Chapter 3.

Chapter 4 describes the experimental work. Materials and equipments used in the test program, the specimen details and the test procedure used are reported here.

The presentation and analysis of experimental test are given in Chapter 5.

Chapter 6 explains the finite element analysis used in this study. Some basic information about modeling of reinforced concrete structures using ANSYS is discussed here. In this chapter, test results from the experimental work are compared with the Finite Element Analysis.

Chapter 7 describes the strength and serviceability of the sandwich section. The crack propagation of each test specimen, the stiffness and load deformation behavior of beams as well as the comparison of the experimental results with design prediction given by the code are discussed here.

Chapter 8 summarizes the findings of this investigation and presents a set of conclusions. Recommendations for further work are also given in this chapter.

CHAPTER 2

LITERATURE REVIEW

2.1 Background

The market trend in modern time, have created a demand for the "open floor plan" that provides the flexibility in designing the layout of the floor without any restrictions by the structural elements. This has been giving the significant economical advantages for car parks, schools, gymnasiums as well as storage facilities and office buildings (Matthew and Bennett 1990).

However the constructions of longer span floors generally have a greater structural depth leading to a higher self weight which limits the span and increases both the material and construction costs. These problems have been partially overcome through the use of new material technologies such as high performance lightweight concrete and through the use of new slab technologies such as Prestressed Hollowcore (Prestressed Hollow-core Concrete Slabs, 2001) and BubleDeck slabs (BubbleDeck technology, 2008). Both of these technologies focus on enhancing the span by reducing the weight of the slab and overcoming concrete's natural weakness in tension.

2.2 Lightweight Concrete

Lightweight concrete can either be made with lightweight aggregate, foamed technology, or autoclaved aerated technology. The benefits of lightweight concrete are numerous and have been well recognized. Bobrowski (1980) highlighted the implementation of lightweight concrete in many constructions. There are five commercially available synthetic lightweight aggregates which are considered to be suitable for structural applications in UK namely: Aglite (expanded clay/shale), Leca (expanded clay), Foamed slag (blast-furnace slag), Lytag (sintered pulverized-fuel ash) and Taclite (sintered pulverized-fuel ash / furnace bottom ash). Of these Lytag is the most commonly used for structural concrete (Horler 1980). Other lightweight materials such as polyurethane foam was considered to make the lightweight concrete (Mounanga et al 2008).

Lai et al (1996) replaced 10% of coarse aggregate with expanded polystyrene beads for making lightweight structures. From the test it was found that the moment carrying capacities for reinforced normal weight and polystyrene concrete beams were similar. However beam with polystyrene deflected considerably more than the corresponding beams with normal weight concrete due to the lower modulus of elasticity of the polystyrene .

Foamed concrete, or cellular concrete, is either cement or mortar in which foaming agent is added to create air-voids within it. The density of foamed concrete varies in a wide range of 400 to 1600 kg/m^3 depending on the foam dosage. Literature classification on the properties of foamed concrete (Ramamurthy et al. 2009) and its historical use in construction application (Jones & Mcarthy 2005) is published recently.

Narayanan and Ramamurthy (2000), investigates the structure and properties of aerated concrete. Aerated concrete is relatively homogeneous when compared to normal concrete. The properties of aerated concrete depend on its microstructure (void-paste system) and composition, which are influenced by the type of binder used, methods of pore-formation and curing. For domestic construction, AAC can be used as load-bearing walls when integral with reinforcing frame (Moulia & Khelafi 2007). The Masonry Structures Code of Australia (AS3700-2001) includes provisions for AAC block design. Other researchers have been utilized the lightweight aggregate in structural application for example in reinforced concrete beams (Bungey & Madandoust 1994, Ahmad et al. 1994), with high strength fiber (Kayali et al. 2003), and as an infill in reinforced concrete columns (Moulia & Khelafi 2007).

Lightweight concrete floors are typically 25% to 35% lighter than regular concrete aggregate mixes, and high strength structural lightweight concrete mixtures can also be designed to achieve similar strengths as normal weight concrete. However, the pouring and finishing of lightweight concrete does require specialist attention to ensure that the finished product is both consistent with the design requirements and specifications (Al-Khaiat and Haque 1997).

2.3 Hollow Structure

Research by Alnuaimi et al (2008) compared between solid and hollow reinforced concrete beams. Results from testing 7 pairs of reinforced concrete beams (solid and hollow beam with the same reinforcement) shows that all solid beams cracked at higher loads than the hollow beams. The hollow beams failed close to the design loads while the solid beams failed in the higher load. This indicates that the core contributes to the ultimate load resistance of the section and cannot be ignored in term of combined load of bending, shear and torsion.

Technologies such as prestressed hollow planks, pre-tensioned, post-tensioned have been commonly used in the industry. This approach is effective and reduces the size of section at a large span. To apply prestress in the construction, specialist is needed, The contractor will not be able to do it with a normal labour.

Precast Hollow-core slabs were developed in the 1950's as an alternative to in-situ cast concrete floor panels allowing an increase in the span length as the dead weight is reduced by up to a third. Hollow-core slabs can also be combined with high strength concrete technology and prestressing to further increase span (Prestressed Hollow-core Concrete Slabs 2001).

Hollow core slabs can be used only in one-way spanning constructions and must be supported by beams and/or fixed walls. When the slabs are installed and grouted together at the keyways, the individual slabs become a system that behaves similarly to a monolithic slab. A major benefit of the slabs acting together is the ability to transfer forces from one slab to another. The ability to distribute loads among several slabs has been demonstrated in published tests.

Hollow-core slabs are excellent in thermal insulators but poor in sound insulators.

It has also been stated in the Hollow-core floor overview report (2007) that a series of Hollow-core slabs will provide a basic diaphragm capable of resisting lateral loads in the form of lateral earth pressures, wind loads or seismic loads by a grouted slab assembly, provided proper connections and details are installed. However, following the Northridge earthquake in California in1994, questions were raised about the integrity of Hollow-core floors after some failures of Hollow-core slab systems. This

leads to load tests on a full-scale model of a Hollow-core floor assembly at the University of Canterbury in 2001, which indicated potentially serious gaps.

2.4 BubbleDeck

Schnellenbach-Held and Pfeffer (2002) investigated the structural behavior of biaxial hollow slab, known as BubbleDeck slab. This technology combines the advantages of material saving and extreme load carrying capacity due to its optimized cross-section.

The basic effect of the bubbles is the weight reduction of the deck. The dead load of the BubbleDeck is 1/3 lesser than a solid deck with the same thickness – and that without effecting the bending strength and the deflection behavior of the deck.

The experiment by Aldejohann and Schnellenbach-Held (2003) shows the similar shear crack behavior of BubbleDeck and the solid slab, The ultimate load of the BubbleDeck was applying most adverse geometrical and material properties- between 55% and 64% of the shear capacity of a massive slab with the same properties.

BubbleDeck gives an exceptional degree of freedom in architectural design – choice of shape, large overhang, larger spans / deck areas with fewer supporting points – no beams, no carrying walls and fewer columns results in flexible and easy changeable buildings. Interior design can easily be altered throughout the buildings lifetime.

The shear capacity is measured to be in the range of 72-91% of the shear capacity of a solid deck. In calculations, a factor of 0.6 is used on the shear capacity for a solid deck of identical height. Areas with high shear loads need therefore a special attention .e.g around columns. That is solved by omitting a few balls in the critical area around the columns, therefore giving full shear capacity. (BubbleDeck technology, 2008).

2.5 The Composite Sandwich Section

The composite sandwich structure is a solution to enhance the structural performance, at the same time makes it lighter and cost effective. Some of the works in the development of composite sandwich sections are by Schaumann et al (2009) who introduced the concrete sandwich slab which consists of three layers, i.e., the

glass fiber reinforced polymer element as the tension skin, lightweight concrete as core material and high performance concrete as the compression skin. Other types of composite sandwich sections are, for instance, composite sandwich panel by fiber glass laminate skin over PVC foam or polyester mat cores (Russo and Zuccarello, 2007), sandwich beam with honey comb core (Abbadi et al, 2009 and Meidell, 2009) and sandwich beam made up of glass fibre-reinforced polymer skins and modified phenolic core material (Manalo et al, 2010).

Hearne et.al (1980) studied the behaviour of AAC blockwork subjected to concentrated loading. Memon et al (2007) introduced the sandwich composite of ferrocement and lightweight aerated concrete. Mousa and Uddin (2009), investigated the FRP/AAC panel based on the theory of sandwich construction with strong and stiff skin. Despite many efforts of investigating the sandwich section to minimize the weight of the structure, there are still limited attempts in incorporating AAC with normal reinforced concrete.

2.6 Numerical Investigation by Using ANSYS

Nowadays, finite element method is a very powerful tool for analyzing a broad range of problems in different environments. The method is employed extensively in the analysis of solids and structures and of heat transfer and fluids. In concrete structures, FEA is a very convenient tool that can simulate and predict the responses of the non linear behavior of concrete members without having to go to expensive and time consuming work in the laboratory.

The finite element method for reinforced concrete structures was introduced by Ngo and Scordelis (1967). Discrete modelling was used to model the bars and a linkage element was introduced to connect bar elements and concrete elements.

Nilson (1968) followed the lines of Ngo and Scordelis (1967) and used a non-linear relationship for the modeling of bond transferred between the concrete and reinforcing bars. He employed a step by step incremental load algorithm to incorporate the non linear behavior and progressive cracking in the specimen.

Arnesen et al (1980) concluded that there are three main things that can lead to succeed in developing the non linear analysis program, i.e: Realistic material model, Efficient discretization technique, and Efficient & reliable solution algorithm.

In this research ANSYS was chosen because of a very useful 3-D reinforce concrete element already provided in its element library. Some of the literature that using ANSYS to perform modeling in the reinforced concrete are presented here.

Mirmiran et al (2000), used ANSYS for the analysis of FRP confined concrete by using Drucker-Prager plasticity, however, the DP model cannot be used to model stiffness and strength degradation.

Many researchers used Solid65 and Link8 in ANSYS to model the reinforced concrete with discrete reinforcement and most of them found that the results predicted by the model were in good agreement with experimental data.

Kachlakev et al., (2001) studied beams externally strengthened with reinforced plastic carbon fibre (CFRC) with no stirrups being used in the experiment. Padmarajaiah and Ramaswamy (2001) used COMBIN14 (spring) elements to model the interface behavior between the concrete and reinforcement to investigate the prestressed concrete with fiber reinforcement. Ibrahim and Mubarak (2009) modeled the continuous concrete beams pre-stressed using external tendons to predict the ultimate load and maximum deflection at mid-span for two spans of beam. This model accounts for the influence of the second-order effects in externally pre-stressed members. Buyukkaragoz (2010) studied about strengthening the weaker part of the beam by bonding it with prefabricated reinforced concrete plate. Nie et al (2008) investigated three type of connection i.e. interior diaphragms, exterior diaphragms and anchored studs of the concrete- filled square steel tubular columns (CFSSTCs) and steel concrete composite beams. ANSYS was used to model those connections under monotonic and cyclic loading. Dahmani et al (2010), found that discrete reinforcement approach give better results than the smeared one.

The steel fiber reinforced concrete were modeled using ANSYS and the finite element failure behavior indicates a good agreement with the corresponding experimental behavior (Özcan et al, 2009). Li Hua et al (2008) who investigated steel fiber in deep beam also used ANSYS to model this behaviour. The result shows that the addition of steel fiber could repress the crack propagation of the deep beam. Good agreement was found between FEA results and test results if the Nilson bond stress slip relationship curve was used to simulate the SFRC beam approximately. Finite Element Analysis with ANSYS can also predict accurately the bond mechanism for both plain and fiber reinforced concrete Ezeldin and Balaguru (1990).

The short discrete fibers added to the brittle concrete matrix improve the composite behavior in the areas of strength and ductility.

Barbosa and Ribeiro (1998) compared the nonlinear analysis with discrete and smeared reinforcement for the same beams. Both models were analysed four times. It is shown that satisfactory results may be obtained from relatively simple and limited models.

CHAPTER 3

DESIGN PROVISION

3.1 Introduction

A brief review of Flexure and Shear design provision in the Australian Standard 3600 (2009) is described here. Previous research regarding shear capacities is also discussed here.

3.2 Flexure Design Provisions in AS 3600

When a beam is to be designed to resist flexure, it will be subjected to compressive and tensile force at the same time. The tensile force will be resisted by the longitudinal reinforcements while the compressive force is resisted by the concrete above the neutral axis.

Rectangular stress block concept was used in which a single parameter γ is used to define both the magnitude and the location of the compressive force which is noted as '*C*'. Uniform stress of magnitude $0.85f'c$ was used to replace nonlinear stress distribution above the neutral axis. The resultant compressive force becomes:

$$C = 0.85f'c\gamma bd_n \qquad (3\text{-}1)$$

where

f'_c = *the characteristic compressive cylinder strength of concrete at 28 days.*

b = *width of the cross section, and*

d_n = *depth of neutral axis from the extreme compressive fibre.*

and acts at a depth:

$$d_c = 0.5\gamma d_n \qquad (3\text{-}2)$$

In AS 3600, the value for γ applies for normal concretes with f'_c up to 50 MPa. The values are:

$$\gamma = 0.85 - 0.007(f'_c - 28) \quad (0.65 \leq \gamma \leq 0.85) \qquad (3\text{-}3)$$

The force in reinforcing steel, noted as 'T' is:

$$T = f_{sy}A_{st} \qquad (3\text{-}4)$$

where

f_{sy} = *the yield strength of reinforcing steel, determined in accordance with clause 6.2.1 of AS 3600 (2001), and*

A_{st} = *the cross-sectional area of tension reinforcement.*

It is essential to design a beam that has ductile behaviour. In AS 3600, to ensure ductile behaviour, the neutral axis parameter ku shall not exceed 0.4.

AS 3600 also stipulates that minimum tensile reinforcement shall be provided in order to satisfy the requirement that $M_{uo} \geq (M_{uo})_{min}$ for rectangular reinforced concrete cross-sections whereby M_{uo} is the ultimate flexural strength and $(M_{uo})_{min}$ is the minimum flexural strength. The formula given in the code for minimum tensile reinforcement is as follows:

$$A_{st\cdot min} \geq 0.22 \left(\frac{D}{d}\right)^2 \frac{f'_{cf}}{f_{sy}} bd \qquad (3\text{-}5)$$

where

$A_{st.min}$ = *the minimum cross-sectional area of reinforcement permitted in a critical tensile zone of a beam in flexure.*

D = *the overall depth of a cross-section in the plane of flexure.*

d = *the effective depth of a cross-section (clause 1.6.3 in AS 3600), and*

f'_{cf} = *the characteristic flexural tensile strength on concrete determined in accordance with clause 6.1.1.2 in AS 3600.*

3.3 Shear Design Provisions in AS 3600

The Australian Standard AS 3600 (2001) shear design equations are based on a variable angle truss model. The shear resistance is made up of concrete and steel stirrup contribution:

$$V_u = V_{uc} + V_{us} \qquad (3\text{-}6)$$

where

$$V_{uc} = \beta_1 \beta_2 \beta_3 bd \left(\frac{A_{st} f'_c}{b_v d_o}\right)^{\frac{1}{3}} \qquad (3\text{-}7)$$

b_v = *effective web width.*

d_o = *distance form extreme compression fibre to the centre of the outermost layer of longitudinal reinforcement, and*

A_{st} = *cross sectional area of longitudinal tensile steel reinforcement*

The factors for the concrete contribution, V_{uc}, according to AS 3600 (2001) are as follows:

β_1 accounts for the size factor of a section. Deeper sections are considered to carry lower shear stress at failure.

$$\beta_1 = 1.1\left(1.6-\frac{d_0}{1000}\right) \geq 1.1 \quad (d_o \text{ in mm}) \qquad (3\text{-}8)$$

β_2 accounts for axial force effects.

β_2 = *1.0 (when no axial force exists)*

β_3 accounts for the presence of a large concentrated load near a support.

$$\beta_3 = \frac{2d_0}{a_v} \quad (1.0 \leq \beta_3 \leq 2.0) \qquad (3\text{-}9)$$

where a_v is the distance of the concentrated load from the support.

For vertical shear reinforcement, AS 3600 gives the perpendicular stirrup contribution as:

$$V_{us} = \frac{A_{sv} f_{sy.f} d_o \cot\theta_v}{s} \qquad (3\text{-}10)$$

where

A_{sv} = *cross-sectional area or shear reinforcement.*
$f_{sy.f}$ = *yield stress of a shear reinforcement.*
θ_v = *angle of inclination of the concrete compression strut.*
s = *spacing of the stirrup.*

To avoid web crushing failure when large amount of stirrup is used, AS 3600 limits the shear capacity to:

$$V_{u.max} = 0.2 f'_c b_v d_o \qquad (3\text{-}11)$$

AS 3600 (2001) also stipulates that a minimum amount of shear reinforcement should be provided before it is effective for shear contribution:

$$A_{sv.min} = \frac{0.35 b_v s}{f_{sy.f}} \qquad (3\text{-}12)$$

The angle of inclination θv is the angle between the axis of concrete compression strut and the longitudinal axis of the member. It varies linearly between 30° when the minimum amount of shear reinforcement is used and 45° when the maximum amount of shear reinforcement corresponding to web crushing is used.

3.4 Shear Capacity

In general, as well established by ASCE-ACI Committee 445 (1998), shear resistance in a reinforced concrete slab without shear reinforcement can be assessed from five main components:

1. Shear capacity in uncracked compressed concrete, which is mainly contributed by the concrete strength and the depth of the uncracked zone as a function of the longitudinal reinforcement properties.
2. Aggregate interlock, which is a function of the crack roughness, the crack width and the concrete strength that allows the shear transfer across a crack in the tensile zone.
3. Dowel action of the longitudinal reinforcing bars intersecting the shear crack, which depends on the amount and size of the longitudinal reinforcement, i.e., a greater influence for larger and more rigid bars.
4. Arch action, which occurs in the uncracked concrete near the end of the elements where *a/d* ratio is less than 2.5.
5. Residual tensile stresses, which are transmitted directly across the cracks with the crack widths smaller than 0.15 mm.

The primary design parameter that significantly affects the shear failure mechanism is the shear span-to-depth ratio, *a/d*, (Bažant and Kim (1984), Marti (1985), Walraven and Lehwalter (1994), and as *a/d* decreases, the shear strength considerably increases due to the arch action.

Choi and Park (2007) proposed the design method in which the shear strength is significantly affected by the change in the shear failure mechanism. As *a/d* decreases, the shear failure mechanism controlled by compression governs, and as a result, the shear strength of the beam increases. Similarly, as the ratio of transverse web reinforcement increases, the shear strength increases. On the other hand, as the ratio of longitudinal web reinforcement increases, the shear strength does not significantly increase.

Choi et al (2007) also mentioned that the compression zone of a beam is subjected to a combination of compressive normal stress and shear stress. Therefore, the interaction between these two stress components must be considered to accurately evaluate the shear strength of the compression zone. The use of concrete with high compressive strength did not significantly increase the shear strength of the specimens as also appointed by Kong (1996). In the proposed strength model, the shear strength of a beam is affected by the depth of the compression zone as well as the tensile strength of concrete. The high compressive strength of concrete increases the tensile strength of concrete, but reduces the depth of the compression zone. For this reason, the shear strength of a beam does not significantly increase.

In the web-shear crack region, which is usually uncracked in flexure, the load causing web-shear cracks can be estimated by equating the principal tensile stress at a critical point in the web to the tensile strength of the concrete (Warner et al. 1998). Using Mohr's circle, the principal tensile stress σ_1 caused by the longitudinal stress, σ, and shear stresses, τ, acting on an element is given by:

$$\sigma_1 = \sqrt{(0.5\sigma)^2+\tau^2} + 0.5\sigma \qquad (3\text{-}13)$$

$$\tau = \frac{VQ}{Ib_w} \qquad (3\text{-}14)$$

where

Q = *the first moment about the centroidal axis of the top (or bottom) portion of the member's cross-sectional area, defined from the level at which τ is being calculated,*

I = *the moment of inertia of the entire cross-sectional area computed about the neutral axis, and*

b_w = *the width of the cross-sectional area, measured at the point where τ is being calculated.*

The recommended value of the maximum principal tensile stress sufficient to cause diagonal cracking is $0.33\sqrt{f_c'}$ in both Australian and American codes. In design, the exact location of the principal tensile stress is usually not known depending on the distribution of longitudinal and shear stresses across the section. However, at a region nearer to support where the bending moment is close to zero, the maximum principle tensile stress occurs at the neutral axis of the cross section. Thus, for a rectangular section without any bending moment and where the maximum principal tensile stress is at the neutral axis of the cross-sectional area.

The shear formula (3-14) is based on the assumption that the shear stress is constant across the width of the section. In a wider section, such as in the present case, shear stresses are not necessarily constant and the maximum shear stress occurred at the edges could be significantly greater than the maximum shear stress based on Equation 3-14.

CHAPTER 4

MANUFACTURE AND TESTING OF LSRC BEAMS AND SLABS

4.1 Introduction

This chapter described the experimental work, details of each test specimens, such as the concrete materials, the AAC blocks, the equipment and the manufacture of the specimens. The test set up, the instrumentation and the testing procedure are also presented.

Five beams were manufactured, 3 for flexure test i.e.: solid beam as control, beam incorporating full amount of AAC blocks, and beam with half amount of AAC blocks. Two more beams manufactured for shear testing purpose; solid beam and beam with full amount of AAC blocks.

Furthermore, to investigate the shear capacity of the slab, 4 slabs were manufactured. One solid slab and 3 sandwich sections i.e.: slab with maximum amount of AAC blocks, half amount of AAC blocks and full amount of curve AAC blocks.

The test program was established to study the behavior of sandwich section subjected to bending moment and shear force.

4.2 Concrete

The concrete was supplied by a commercial ready mix plant in Perth, Western Australia with nominal 28 day compressive strength of 40 MPa. The maximum size of aggregate was 10 mm. Superplastisizer was added on site to increase the workability of the mixes to ensure the easier casting and a good compaction of concrete. The properties of concrete such as, compressive strength test, splitting test, and modulus of elasticity are incorporated in this research.

Twenty six of 100 mm x 200 mm cylindrical samples and nine of 150 mm x 300 mm cylindrical samples were made during the casting of the specimens using the same batch of concrete. The concrete in 100 mm x 200 mm cylinders was cast in two layers on a vibrating table. For 150 mm x 300 mm cylinders was done in three layers. These cylinders were kept under the same environmental conditions as the beams

and slabs. All tests were performed at concrete laboratory, Department of Civil Engineering, Curtin University, Western Australia.

4.2.1 Compressive Strength Test

The concrete compressive strength test was carried out at day 7, day 14, day 21, day 28 and on the testing days (day 40 and 103). Each test consisted of 3 cylinders measuring at 100 mm x 200 mm. The test used the MCC computerized control console in the concrete laboratory as shown in Figure 4.2. The test was performed in accordance with AS 1012.9-1999.

The result on the strength development of concrete are listed in Table 4.1 And shown in Figure 4.1.

Table 4.1 Concrete strength development with curing age

Day	Sample	Diameter	Height (mm)	Mass (kg)	Stress (MPa)	Average
Day 7	1	99.0	201.0	3775	31.45	29.40
	2	99.8	202.0	3840	29.92	
	3	100.3	200.0	3821	26.82	
Day 14	1	99.5	201.7	3785	37.29	35.21
	2	99.4	200.7	3733	31.48	
	3	100.0	201.7	3761	36.87	
Day 21	1	99.4	201.2	3788	38.34	37.53
	2	99.7	201.9	3769	36.12	
	3	99.7	200.5	3801	38.13	
Day 28	1	99.6	203.5	3767	42.62	43.29
	2	99.9	200.8	3782	44.12	
	3	99.8	203.0	3793	43.14	
Day 40	1	99.5	201.6	3621	43.87	43.94
	2	99.7	201.8	3634	44.32	
	3	99.2	201.5	3646	43.62	
Day103	1	99.9	202.5	3668	43.61	43.88
	2	99.9	201.3	3626	45.25	
	3	99.7	202.7	3639	42.78	

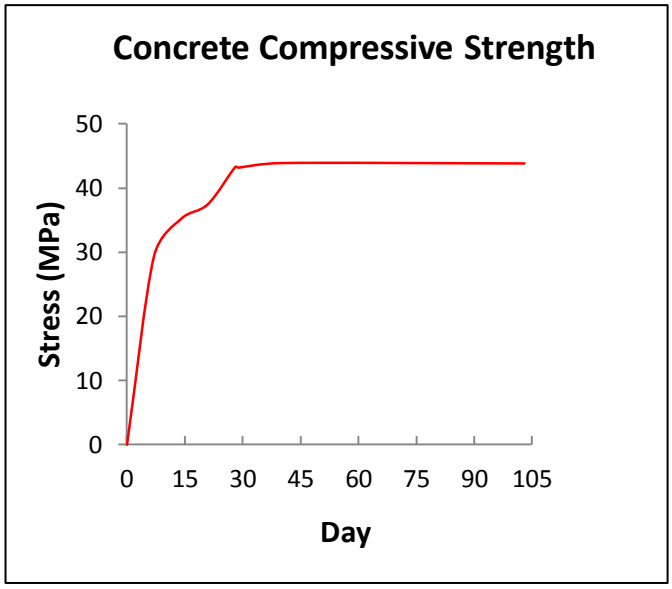

Figure 4.1 Development of concrete strength with age

4.2.2 Indirect Tensile Strength Test

The AS 1012.10-2000 was employed to determine the indirect tensile strength of concrete. The cylinder dimension is 150 mm in diameter and 300 mm in height. The splitting test was performed at day 28, and on the testing day (day 40 and day 103 of concrete age). The results on the splitting tensile strength of concretes are listed in Table 4.2.

Figure 4.2 The MCC computerised controle console for testing concrete compressive and tensile strength

Table 4.2 Concrete splitting tensile test result

Day	Sample	Diameter	Height (mm)	Mass (kg)	Load (kN)	Strength	Average strength (MPa)
Day 28	1	150.00	300.00	12409	238.30	3.37	3.29
	2	149.00	300.00	12434	217.70	3.10	
	3	150.40	300.00	12297	241.80	3.40	
Day 40	1	150.00	300.00	12300	257.40	3.64	3.64
Day 103	1	150.00	298.00	12141	297.70	4.24	3.40
	2	150.00	300.00	12075	237.20	3.36	
	3	150.00	299.00	12120	178.00	2.52	

4.2.3 Modulus of Elasticity

The modulus of elasticity was determined in accordance with AS 1012.17-1997. Figure 4.3 shows the arrangement of the modulus of elasticity test. The modulus of elasticity was taken as the secant modulus measured at 45% of the compressive strength of the cylinder. The result of this test is tabulated in Table 4.3.

Figure 4.3 The modulus of elasticity test set up

Table 4.3 Concrete modulus of elasticity

Day	Sample	Stress	Modulus of Elasticity			Average Modulus of Elasticity (10^3)MPa	
			1	2	3		
Day 28	1	44.09	26477.40	27932.09	27856.42	27.9	29.6
	2	42.32	28743.24	30487.88	30556.91	30.5	
	3	43.27	29072.45	30577.18	30402.60	30.5	
Day 40	1	44.32	29900.31	31217.42	31106.47	31.2	31.7
	2	43.62	30323.01	32361.11	32280.08	32.3	

4.3 Construction of LSRC Section

As per any reinforced concrete members, the construction of LSRC members can be either fully precast, semi-precast, or cast in-situ. Lightweight blocks can be technically placed between the lower and upper reinforcements of the section. In a beam member, the encasing shear stirrups can be installed before or after the placement of the blocks. When preparing for the experiment, the casting bed and steel mould were prepared and secured; lower and upper reinforcing steels and shear stirrups were prefabricated. Lightweight blocks were inserted within the encasing stirrups through the side of the beam. This method of construction is typical for either precast or cast in-situ members.

When dealing with a large concrete member such as a long span beam or a large floor construction, it is of advantage for constructors to consider semi-precast construction method. The semi-precast construction helps resolve, to a certain extent, the complication due to the heavy weight of the structure. LSRC members are also suitable for semi-precast construction. The lower part of concrete section can be cast with the lower reinforcing steels in which the shear stirrups and lightweight blocks are already put in place. Alternatively, the precast can be done with the portion below the underside of the blocks, which means that the concrete can be cast prior to the placement of the blocks. If this is the case, side formworks will be required when preparing the upper part of the section for concreting. It is necessary to ensure that the section is monolithic by making sure during casting that the concrete can flow in properly through to the sides of the beam and in the gaps between the lightweight blocks.

The manufacture of beams and slabs involved pouring the fresh concrete in layers into the moulds. Hand-held mechanical vibrators were used to compact the fresh concrete. The beam and slab specimens were covered in hessian and plastic sheets to minimize the loss of moisture after initial setting of the concrete, and routinely watered each day until day 5 when the external sides of the formwork were stripped. The beams and slabs were removed from the formwork 7 days after casting and stored just outside the concrete laboratory until the time of testing.

4.3.1 Beams

The tested beam had a rectangular cross section, with a constant width and depth of 200 mm by 300 mm. All beams were provided with top and bottom longitudinal bar. Bottom bars were deformed bars (designated as N-bars) used in Australian practice. N20 bars were used as bottom steel in all beams. For top steel, round bars were used (designated as R-bars). The tensile strength at yield was 560 MPa for the N-bars and 300 MPa for the R-bars. For shear reinforcement, 6mm diameter hot-rolled plain round rebar were used. The stirrups were vertical rectangular closed ties with 139^{o} hooks for good anchorage. The beam length was 3000 mm, with 2800 mm clear span when set up for testing. Five beams were manufactured for two series of four-point test – the flexural test and the shear test.

The flexural test was to compare the flexural capacity between the solid and LSRC beams. Three beams were prepared, one solid (SB1F) and two with AAC blocks (LB1F and LB2F). LB1F beam had the maximum number of blocks that could be placed in it, while LB2F has half the amount of that contained in LB1F. In the shear test, two beams were prepared, one solid (SB1S) and one with AAC blocks (LB1S). AAC blocks were supplied by Ecobrick based in Canning Vale, Western Australia. The standard dimensions of the AAC blocks used were 300 mm x 180 mm x 75 mm. Two blocks were tied together that create the thickness of 150 mm. These blocks would be placed within the tension region of the beam cross-section when subject to bending, i.e., below the calculated depth of the neutral axis. It is therefore necessary to cut the blocks to fit within this depth. The cross section of AAC blocks became 115 mm x 160 mm. To ensure the good grip between the AAC blocks and the concrete, there were 43 mm gaps between the blocks. Steel bar, 10 mm in diameter, was used to tie the blocks together. As a result, when the tied blocks were placed, there were gaps between the blocks and the stirrups, and the blocks and the longitudinal bars. These gaps were useful in enhancing the grip of the reinforcing bars in the concrete section. Figure 4.4a, 4.4b, and 4.5 show the details of LSRC beam with AAC blocks infill.

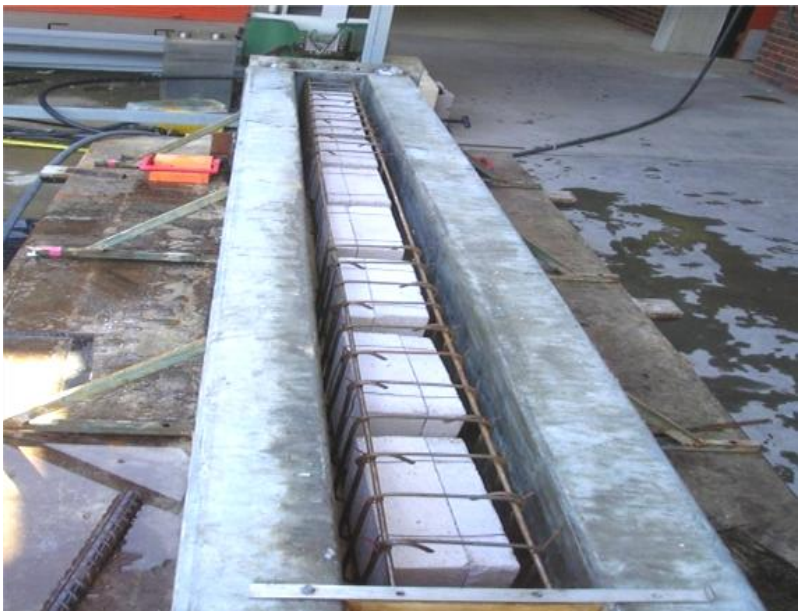

Figure 4.4a LSRC beam with full amount of AAC blocks

Figure 4.4b LSRC beam with half of AAC blocks infill

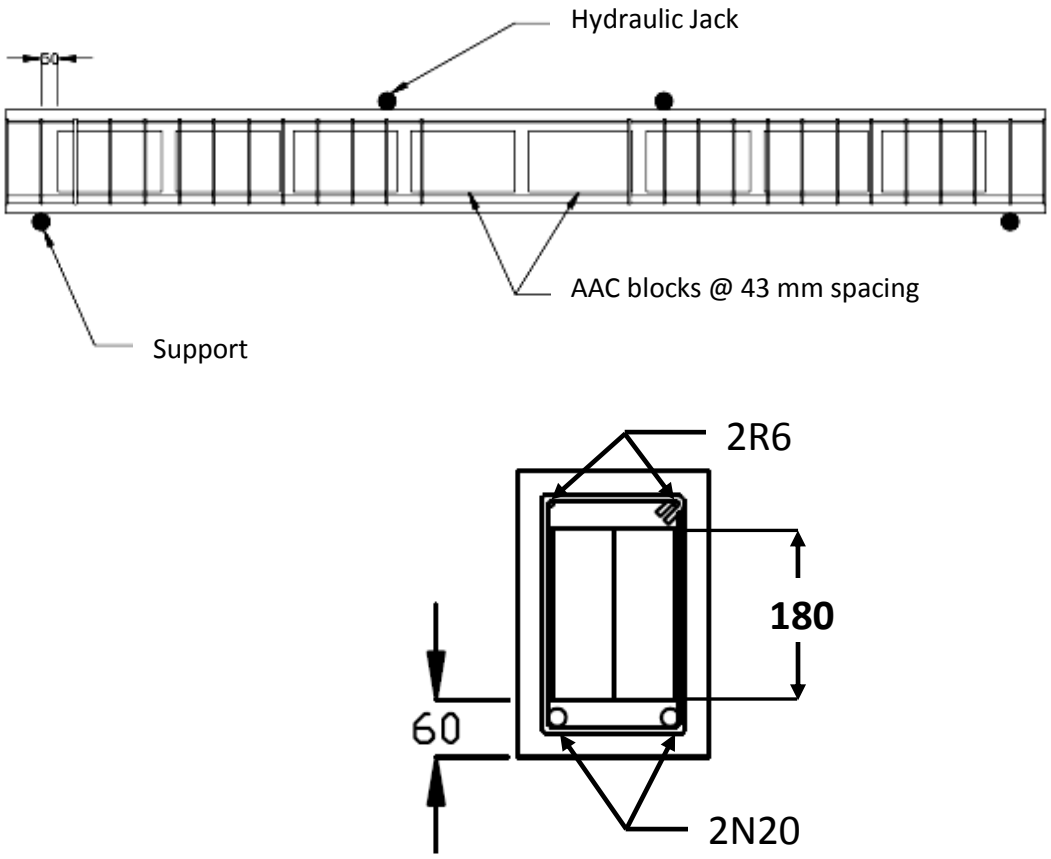

Figure 4.5 Beam details of sandwich section

Table 4.4 Details of tested beams

ID	Section	% Weight reduction	Testing
SB1F	Solid-no blocks	0	Flexure
LB1F	With 8 blocks	19	Flexure
LB2F	With 4 blocks	9.5	Flexure
SB1S	Solid-no blocks	0	Shear
LB1S	With 8 blocks	19	Shear

4.3.2 Slabs

Four slabs were manufactured, one solid (SS1), and three LSRC sections. All slabs had the same dimensions and reinforcement details. Slabs were 3000 mm long, 1000 mm wide, and had the total depth of 250 mm. The primary reinforcement used in the bottom of the slab was N12-100, in the top of slab was the minimum N12-300 and in the secondary directions in the top and bottom was N12-300. The shear span-to-depth ratio was equal to 2. The standard dimension of an AAC block used was 300 mm long, 180 mm wide and 75 mm thick. Two blocks were put together to create the total block thickness of 150 mm. LS1 contained 64 standard blocks, which were the

maximum number of blocks that could be placed within the specimen. LS2 contained 32 blocks, half of that contained in LS1, while LS3 had the same amount of blocks as in LS1 but the corners of the blocks were cut off to investigate the shape effect on the slab. In all LSRC slabs, blocks were placed evenly in both directions. The minimum gaps between the blocks in LS1 were 50 mm and 43 mm in the cross-section and the longitudinal directions of the slab, respectively. The details of the tested slabs are shown in Figure 4.6, 4.7, and 4.8.

Weight of Slabs

In the tested LSRC slabs, AAC Blocks were used as AAC blocks infill. The density of AAC Blocks was 550 kg/m^3 and the total weight reductions for each type of slab were between 14-27% of the equivalent solid slab. Table 4.5 presents a detailed breakdown of each slab. The maximum weight reduction was in LS1 which contained the maximum amount of AAC Blocks.

Table 4.5 Details of tested slabs

ID	No of blocks	Vol Blocks (m^3)	Vol Concrete (m^3)	% Concrete	% wt reduction
SS1	-	-	0.75	100.0	-
LS1	64	0.26	0.49	65.3	27
LS2	32	0.13	0.62	82.6	14
LS3	64	0.16	0.59	78.6	17

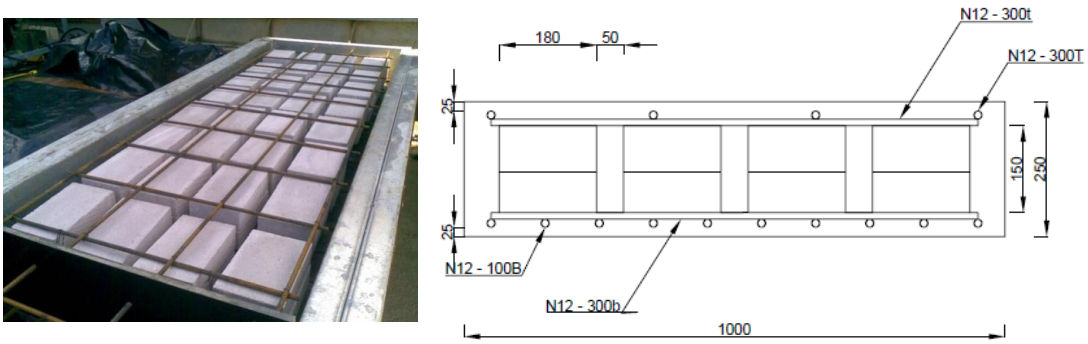

Figure 4.6 LS1 with full amount of AAC blocks

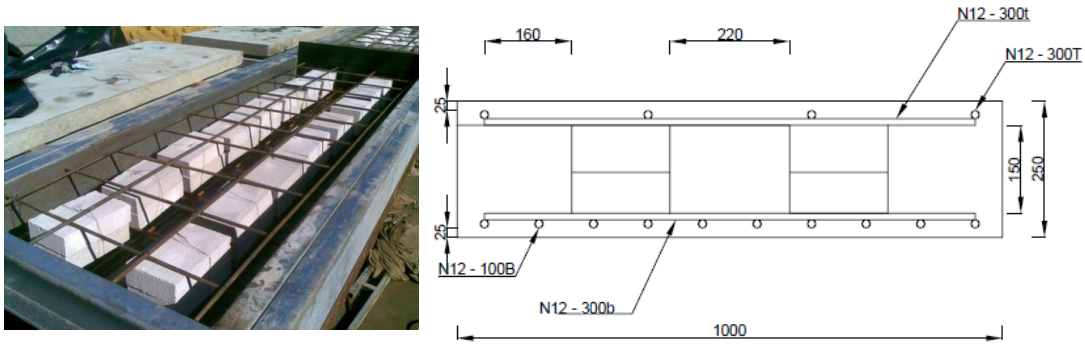

Figure 4.7 LS2 with half amount of AAC blocks

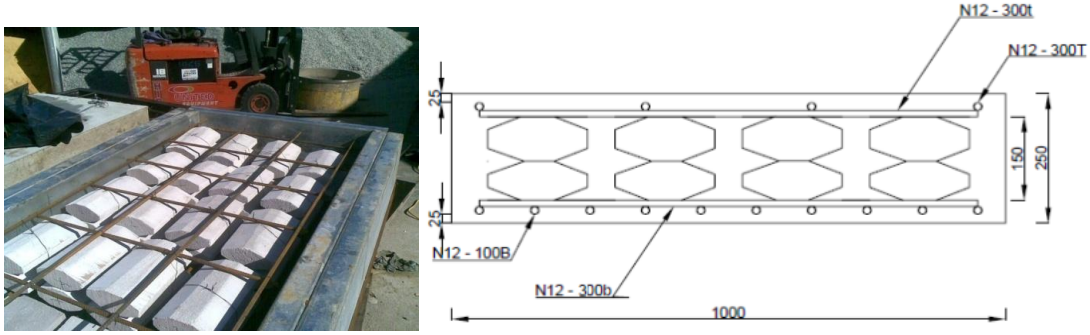

Figure 4.8 LS3 with full amount of curved AAC blocks

4.4 Test Set Up and Loading Procedure

4.4.1 Beams

Three beams were designed to fail in flexure, and two beams to fail in shear. The beams were simply supported and were subjected to two point loads. The distance between the two point loads was 800 mm and 1680 mm in the flexure and shear tests respectively. The typical test set up is as shown in Figure 4.9 and 4.10**.** The beams were loaded to failure using a 20 tonne capacity hydraulic jack to apply each of the two point loads. The jacks were attached to a reaction frame. Two supporting frames with 200 mm long x 150 mm diameter steel rollers were used as the end support.

To ensure a uniform dispersion of force during loading and to eliminate any torsion effects on the beam due to slight irregularities in the dimension of the beams, plaster of paris (POP) and 100 mm wide x 250 mm long x 20 mm thick distribution plates were placed on the rollers and also under the jacks.

The vertical deflections of the test beams were measured using Linear Variable Differential Transformers (LVDTs) which were placed at 200 mm spacing within 2.8 metres span. LVDTs were also attached on each loading jack to capture the vertical deflection at the loading point. The LVDTs were attached to a truss frame as seen in Figure. 4.11 and 4.12. With this arrangement, the curvature of the beam can be identified in relation to the loading increment. During the initial set up of the LVDTs, the instruments were calibrated before the test commenced. An automated data acquisition system with a Nicolet data logger system was used to record the load-deformation from the jacks and the LVDTs.

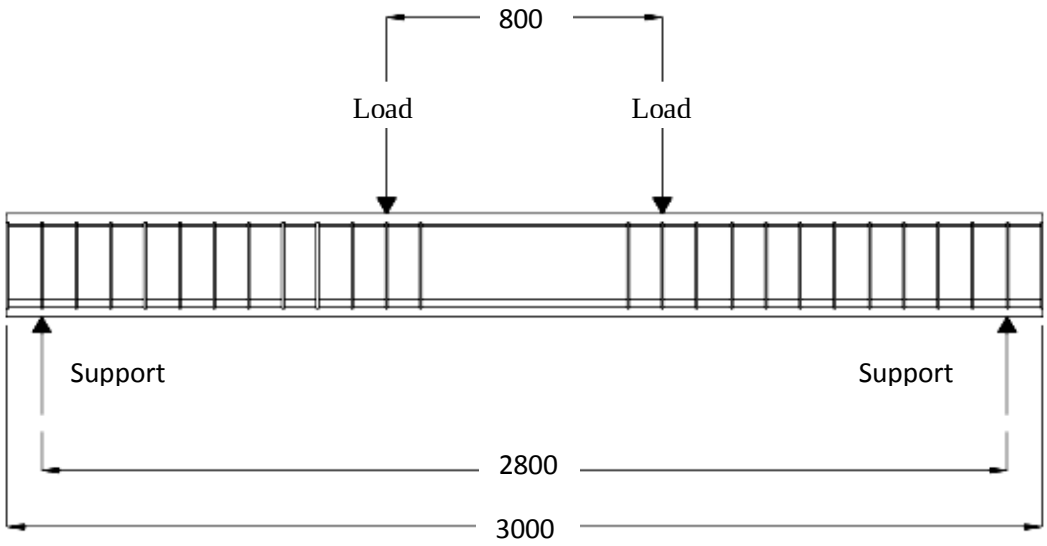

Figure 4.9 Load and support arrangement for flexure test

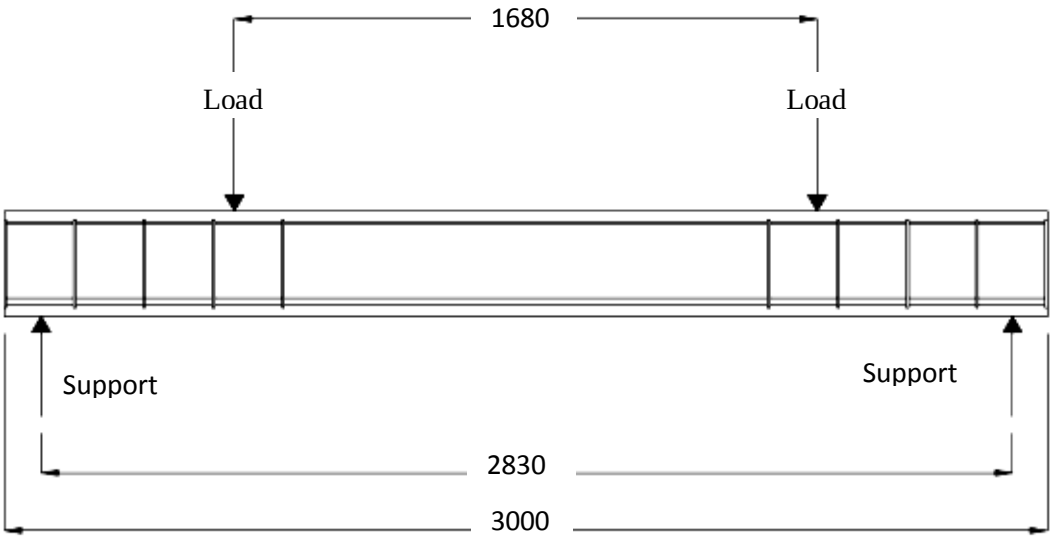

Figure 4.10 Load and support arrangement for shear test

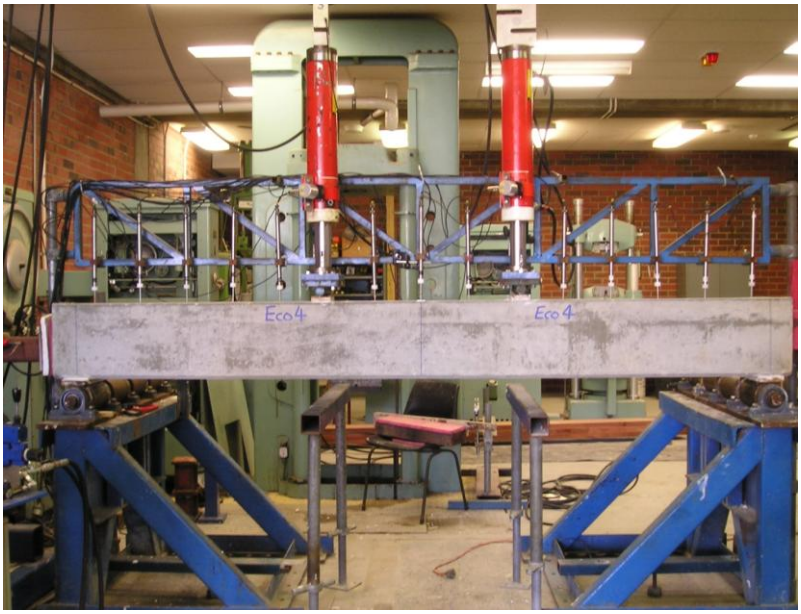

Figure 4.11 Test set up for flexure

Figure 4.12 Test set up for shear

Test Procedure

All the beams were loaded to failure. Small load was applied initially to ensure the test set-up and the instruments worked properly. The beam was then unloaded and initial reading was recorded.

During loading process, all cracks formed was redrawn with permanent marker and noted with the load when the crack appears. This will give a better visual on the crack propagation during loading.

After failure, each beam was photographed to show the crack pattern and the mode of failure. The photographs of the beams after failure are given in the appendices.

4.4.2 Slabs

The Heavy Loading Frame located in the concrete lab at Department of Civil Engineering, Curtin University, was used for the tests. The slabs were supported on roller supports and two hydraulic jacks were used to apply the load with 200 kN loading capacity for each jack which created a combined maximum loading capacity of 400 kN under force control. The applied load limitation had restricted the setup on the spanning arrangement of the slabs. Slabs were to be tested in shear, therefore, the bending moment induced by the load tests should not be more critical than the corresponding shear. As a result, the slab specimen was set with the clear span of 2000mm, as shown in Figure 4.13. The two locations of the jacks are as depicted in Figure 4.14. The shear span-to-depth ratio was equal to 2 at the testing end of the slab where critical shear failure was expected.

The applied load when the slab reached the predicted shear capacity was expected at 232 kN. Hinges were used at the top of the jacks to allow the jacks to move with the slab during testing. A transverse spreader steel beam was used to transform the two-point loadings to a uniform one-way action across the slab width. Plaster was applied to the underside of the bearing plate which was located directly under the spreader beam above the slab. This plaster ensured that the load applied to the slab was distributed evenly. The cantilevering end of the slab was not affected. For safety during load test, the slab was restricted from moving at one end by a rubber pad which did not prohibit the vertical deflection of any part of the slab when under load.

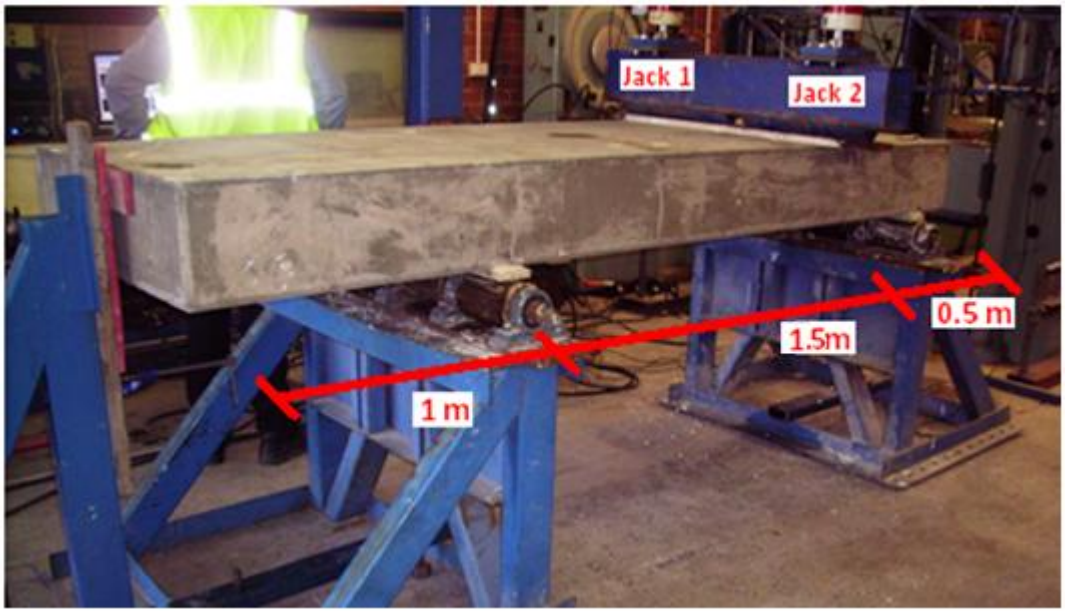

Figure 4.13 The experiment set up for slab specimen

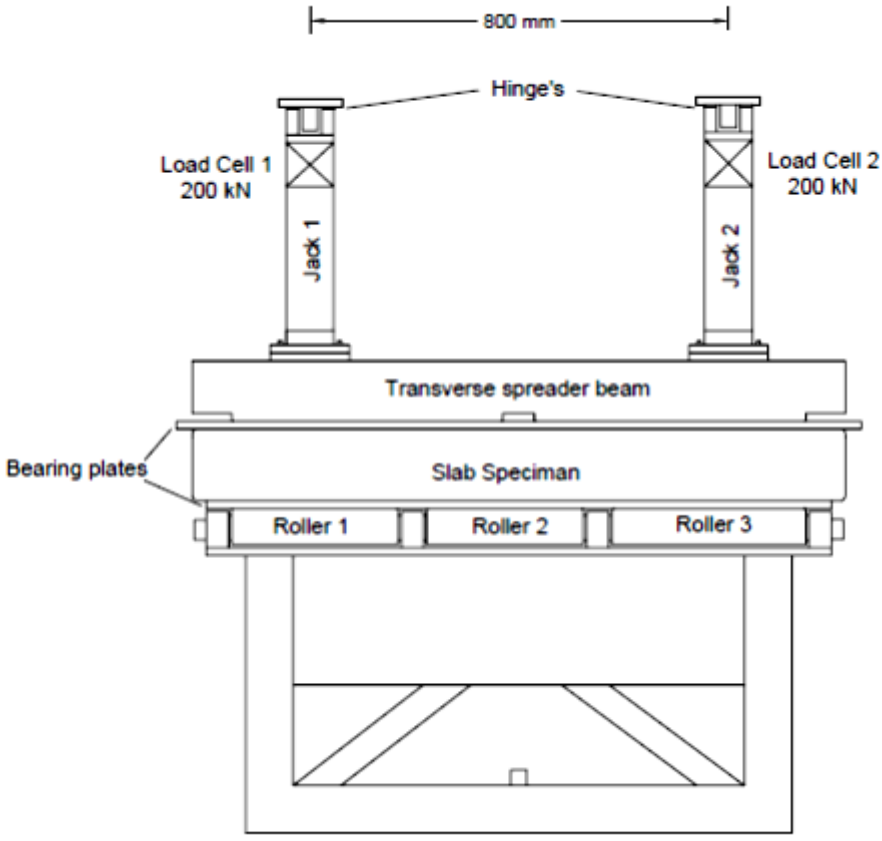

Figure 4.14 Test set up – Uniform one way action

Test procedure

During load test, a Linear Variable Differential Transformer (LVDT) was attached to each load cell. Both LVDTs were calibrated and setup to measure the displacement of the slabs associated with the applied loads. The testing involved firstly loading the slab with 100 kN and then releasing the full load. The process of loading the slab then releasing the load was then repeated for a number of loadings up until a loading of 320 kN which was the maximum allowed loading using the deformation controlled system. At this point, the loading was again released to zero and then reapplied by force control until failure of the slab occurred. As part of the force controlled test, an additional deflection dial gauge was setup. This dial gauge was used by the technician to measure the rate of displacement and approximately keep the displacement of the loading cells constant throughout the test until failure. The load and deformation were recorded by LDS Nicolet data acquisition system. During loading, the formation of the cracks on the sides of the slabs were also manually marked and recorded. The photographs of the slabs after failure are given in the appendices.

CHAPTER 5

EXPERIMENTAL RESULT

5.1 Introduction

The test results are presented in this chapter. The behavior of the specimens during the laboratory experiment is discussed. The effects of varying amount of blocks on the test beams are elaborated in this chapter.

5.2 Beams

5.2.1 Flexure Behaviour

The failure loads of the solid and LSRC beams under the flexure test were found to be of insignificantly different. It was found that beam LB1F, which had the maximum number of AAC blocks, failed at an average load of 78.9 kN, LB2F and SB1F beams failed at 78.6 kN and 78.5 kN, respectively. These load values were taken from the average of the loads applied from the two hydraulic jacks.

Under the flexural test, the main flexure cracks were developed within the two loading points and widen up as load increased. At failure, the concrete in the compression region crushed. It was seen that the exposed reinforcing steel in this region buckled. It is also evident that the sandwich sections have a more brittle failure .The typical crack formations at failure under the flexural test of solid and LSRC beams are as shown in Figure 5.1a, 5.1b, and 5.1c.

Figure 5.1a The typical crack formations at failure under flexural test of control beam

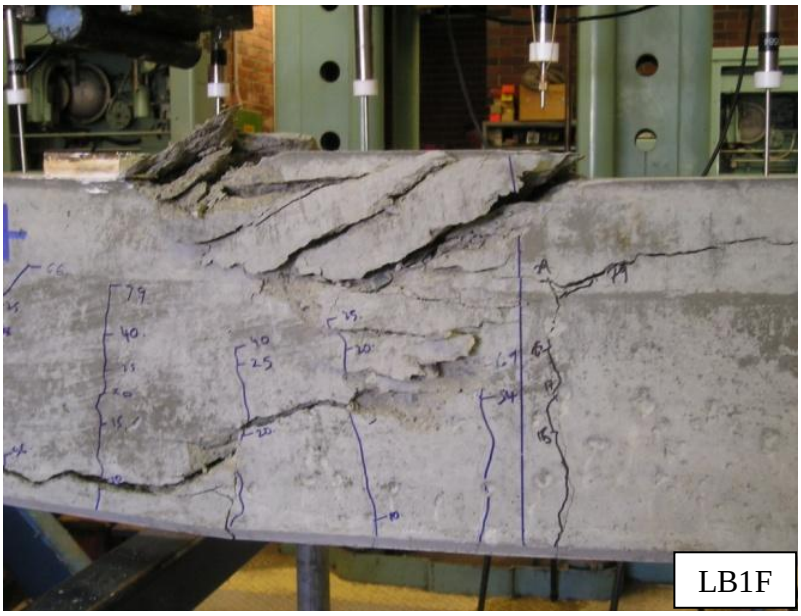

Figure 5.1b The typical crack formations at failure under flexural test of beam with full amount of AAC blocks

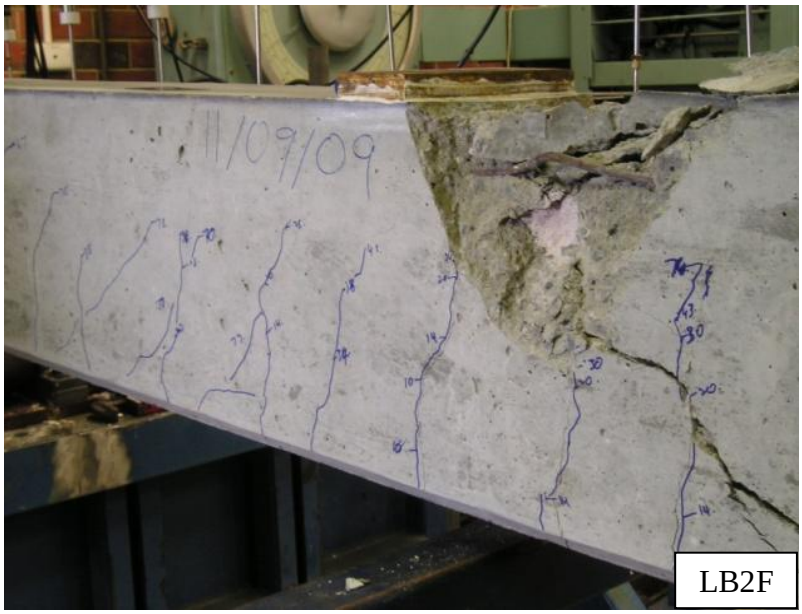

Figure 5.1c The typical crack formations at failure under flexural test of beam with half amount of AAC blocks

The load-deformation behavior of all the tested beams was found to be similar and followed the same trend. The loads versus deflections at the mid-span of all the beams under flexure are plotted in Figure 5.2.

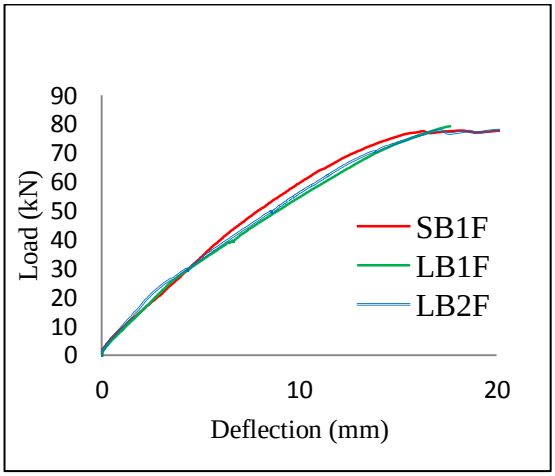

Figure 5.2 Load versus deflection

The graph shows that in the linear range, surprisingly the sandwich section incorporating half amount of AAC blocks (LB1F) is stiffer by 6.4%. However, after the first cracking occur, the stiffness different on the three beams can be clearly seen. The stiffness of the sandwich beams decrease by 5.6 % and 4.1% for LB1F and LB2F respectively. Before cracking the stiffness of the sandwich beam is similar to

the equivalent solid beam. This finding is as expected, because the area underneath the neutral axis does not contribute to the strength of concrete in bending.

5.2.2 Shear Behaviour

When a beam is more critical in shear, rather than in flexure, an LSRC beam is expected to exhibit lower shear resistance than the equivalent solid beam. This is because the inserted AAC blocks in an LSRC beam have lower compressive strength than the normal concrete. As a result, an LSRC beam has less effective concrete area to resist the shear when compared to the solid beam of identical height. Based on the two beam tests, the failure loads of SB1S and LB1S were 128 kN and 102 kN, respectively. A significant 20% reduction in the shear capacity of LSRC beam compared to the equivalent solid beam.

For beams tested in shear, the behaviors of the two tested beams were similar. Small flexure cracks occurred first at the midspan region of the beam. Subsequently, the flexure cracks extended as flexure-shear cracks were developed between the support and the loading point. As the load approaching the failure load, critical web shear cracks were developed diagonally within the shear span. The cracks continued to widen as the load increased, and failure occurred soon after depicting a typical sudden type of shear failure. The typical progressions of the cracks and the failure modes of the beam tested in shear are shown in Figure 5.3a and 5.3b**.**

Figure 5.3a The crack formation at failure under shear test of control beam

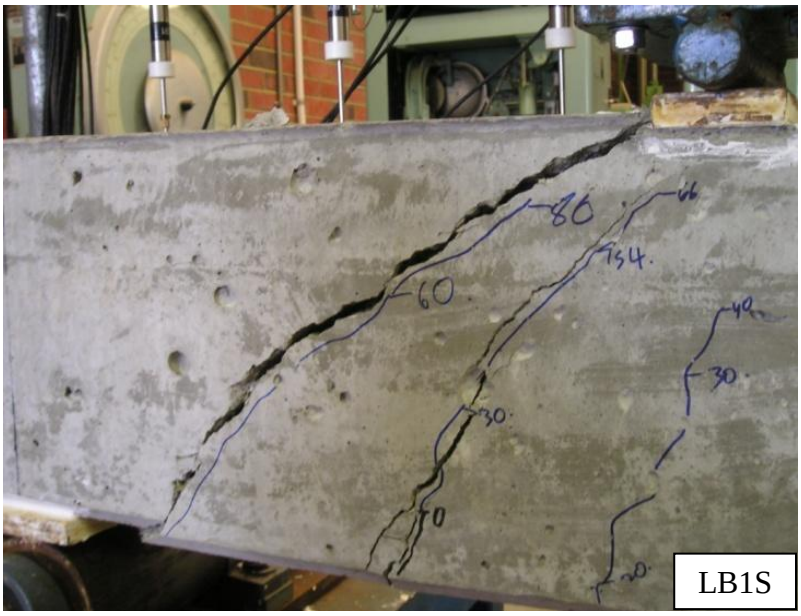

Figure 5.3b The crack formation at failure under shear test of LSRC beam

The loads versus deflections at the mid-span of the beams under shear are plotted in Figure 5.4**.**

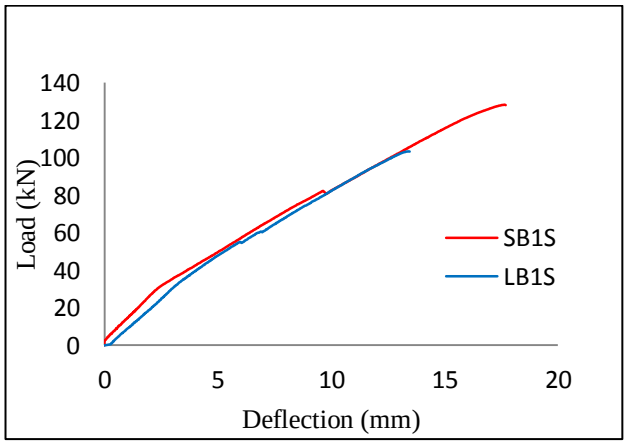

Figure 5.4 Load versus deflection for shear test

The load deflection behaviour of the beam which fail in shear shows the lost of stiffness for LB1S from the very beginning. In the linear area the stiffness difference is about 16.7%, however after the first cracking the stiffness difference between this two beams decreased to 2.9%. After the second cracking in the solid slab, the stiffness of the control beam become similar to the sandwich one.

After the test, it was of concern to determine whether the inclination of the critical shear crack was influenced by the position of the AAC blocks within the crack region. After the beam failed, the beam was cut using concrete saw to examine the

actual position of the blocks. It was found that the cracks propagated right through the blocks as if the section was monolithic. This behavior indicates good bonding between the concrete and the blocks.

Figure 5.5a Bond between the AAC blocks and the concrete

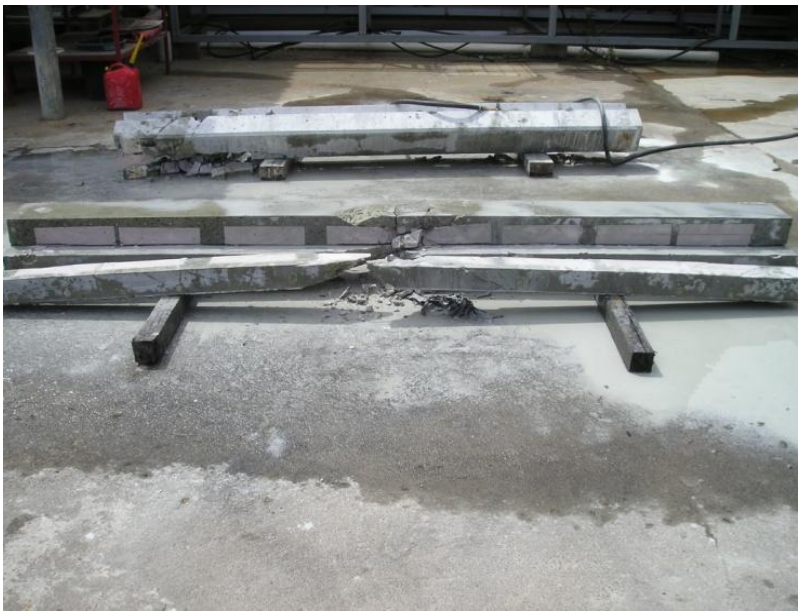

Figure 5.5b Location of AAC blocks within the sandwich section

5.3 Slabs

All slabs were tested both ends, described as Test 1 and Test 2 in Table 5.1. This type of experiment was adopted because of a limitation in the laboratory arrangement while preparing the slab samples.

The solid slab SS1 failed at 400 kN and 358 kN in the first and second tests, respectively. The lower capacity obtained in the Test 2 was as expected as there were some initial flexural cracks caused by Test 1 of the slab.

Table 5.1 Summary of the load results, unit in kN

Slab	Test	1st Flexural Crack	1st Shear Crack	2nd Shear Crack	Ultimate Load	Ultimate Shear
SS1	1	100	340	340	400	300
SS1	2	100	340	340	358	268
LS1	1	100	290	304	376	282
LS1	2	100	270	300	360	270
LS2	1	100	290	340	350	262
LS2	2	70	290	340	340	255
LS3	1	80	320	330	402	301
LS3	2	100	320	370	373	278

In both LS1 and LS2 slabs, the longitudinal reinforcement was the same, the only varying parameter between the two slabs was the amount of AAC blocks. LS1, which had more numbers of the blocks in it, failed unexpectedly at a slightly greater load than LS2 in both tests. The failure loads from Test 1 and Test 2 of LS1 are 376 kN and 360 kN, and of LS2 are 350 kN and 340 kN, respectively. These failure loads were from the combined loading from both jacks. These two jacks were loaded at the same rate so the reading from each jack showed the same number.

In slab LS3, the shape of the inserted AAC was altered by trimming of the four corners of the bricks in order to investigate the shape effect. The test results show that the failure loads of LS3 were almost equal to the failure loads of the solid slab. These results indicate that cutting off the four corners increased the resistance to shear of the tested LSRC slab. This finding deserves attention as it means that it is possible to develop an LSRC section that has the same flexural and shear strength as that of the solid section. The trade off for this is the less weight reduction of the slab. In order to increase the weight reduction, it is recommended that the shape of the AAC blocks infill can be altered only at the region where shear is known to be critical.

5.3.1 Mode of Failure

The stresses in a typical cross-section of a reinforced concrete member are the combination of longitudinal and shear stresses. When the member is subjected to

bending, transverse tensile cracks form when the tensile strength of the concrete is reached. Flexural tensile cracks occur as vertical lines, which are originated in the region where the bending moment is large and the shear small. The typical flexural crack patterns will be disturbed whenever there are changes in the member geometry and loading (Warner et al. 1998). Cracks that form in the region where both the bending moment and the shear force are significant are inclined cracks, which are called flexural-shear cracks. If shear becomes large in any region of the member, inclined tensile cracks form and can lead to a premature 'shear' failure. This type of cracks is referred to as web-shear cracks, or diagonal tension cracks. Formation of inclined cracks as well as post-cracking behaviour depends on the relative magnitudes of the bending moment and shear force. Sengupta and Menon (2009) describes five possible modes of shear failure, namely diagonal tension failure, shear compression failure, shear tension failure, web crushing failure and arch rib failure. In a previous investigation by Taylor (1974) into the contribution of each component in carrying shear in reinforced concrete beams, it was found that the compression zone carried 20-40%, aggregate interlock carried 33-50% and dowel action 15-25% of the shear.

All four slabs tested in this experiment have been designed to have a low span-to-depth ratio and adequate flexural reinforcement so that they fail in shear. Based on the test results, the slabs exhibited diagonal tension failure and shear compression failures. When the ultimate shear at failure was reaching, inclined crack propagated rapidly and there was crushing of the concrete at the compression edge of the slab above the tip of the inclined crack.

The main shear cracks appeared uniformly on both the left and right hand side of the slab at a loading when the first shear crack occurred. The crack then extended diagonally on both sides from the loading point to about 80 - 100 mm in front of the support point. The slab then continued to take slightly increased load and failed suddenly in a shear compression failure at the ultimate load. Shear crack is shown in Figure 5.6. In LS1 Test 2, a tensile splitting failure was observed within the shear span at the level of the top longitudinal reinforcement. The crack then extended along the level of the top reinforcement for about 400 mm before extending diagonally downwards above the support. This resulted in the spalling of the concrete above the top reinforcement when failure occurred as shown in Figure 5.7.

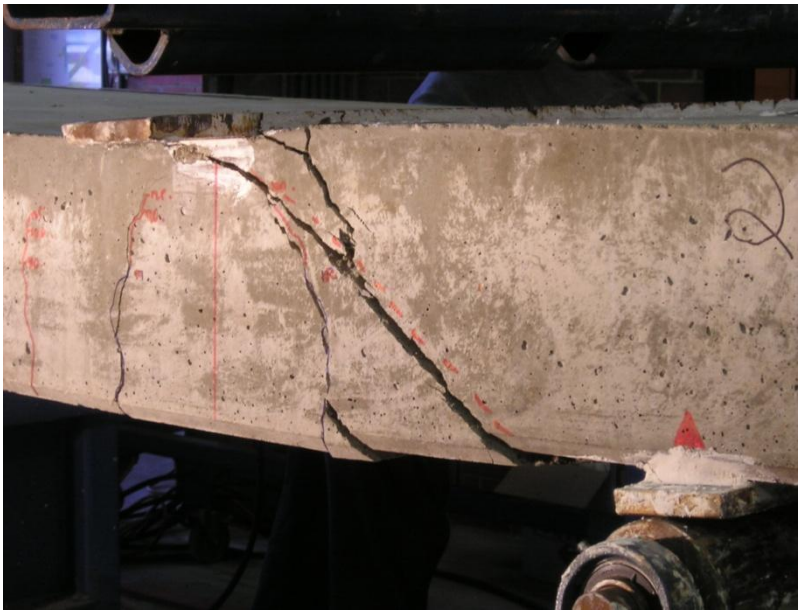

Figure 5.6 Typical shear compression failure

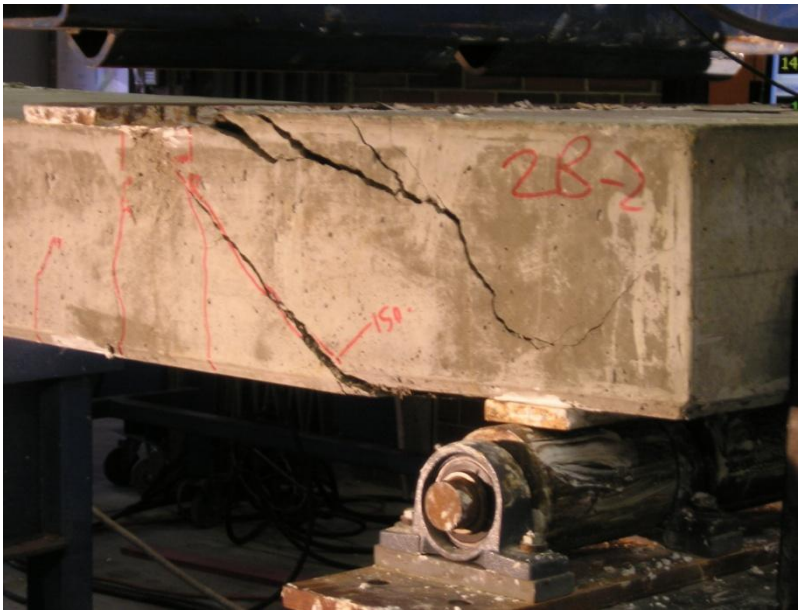

Figure 5.7 Spalling of the concrete above the top reinforcement

5.3.2 Load-Deflection Behaviour

The load versus deflection behaviours of all the tested slabs are plotted together in Figure 5.8 for comparison. The data from this graph was taken from the second test of the slabs. Due to the software related problems, there is no deflection information available for SS1 and LS3 test 1. The responses of all the slabs to the applied load were similar. The initial slope of the load-deflection relationship is constant until the

first flexural crack developed. After the initiation of the first crack, the slope of the graph becomes shallower with a decrease in the stiffness of the slab.

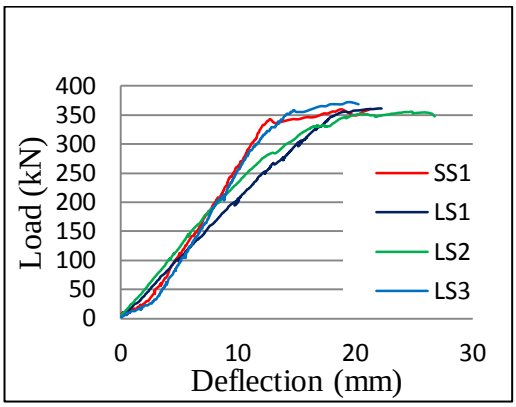

Figure 5.8 Load versus deflection of tested slabs

On closer examination of the failed sandwich slab, it can be seen that the primary shear crack went directly through the AAC blocks not around them, as shown in Figure 5.9. This shows the good bonding between concrete and the AAC blocks.

Figure 5.9 The shear crack passing through the AAC blocks

The next chapter will discuss the Finite Element Analysis with ANSYS. The load deflection relation of beams and slabs from the experimental investigation will be compared with modeled beams and slabs with ANSYS.

CHAPTER 6

NUMERICAL INVESTIGATION

6.1 Introduction

The finite element method is a very powerful tool for analyzing non linear behavior of concrete members without having to go to expensive and time consuming work in the laboratory. ANSYS 12.1 was employed to simulate the flexural and shear behaviour of the beam by finite element method as well as the shear behavior of slab element type

6.2 ANSYS Theory

The concrete was modeled with solid65, and a link8 element was used to model the steel reinforcement. By taking advantage of the symmetry of the beam layout, only half of the beam is being modeled. In case of slab, only half of the slab width (500 mm) was modeled.

The explanation about modeling the reinforced concrete with ANSYS for this study is discussed here.

6.2.1 Material Properties

a. Concrete

An eight-node solid element, solid65, was used to model the concrete. The solid element has eight nodes with three degrees of freedom at each node-translation in the nodal x, y and z directions. The element is capable of plastic deformation, cracking in three orthogonal directions, and crushing. The geometry and node locations for this element type are shown in Figure 6.1.

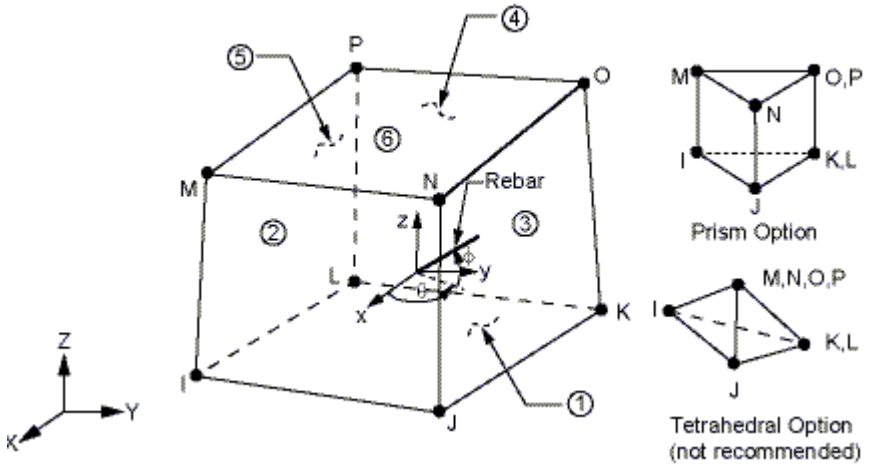

Figure 6.1 Solid65-3D reinforced concrete solid (ANSYS 12.1)

b. Steel Reinforcement

To model concrete reinforcing, there are two methods that can be followed. In the first method, the reinforcement is simulated as spar elements with geometric properties similar to the original reinforcement. The second idealization of steel reinforcement is the smeared concrete element method in which the concrete and the reinforcement are discretized into elements with the same geometrical boundaries. This study follows the first method.

A link element was used to model the steel reinforcement. Two nodes are required for this element. Each node has three degrees of freedom, - translation in the nodal x, y, and z directions. The element is also capable of plastic deformation. The geometry and node locations for this element type are shown in Figure 6.2

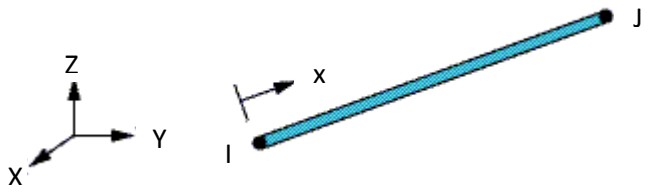

Figure 6.2 link8- 3D spar (ANSYS 12.1)

Failure criteria for concrete

The model is capable of predicting failure for concrete materials. Both cracking and crushing failure nodes are accounted for. The two input strength parameters i.e ultimate uniaxial tensile and compressive strength – are needed to define a failure surface for the concrete. Consequently, a criterion for failure of the concrete due to a multiaxial stress state can be calculated (William and Warnke 1975).

A three-dimensional failure surface for concrete is shown in Figure 6.3. The most significant nonzero principal stresses are in the x and y directions, represented by σ_{xp} and σ_{yp} respectively. Three failure surfaces are shown as projections on the σ_{xp} - σ_{yp} plane. The mode of failure is a function of the sign σ_{zp} (principal stress in the z direction). For example, if σ_{xp} and σ_{yp} are both negative (compressive) and σ_{zp} is slightly positive (tensile), cracking would be predicted in a direction perpendicular to σ_{zp}. However, if σ_{zp} is zero or slightly negative, the material is assumed to crush (ANSYS 12.1).

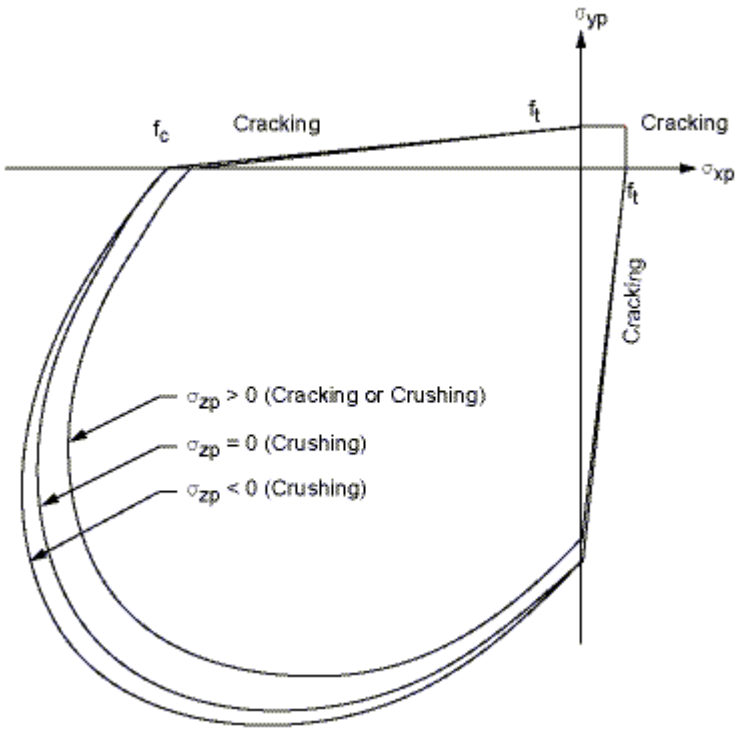

Figure 6.3 3-D failure surface for concrete (ANSYS 12.1)

6.2.2 Nonlinear Solution

In nonlinear analysis, the total load applied to a finite element model is divided into a series of load increments called load steps. At the completion of each incremental solution, the stiffness matrix of the model is adjusted to reflect nonlinear changes in structural stiffness before proceeding to the next load increment. The ANSYS uses the Newton-Raphson equilibrium iterations for updating the model stiffness.

In a concrete element, cracking occurs when the principal tensile stress in any direction lies outside the failure surface. After cracking, the elastic modulus of the concrete element is set to zero in the direction parallel to the principal tensile stress direction. Crushing occurs when all principal stresses are compressive and lie outside the failure surface; subsequently, the elastic modulus is set to zero in all directions (ANSYS 12.1) and the element effectively disappears.

A pure " compression" failure of concrete is unlikely. In a compression test, the specimen is subjected to a uniaxial compressive load. Secondary tensile strains induced by Poisson's effect occurs perpendicular to the load. Because concrete is relatively weak in tension, these actually cause cracking and the eventual failure (Mindess and Young 1981; Shah et al.1995). Barbosa and Ribeiro (1998), Kachlakef (2001) and Wolanski (2004) found that if the crushing capability of the concrete is turned on, the finite element beam models fail prematurely. Crushing of the concrete started to develop in elements located directly under the loads. Subsequently, adjacent concrete elements crushed within several load steps as well, significantly reducing the local stiffness. Finally, the model showed a large displacement, and the solution diverged. However ANSYS will generate the complete load deflection diagram when the crushing of concrete has been disabled. In this case failure of the model has been determined by yielding of reinforcing steel (Barbosa and Ribeiro 1998).

In this study, the crushing capability was turned off and cracking of the concrete controlled the failure of the finite element models.

6.3 Beam and Slab Modelling

6.3.1 Concrete Properties

For concrete, ANSYS requires an input data for material properties, which are Elastic modulus (E_c), ultimate uniaxial compressive strength (f_c'), ultimate uniaxial tensile strength, Poisson's ratio (ν), shear transfer coefficient (β_t). The value of f_c' used in this study was 43 MPa. The uniaxial tensile cracking stress was 3.4 MPa, which was calculated based on AS1012.10-2000. The modulus of elasticity of concrete was 32000 MPa which was determined in accordance with AS1012.17-1997. Poisson's ratio for concrete was assumed to be 0.2 for all the slabs. The modulus of elasticity for AAC was 8000 MPa, and f_c' = 3.5 MPa.

The shear transfer coefficient, β_t, represents the conditions of the crack face. The value of β_t, ranges from 0 to 1 with 0 representing a smooth crack (complete loss of shear transfer) and 1 representing a rough crack (i.e., no loss of shear transfer) as described in ANSYS. The value of β_t specified in this study was 0.4. Based on a study by Kachlakef et al (2001) convergence problem occurred when the shear transfer coefficient for the open crack was lower than 0.2. In the present case, after a number of trial and error by varying numbers of β_t, the value of 0.4 was chosen for this study. The shear transfer coefficient for a closed crack β_c was taken as 1.

The simplified stress-strain curve for concrete and AAC blocks for beams and slabs model is constructed from six points connected by straight lines by using simplified model by Kachlakef et al (2001) as shown in Figure 6.4 in which the numerical expression by Desayi and Krisnan (1964), Equations 6-1 and 6-2, were used along with Equation 6-3 (Gere and Timoshenko, 1997) to construct the uniaxial compressive stress-strain curve for concrete in this study.

$$f = \frac{\mathrm{E}_c \varepsilon}{1 + \left(\frac{\varepsilon}{\varepsilon_0}\right)^2} \qquad (6\text{-}1)$$

$$\varepsilon_o = \frac{2 f'_c}{\mathrm{E}_c} \qquad (6\text{-}2)$$

$$E_c = \frac{f}{\varepsilon} \qquad (6\text{-}3)$$

where f and ε are the stress and the corresponding strain, respectively. The strain at the ultimate compressive strength is denoted by ε_o. The compressive stress at 0.3 of the compressive strength was used as the first point of the multi-linear stress-strain curve.

In this study, an assumption was made of perfectly plastic behavior after point no 5 (Kachlakef et al 2001).

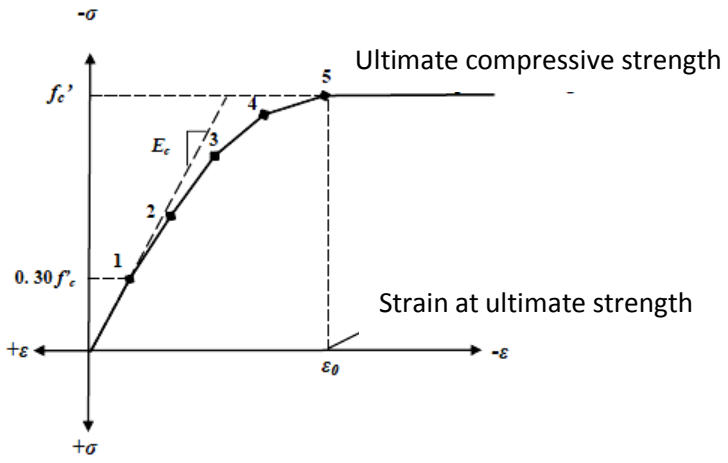

Figure 6.4 Simplified compressive uniaxial stress-strain curve for concrete (Kachlakef 2001)

Table 6.1 The stress strain for concrete

Strain	Stress (Pa)
0.000403125	12,000,000
0.000933680	26,660,000
0.001478400	36,317,800
0.002166000	41,314,400
0.002687500	43,000,000

Table 6.2 The stress strain for AAC blocks

Strain	Stress (Pa)
0.00013125	1,050,000
0.00030400	2,170,000
0.00048700	2,960,000
0.00065600	3,360,000
0.00087500	3,500,000

6.3.2 Steel Reinforcement

In the finite element models, steel bars were assumed to be made of an elastic-perfectly plastic material and the behaviour in tension and compression was identical. Poisson's ratio of 0.3 was used, and the elastic modulus, E_s = 200,000 MPa.

6.4 Comparison of Finite Element Analysis and Experimental Results

6.4.1 Beams

6.4.1.1 Beams Fail in Flexure

The load deflection characteristics from the finite element analysis (SB1F, LB1F and LB2F) are plotted to compare with the flexural test results in Figure 6.5a and 6.5b. All results show similar trend of the linear and nonlinear behavior of the beam. In the linear range, the load-deflection relation from the finite element analysis agrees well with the experimental results. After the first cracking, the finite element still follow the same stiffness as in the experimental one. However after the second cracking occurs in the finite element analysis the loss of stiffness can be clearly seen until it fail at same load as the experimental one. Based on these results, the concrete replacement by AAC blocks, as tested on LB1F and LB2F, has virtually no effect on the flexural strength of the section, which is as expected.

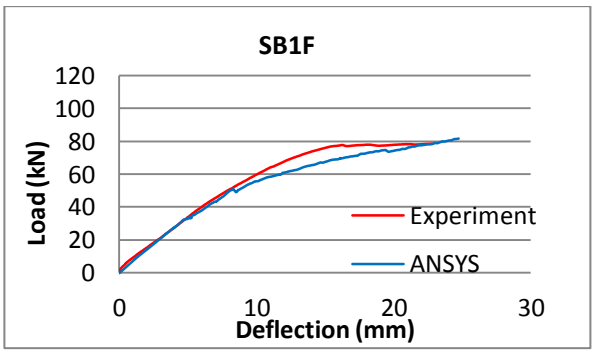

Figure 6.5a Load deflection relation of solid beam failed in flexure

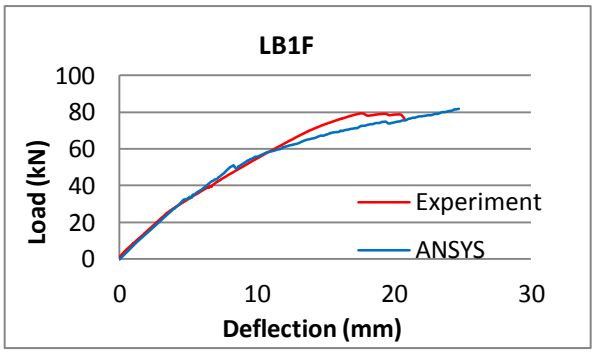

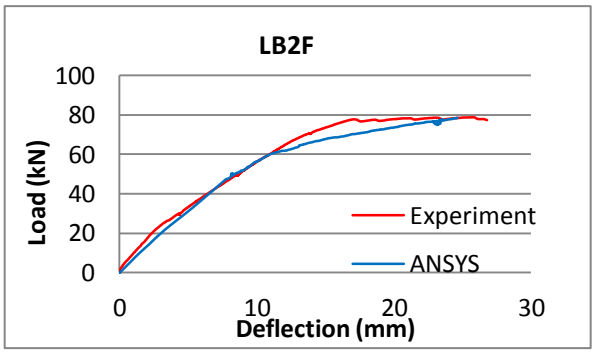

Figure 6.5b Load deflection relation of LSRC beams failed in flexure

6.4.1.2 Beams Fail in Shear

The typical finite element model of beams fail in shear are illustrated in Figure 6.6a and 6.6b.

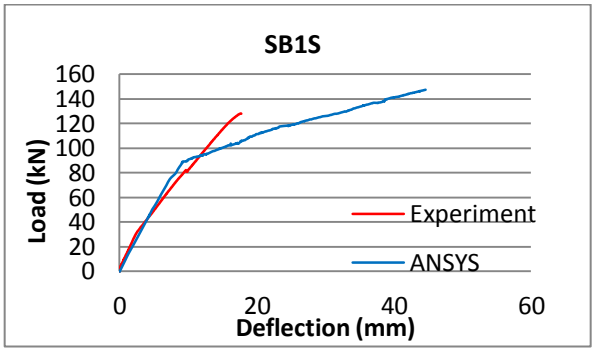

Figure 6.6a Load deflection relation of solid beam failed in shear

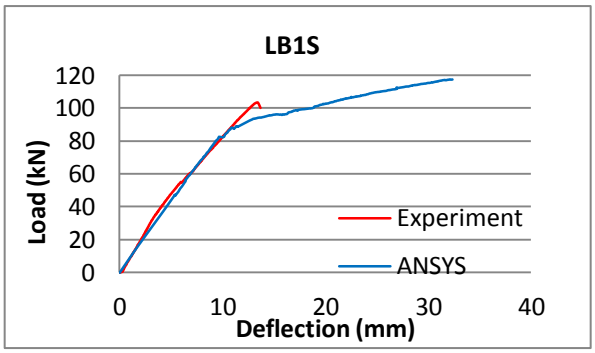

Figure 6.6b Load deflection relation of LSRC beams failed in shear

For beam failed in shear, generally ANSYS could capture the same trend of the load deflection behavior from the experimental data. The graph shows the stiffness in the linear range is nearly the same for both the ANSYS model and the equivalent beam. After the first crack occurred the beam incorporated AAC blocks keep maintain the same stiffness, however in the solid beam the ANSYS model overestimate the experimental data by 7.3%. The yielding steel occurs earlier in the finite element analysis resulting in loss of stiffness and the bigger deflection in comparison with the experimental one.

6.4.2 Slabs

Analyses were made of the developed numerical model for the solid slab and LSRC slabs. The experimental results plotted here were from the second test. It was not able to collect the deflection information for SS1 and LS3 test one, due to the software related problems.

The support condition was assumed as hinge-hinge. The four graphs show similar results in both linear and nonlinear behavior of the slabs. The typical finite element model of the slabs and the results at failure are illustrated in Figure 6.7, 6.8, 6.9, and 6.10.

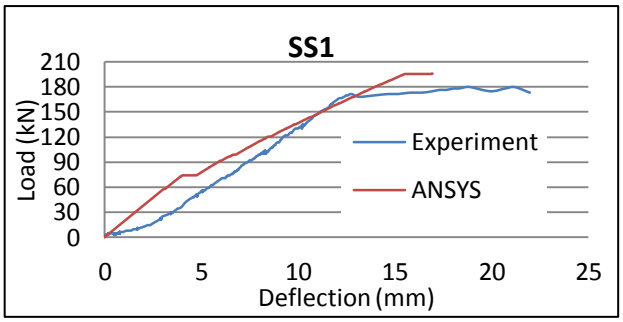

Figure 6.7 Load deflection relation of solid slab

Figure 6.7 shows that the finite element model is stiffer than the actual slab by 14.5% in the linear range. After the first cracking the stiffness of ANSYS model decrease. At the load of 150 kN the finite element model and the actual slab have almost the same stiffness. The yielding point for steel in the FEA model is higher than the experimental one by10%.

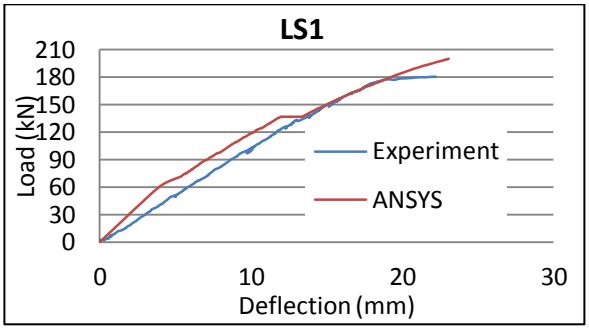

Figure 6.8 Load deflection relation of sandwich slab with full amount of AAC blocks

The load deflection of slabs incorporating the maximum amount of AAC blocks show the greater stiffness for the numerical model for about 13.2%. After the second cracking in ANSYS model, the graph shows the same stiffness with the experimental data.

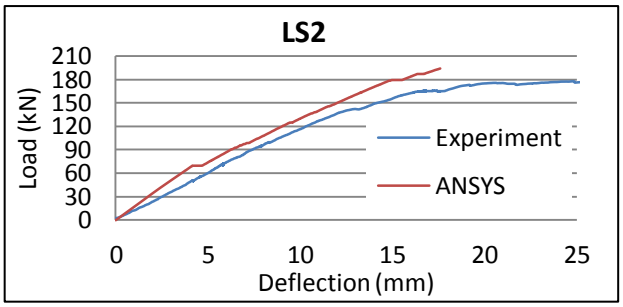

Figure 6.9 Load deflection relation of sandwich slab with half amount of AAC blocks

The finite element model is stiffer than the actual slab in the linear range by 9.16%. The first cracking load for finite element model is 71 kN which is higher than the load for the experimental one by 29.3%. After the first cracking it is evident that yielding of the steel reinforcement create the large deflection.

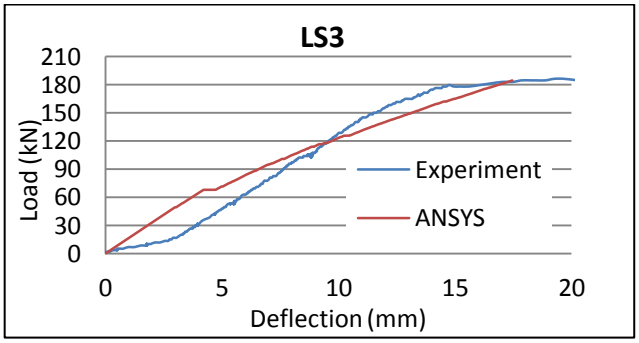

Figure 6.10 Load deflection relation of sandwich slab with curved AAC blocks

The Finite element model experience the stiffer stiffness in the linear range by 19.75%. After the first cracking the stiffness is decreasing but it is still higher than the experimental one. After the steel yielding the experimental one is stiffer than the FE model by 7.3%.

There are several factors that may cause the greater stiffness in the finite element models. The data plotted for the experimental one were from the second test. There might be crack inside the slab already due to the first test that reduce the stiffness of the slabs . Kachklakef et al. (2001) pointed out some factors that make higher stiffness in the Finite Element modeling due to the factors that have not been incorporated into the models such as drying shrinkage, and bond between the concrete and reinforcing steel.

CHAPTER 7

STRENGTH AND SERVICEABILITY OF LSRC BEAMS AND SLABS

7.1 Introduction

Strength and Serviceability requirements are two important parameters in designing reinforced concrete. Kara and Dundar (2009) pointed out that to ensure serviceability criterion is satisfied, it is necessary to accurately predict the cracking and deflection of reinforced concrete structures under service loads. For accurate determination of member deflection, the prediction of flexural and shear stiffness of members after cracking becomes important. Therefore, an analytical model which can include the effects of nonlinearity due to the concrete cracking on the flexural and shear stiffness of the members and accurately assess the deflection would be very useful. To ensure serviceability of LSRC beams and slab, this chapter will discuss the crack propagation of each specimen with finite element analysis, the stiffness of beams and deflection prediction by code. On the second part the flexure and shear behaviour of beams from the experimental results will be compared with the predictions based on the provisions from AS 3600 (2009) while the shear capacity of the slabs is also compared with other standards.

7.2 Crack Investigation

The output of ANSYS such as stresses and strains are calculated at integration points of the concrete solid element. The element stress direction is parallel to the element coordinate system. A cracking sign represented by a circle appears when a principle stress exceeds the ultimate tensile strength of the concrete. The cracking sign appears perpendicular to the direction of the principal stress as illustrated in Figure 7.1.

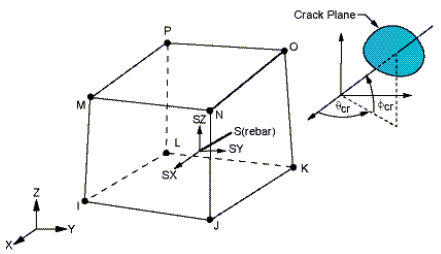

Figure 7.1 Concrete solid element stress output (ANSYS 12.1)

In the finite element analysis the load was applied on 11 nodes in the negative direction of y axis. The development of cracks for each beams and slabs is presented here and compared to failure photograph from experimental investigation.

7.2.1 Crack Development of Solid and LSRC Beams

1. SB1F

In the control beam which failed in flexure, the crack started to occur underneath the loading point at 32.895 kN load level. This flexural crack expanded as the load level increased. Figure 7.2a shows the crack propagation until load level 89.864 kN. The crushing capability of ANSYS was disabled to avoid premature fail of the model as appointed by Barbosa and Ribeiro (1998), Kachlakef (2001), and Wolanski (2004).

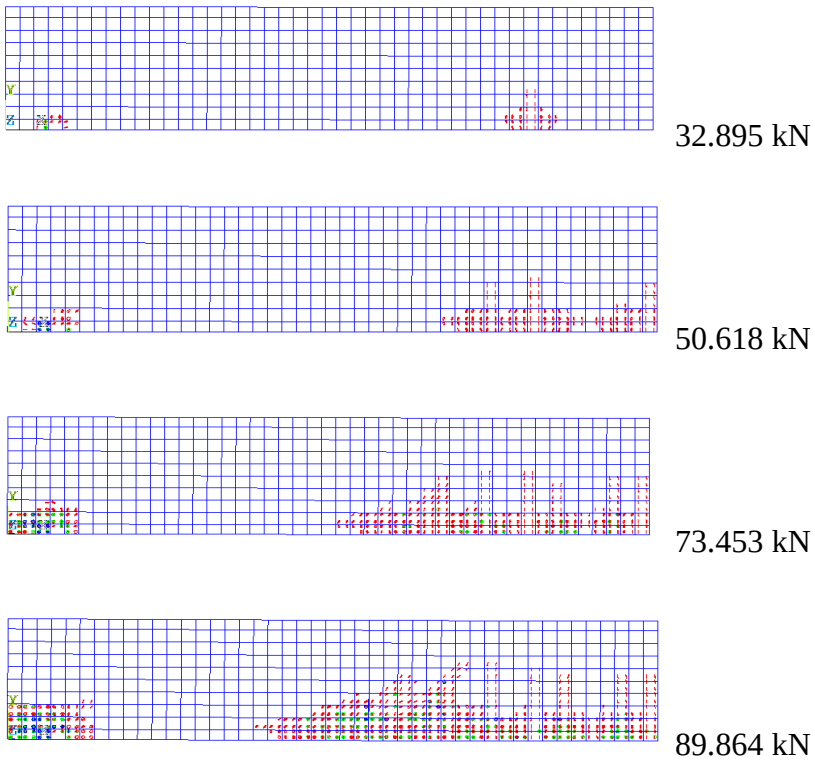

Figure 7.2a Crack propagation of SB1F from ANSYS

Figure 7.2b Crack propagation of SB1F from experiment

2. LB1F

The crack pattern of the beam contains maximum amount of AAC blocks is illustrated in Figure 7.3a. The flexural cracks started to occur at 32.167 kN. Figure 7.3a shows the crack pattern up to 76.784 kN load level. It is clear that the ANSYS model for LB1F shows more cracks compared to the SB1S. The crack of AAC blocks is noticeable in this model which related to the brittle failure in the actual beam.

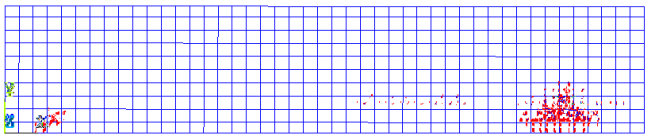

32.167 kN

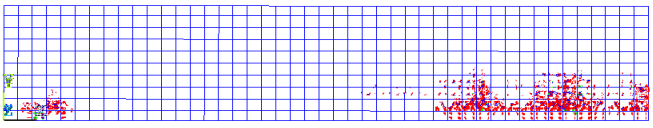

47.747 kN

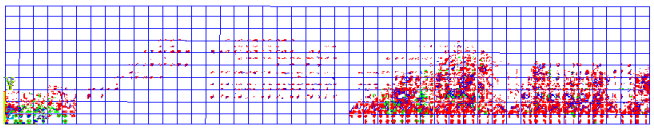

64.187 kN

Figure 7.3a Crack propagation of LB1F from ANSYS

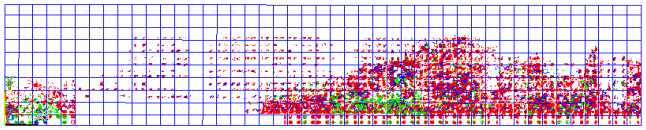

68.453 kN

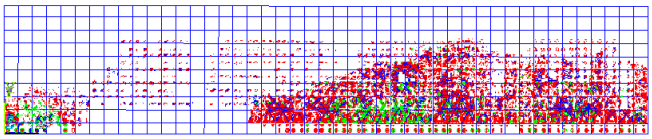

76.784 kN

Figure 7.3a (continued) Crack propagation of LB1F from ANSYS

Figure 7.3b Crack propagation of LB1F from experiment

3. LB2F

This beam contains half amount of AAC blocks. The flexural crack started to appear at the load level of 32.898 kN. The increasing load caused the crack propagation in the beam. Figure 7.4a shows the crack pattern of this beam up to 78.608 kN.

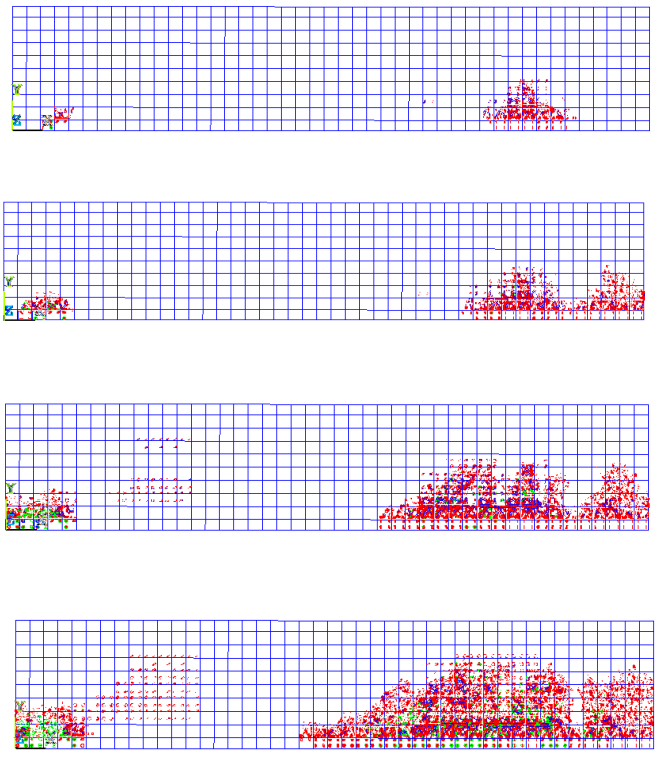

Figure 7.4a Crack propagation of LB2F from ANSYS

Figure 7.4 b Crack propagation of LB2F from experiment

The first flexural crack occurs on the solid and the LSRC beams were almost at the same load level (32 kN). This finding is just as expected. Before the first crack, the LSRC beams behave the same as the solid one. The crack patterns of these three beams are almost similar. The only different is, the LSRC beams have more cracks

compared to the equivalent solid beam due to the crack which also appear in the AAC blocks. The noticeable cracks of the AAC blocks in ANSYS model correlated to the brittle failure in the LSRC beams.

4. SB1S

The first flexural cracks appeared at 79.575 kN load level in the control beam which failed in shear. These cracks kept propagating with increasing load. The shear crack started to occur at 105kN at the same time with crack at the surface. The beam failed at the the load level of 141.779 kN. The crack propagation of SB1S is illustrated in Figure 7.5a.

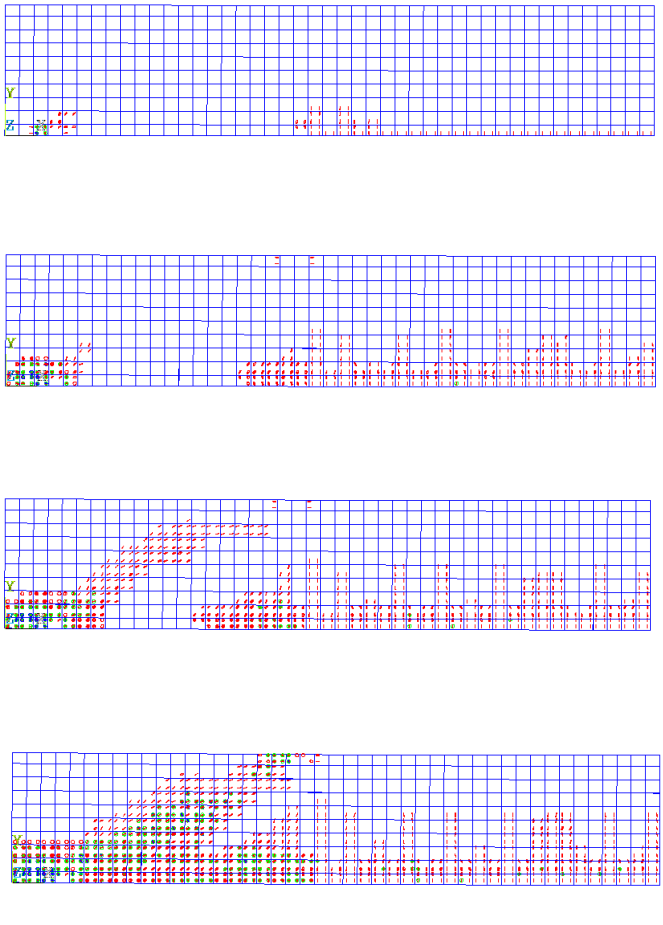

Figure 7.5a Crack propagation of SB1S from ANSYS

Figure 7.5b Crack propagation of SB1S from experiment

5. LB1S

The crack propagation of beam contains AAC blocks and designed to fail in shear is illustrated in Figure 7.6a. Small flexural cracks started to occur underneath the loading point at 76.322 kN. However it is obvious that crack started to happen at the section where AAC blocks available, just before the first flexural crack. The shear crack developed between the support and loading point until it failed at 125.379 kN

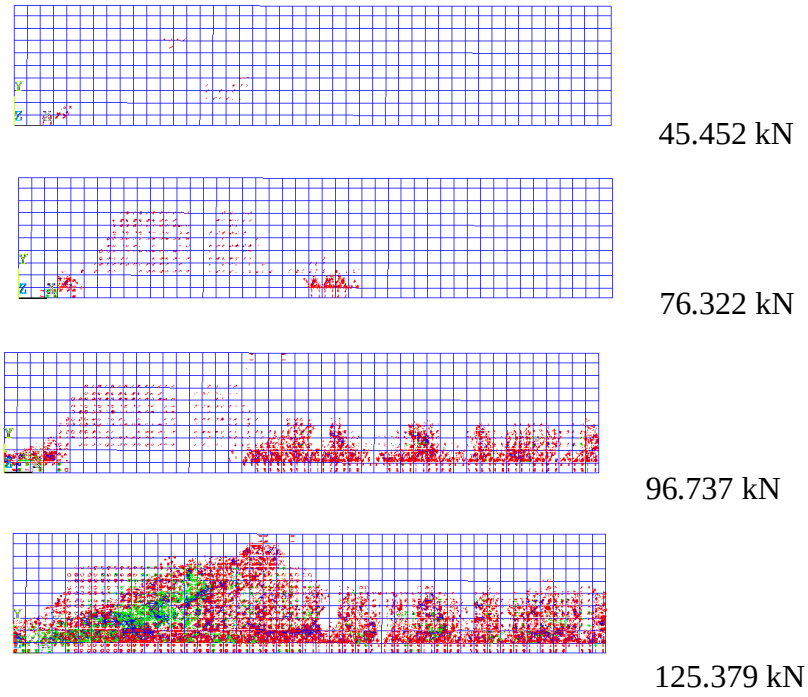

Figure 7.6a Crack propagation of LB1S from ANSYS

Figure 7.6b Crack propagation of LB1S from experiment

For beams tested in shear, the behaviors of the two tested beams were similar to the crack behavior in the experimental investigation. Small flexural cracks occurred first at the midspan region of the beam. Subsequently, the flexure cracks extended as flexure-shear cracks were developed between the support and the loading point. At the load approaching the failure load, critical web shears crack were developed diagonally within the shear span. The cracks continued to widen as the load increased, and failure occurred soon after depicting a typical sudden type of shear failure. The brittle failure of the LSRC beam failed in shear is related to the cracks in the AAC blocks.

7.2.2 Crack Development of Solid and LSRC Slab

1. SS1

The cracks started to occur underneath the loading point at 74 kN load level. This flexural crack expanded as the load level increased. At 121.03 kN, the first flexural crack propagated upward, and the shear crack started to occur at the loading point. These flexural and shear crack kept continuing along with the increasing load level. The flexural crack reached the surface at 188 kN and the slab failed suddenly at the maximum load where the shear crack reached the surface.

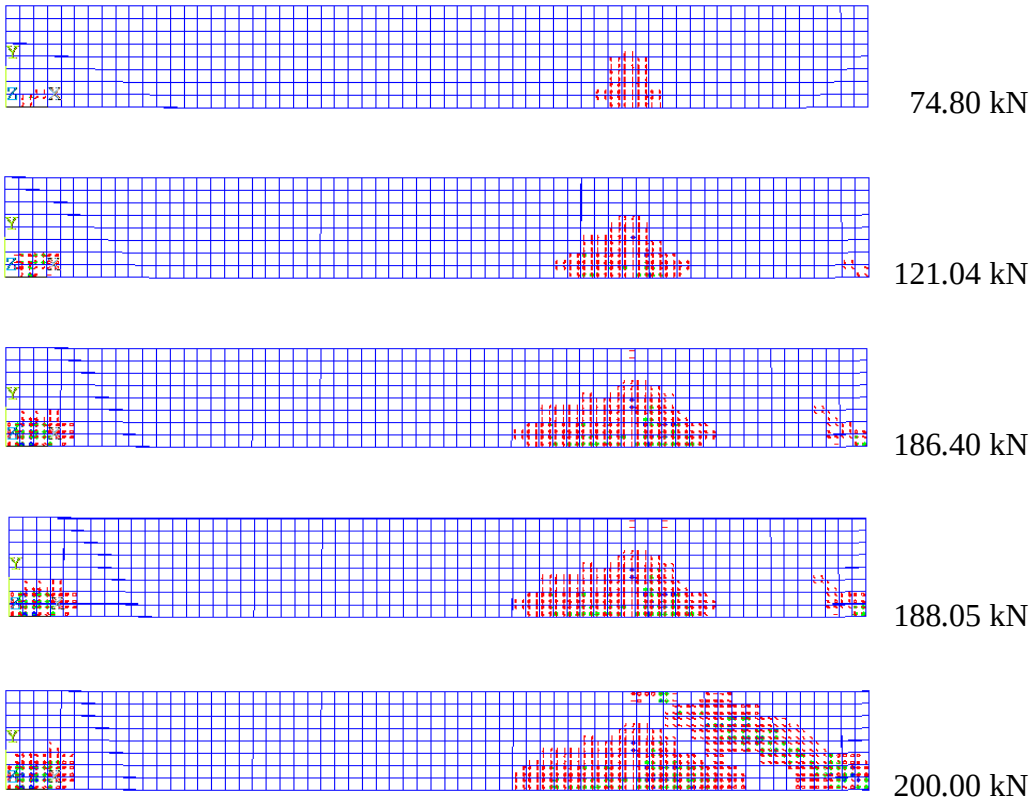

Figure 7.7a Crack propagation of SS1 from ANSYS

Figure 7.7b Crack propagation of SS1 from experiment

Figure 7.7b (continued) Crack propagation of SS1 from experiment

2. LS1

The crack at the AAC blocks which is located between support and loading point occurred at 62.06 kN. The first flexural crack was spotted at 71.37 kN load level which kept propagating with the increasing load. This slab failed at 163.5 kN.

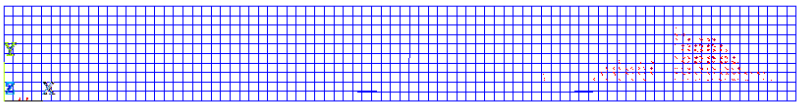

62.061 kN

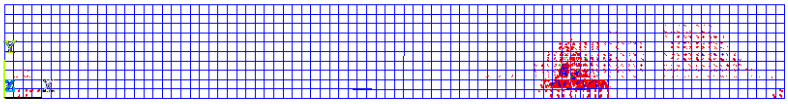

71.376 kN

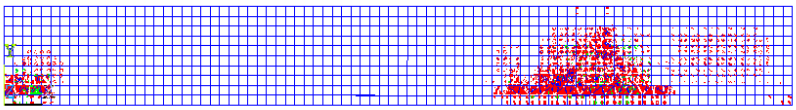

135.952 kN

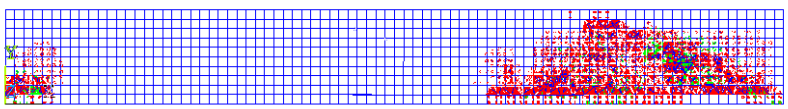

163.519 kN

Figure 7.8a Crack propagation of LS1 from ANSYS

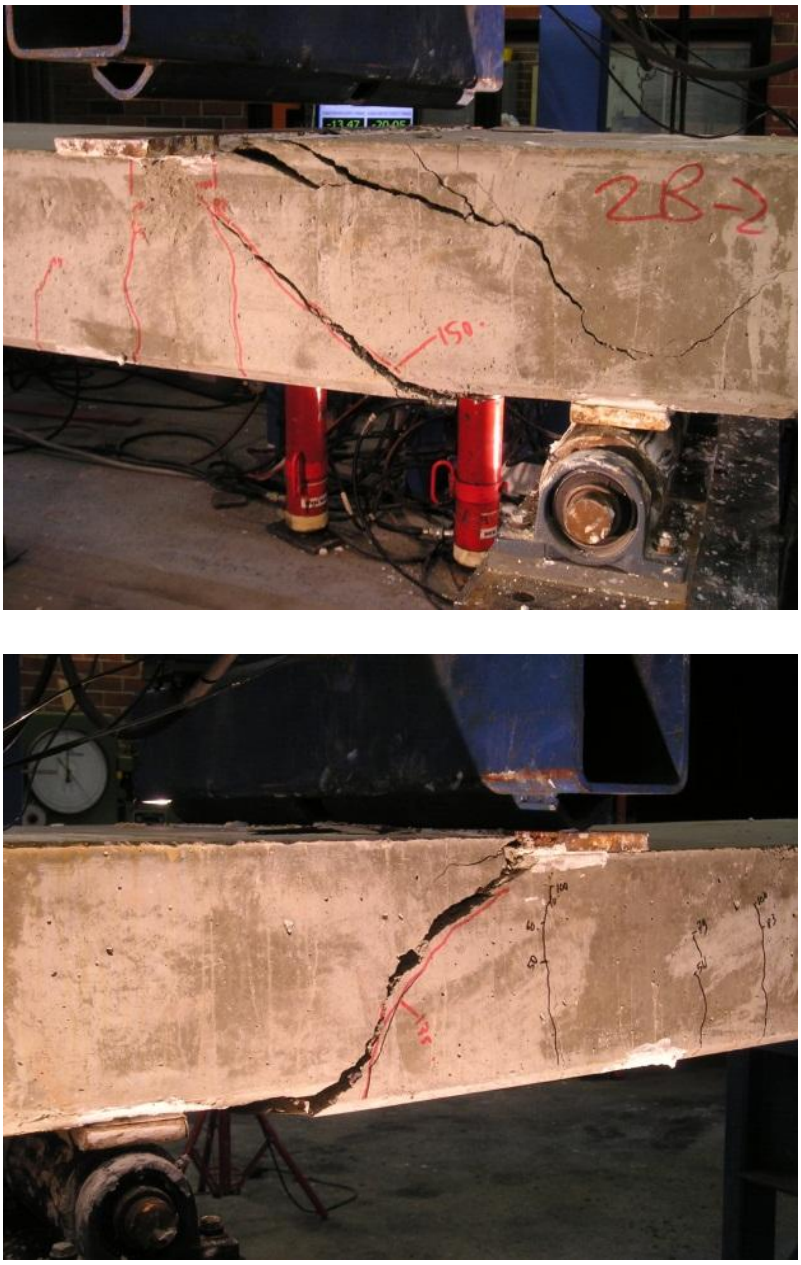

Figure 7.8b Crack propagation of LS1 from experiment

3. LS2

The first crack appeared at 63 kN where the AAC blocks available. At 71 kN the flexural crack started to happen. The cracks kept spreading along with the increasing of load level as illustrated in Figure 7.9a. The flexural crack in the surface occurred at 136 kN. The slab finally failed after the shear crack reached the surface at 194 kN.

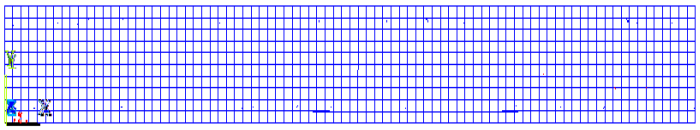

63.793 kN

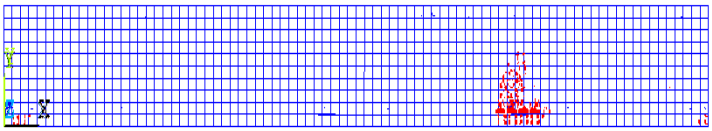

71.001 kN

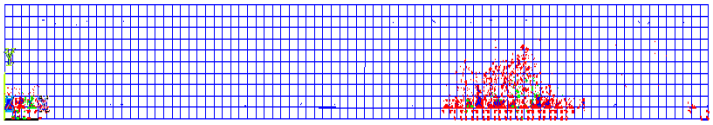

124.323 kN

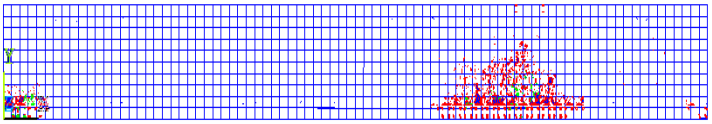

136.648 kN

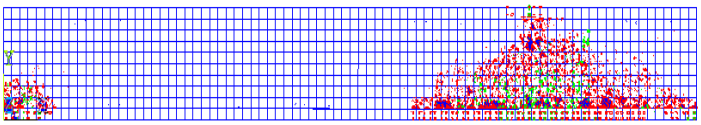

194.258 kN

Figure 7.9a Crack propagation of LS2 from ANSYS

Figure 7.9b Crack propagation of LS2 from experiment

4. LS3

The AAC blocks in the shear region started to crack at 56.228 kN. At 67.7 kN, the first flexural crack underneath the loading point started to occur, and the cracks kept propagating with the increasing load. The crack reached the surface at 136.61 and the beam failed at 184.178 kN.

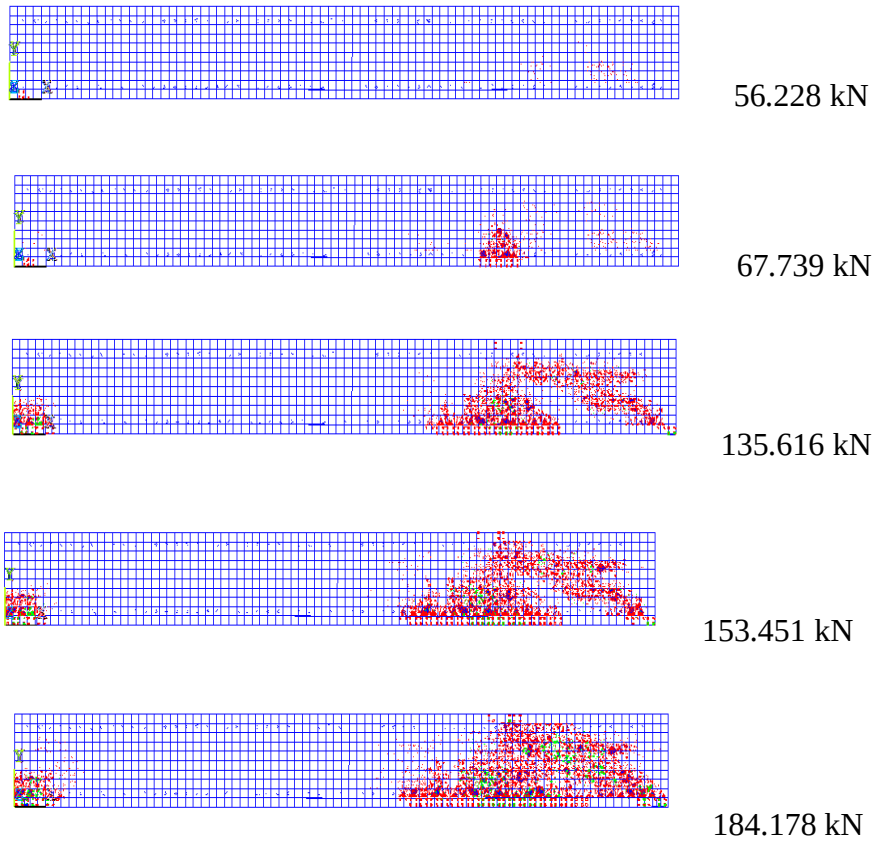

Figure 7.10a Crack propagation of LS3 from ANSYS

Figure 7.10b crack propagation of LS3 from experiment

Figure 7.10b (continued) Crack propagation of LS3 from experiment

In general, the first flexural cracks appear underneath the loading point. The crack start to propagate horizontally and vertically as the loading level increased. The shear crack reached the surface at the maximum load and the slab failed. It is obvious for the LWRC slabs, that the cracks started to occur in the lightweight concrete which is located at the shear region before the first flexural crack. The brittle failure was also noticeable in the LWRC slabs compared to the actual beam.

The crack propagation from ANSYS agrees quite well with the results from the experimental investigation.

7.3 The Stiffness Comparison Between Solid and Sandwich ection.

It is obvious that after the first crack the stiffness of sandwich section decrease because the lower EI of the combine materials. An attempt was made to compare between the sandwich sections with the hollow one, for beam failed in flexure by modeling it with ANSYS. It can be clearly seen that the stiffness decrease along with the decrease of the cross section of concrete. The graph for LSRC beam lay between the solid beam and the hollow one. The lower modulus of elasticity of AAC blocks influences the stiffness of the section.

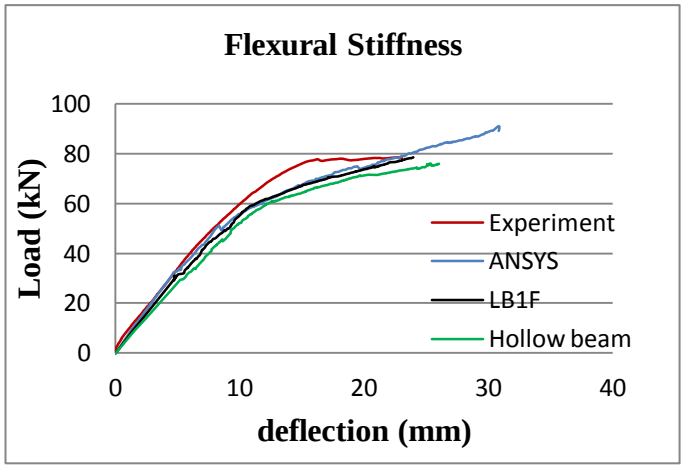

Figure 7.11 Load versus deflection showing the stiffness of beams

7.4 Correlation of Load-Deformation Behaviour with Predictions by Code.

The four point test was adapted in this study.

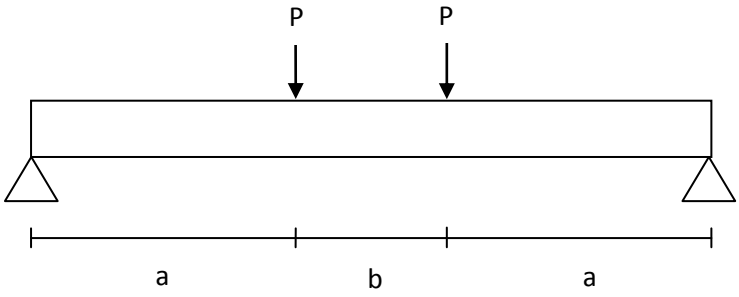

In order to predict the load-deformation behavior for beam, the following deflection at midspan equation was used: $\Delta = \frac{Pa}{24E_c I_{ef}}(3\ell^2 - 4a^2) + \frac{5w\ell^4}{384E_c I_{ef}}$ *(7-1)*

where

Δ = *Deflection at midspan (mm)*

P = *Load applied (N).*

E_c = *Modulus of elasticity of concrete (MPa).*

I_{ef} = *Effective second moment of area (mm^4).*

ℓ = *Distance between the two supports (mm).*

a = *Distance between the load to the nearest support (mm).*

w = *Uniformly distribution load.*

From the code, the formula to determine I_{ef} is given as follows in clause 8.5.3.1:

$$I_{ef} = I_{cr} + (I - I_{cr})(M_{cr} / M^*)^3 \leq I_{e.max} \quad (7\text{-}2)$$

where

I_{cr} = *second moment of area of cracked reinforced section.*

I = *second moment of area of the cross-section.*

M_{cr} = *bending moment causing cracking of the section.*

M^* = *the design bending moment.*

The second moment of are of cracked reinforced section can be determined using the formula derived from analysis by transformed section. The formula is as follows:

$$I_{cr} = \frac{1}{3} b d_n^3 + (n-1) A_{sc} (d_n - d_{sc})^2 + n A_{st} (d_{st} - d_n)^2 \quad (7\text{-}3)$$

where

A_{sc} = *the cross-sectional area of compressive reinforcement.*

d_{sc} = *the distance from the extreme compressive fibre of the concrete to the centroid of the compressive reinforcement.*

d_{st} = d_o

The moment in the midspan can be calculated by the equation (7-4)

$$M = \left(P + \frac{w\ell}{2} \right) \times \frac{\ell}{2} - \left(P \times \frac{b}{2} \right) - \left(\frac{1}{2} w \frac{\ell}{2}^2 \right) \quad (7\text{-}4)$$

The effective second moment of area (I_{ef}) of a reinforced concrete beam section after cracking has occurred lies in the range of:

$$I_{cr} < I_{ef} < I_g$$

The sectional stiffness varies according to the following condition:

- If $M < M_{cr}$, the stiffness is $E_c I_g$
- If $M \geq M_{cr}$, the stiffness is $E_c I_{ef}$

Table 7.1 shows the EI_{ef} values for the test beams. Equation (7-2) was used to determine the I_{ef} . The *M* and *Mcr* are derived from equation (7-4) by referring to the *Pu* and *Pcr* of the beam from the experimental investigation. For solid beam, *w* (uniformly distributed load) was calculated by multiplied the area of beam cross

section with density of concrete (2400 kg /m^3). For LSRC beam, the AAC cross section was multiplied by the AAC density (550 kg/m^3) and adds with the remaining concrete multiplied by its density. The Δ can be determined after knowing the value of $EI_{ef.}$

Once the crack occurs in concrete The EI_{ef} in the sandwich section will be influenced by the modulus of elasticity of both concrete and AAC blocks. In this study it is calculated based on the percentage of concrete and AAC blocks volume available in the sandwich section.

The difference of EI_{ef} of the solid beam to LSRC beams is about 4.5%. This hand calculation agrees well with the experimental results explained in chapter 5.

Table 7.1 Calculated EI values based on test results

Beam	Pcr (kN)	Pu (kN)	EI_{ef}	Δ mm	Δactual mm
SB1F	20.5450	76.8476	5.34E+12	15.41	15.449
LB1F	23.3207	79.4360	5.11E+12	16.90	17.603
SB1S	30.2527	128.2328	5.28E+12	16.12	17.661
LB1S	31.6404	103.4676	5.15E+12	14.21	13.439

7.5 Moment Curvature

The role played by the moment-curvature relation for a beam can be compared with the role of the stress-strain relation for a material in uniaxial stress. For a given cross section and given concrete strength, the shape of the moment-curvature relation is strongly affected by the area of the tensile steel present (Warner et al, 1998).

The moment curvature of solid beam and sandwich beam with maximum amount of AAC blocks is presented in Figure 7.12.

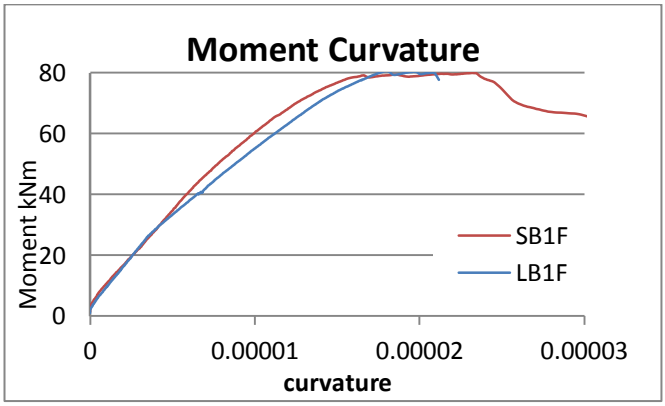

Figure 7.12 Moment Curvature diagram for SB1F and LB1F

The data for this graph is obtained from load and deflection of the experimental results. The moment of this graph was determined by using Equation (7-4). The curvature was determined from the parabola curvature:

$$\kappa = \frac{-8h}{L^2} \qquad (7\text{-}5)$$

where:

h = the deflection

L= the span length

7.6 Correlation of Test Results with Design Prediction

7.6.1 Beams

The test results on the failure loads of the beams are compared with the predicted values obtained from design equations based on Australian standard for concrete design AS3600 (2009).

The predicted flexural capacity was calculated from the solid beam section, which was equal to 82.7 kNm. Based on the test results of the maximum load at failure, the moment of the tested beams was 78.5, 78.6 and 78.9 kNm for solid, LB2F and LB1F, respectively. These results show good correlation with the ultimate design moment value, having only 5% difference. Based on these results, the concrete replacement by AAC blocks, as tested on LB1F and LB2F, has virtually no effect on the flexural strength of the section, which is as expected.

The predicted shear capacity obtained from the design calculation based on AS3600-2009 also shows good correlation with the LSRC beams. The design value of the shear capacity appears to be conservative for the solid beam. The test/predicted shear capacity ratios for the solid and LSRC beams were 1.27 and 1.01, respectively. Therefore, design adjustment needs to be made should the designer wish to maintain the same level of conservativeness in predicting the shear capacity of an LSRC beam, as that of an equivalent solid beam.

7.6.2 Slabs

As described in the previous section, there are a number of mechanisms that contribute to shear transfer in concrete. Opinions vary around the world on the relative importance of each of these mechanisms in the total shear resistance. As a result, various different models and formulas have been developed to predict the shear capacity of a reinforced concrete member with and without shear reinforcement.

Current concrete design codes provide empirical shear strength equations that are simple to use. The tested slabs were designed based on AS3600 (2009), the shear capacity was expected at 195 kN. A comparison with other design codes has been made. The predicted shear capacity of the slabs, which are governed by the flexural shear capacity, is equal to 245 kN and 147 kN based on ACI 318M-02 and Eurocode 2, respectively. Table 7.2 shows the ratio of the shear capacity between the test values and the design values based on the codes.

It is clearly evident from this table that all the codes conservatively estimate the shear capacity of the slabs. Both the Australian and USA design codes give the same value for the web shear capacity as this value is less than the flexural shear capacity. The design formulas for calculating the shear capacity of a solid slab can safely predict the shear capacity of an LSRC slab.

Table 7.2 Ratio between test results and predicted shear capacity

Slab	Test	AS3600	ACI318-02	Eurocode 2
SS1	1	1.54	1.22	2.04
SS1	2	1.37	1.09	1.82
LS1	1	1.45	1.15	1.92
LS1	2	1.38	1.10	1.84
LS2	1	1.34	1.07	1.79
LS2	2	1.30	1.04	1.73
LS3	1	1.54	1.23	2.05
LS3	2	1.43	1.14	1.90

CHAPTER 8

CONCLUSION AND RECOMMENDATION

8.1 Introduction

This chapter presents the conclusions of this research program as well as recommendations for future research. The research involved experimental and numerical programs to study the strength and deformation characteristics of reinforced concrete beams and slabs and compared them with those of the sandwich section. The objectives of the research were successfully achieved. The behaviour of solid and LSRC of beams and slabs were investigated. The FEA analysis with ANSYS was developed to predict the load deflection response as well as crack propagation of each specimen to ensure the serviceability of the structure.

8.2 Beams

A newly developed LSRC section has been proposed. LSRC beams under flexure and shear have been experimentally and numerically investigated. Based on the test and the numerical results, the following conclusions can be drawn:

1. Under the flexure test, there was insignificant difference of less than three percent in the flexural capacity between the solid beam and the beams filled with AAC blocks. The predicted load at failure matched very well with the failure loads obtained from all the tests. These results show that the proposed LSRC sections performed well under flexure.
2. The AAC block and the concrete show a good bonding. There were 43 mm gaps between the blocks in the LB1F and LB1S, and 10 mm gaps between AAC blocks with the reinforcement. These gaps will ensure the concrete move freely between the AAC blocks.
3. The results show that the flexural capacity of the two LSRC beams is actually higher than the solid beam. This is due to the selfweight reduction of the tested beam, which was about 9.5 - 19% of the equivalent solid beam. At failure load, the bending moments caused by the applied load and the selfweight of the solid

beam and of the LSRC beams, taken into account the weight reduction by AAC blocks infill, were almost equal in all the tested beams under flexure.

4. Based on the shear tests, the LSRC beam had lower shear capacity than the equivalent solid beam. The reduction of the shear capacity is 20%, which is quite significant in design. This result deserves more attention in order to determine the influence of the shear capacity in an LSRC beam.
5. The shear design provision of AS3600 (2009) is conservative. However, it is recommended that similar level of conservativeness should be maintained because the shear failure is sudden in nature.
6. Finite element model based on computer program ANSYS (12.1) has been developed to predict the behavior and strength of lightweight sandwich reinforced concrete beams. The model is verified against the experimental results. The result from Finite element analysis agrees quite well with the experimental one.
7. For beams failed in flexure, the similar trend of actual beam with ANSYS modeled beam is obvious. After the first cracking, the finite element model still follow the same stiffness as in the experimental one. However after the second cracking occurs in the finite element analysis the loss of stiffness can be clearly seen until it fails. Based on these results, the concrete replacement by AAC blocks, as tested on LB1F and LB2F, has virtually no effect on the flexural strength of the section, which is as expected.
8. For beams failed in shear, the graph shows the stiffness in the linear range are nearly the same for the ANSYS model and the experimental one. After the first crack occurred the beam incorporated AAC blocks keep maintain the same stiffness, however in the solid beam the ANSYS model overestimate the experimental data by 7.3%. The steel yield occur earlier in the finite element analysis resulting in loss of stiffness and the bigger deflection in comparison with the experimental one.
9. The crack propagation in ANSYS is also in good correlation to the laboratory results. ANSYS could predict the similar behavior of crack propagation in each beams specimen. The crack in AAC block correlated to the brittle failure of the sandwich beams.

8.3 Slabs

Experimental results of the strength and behaviour of LSRC slabs subjected to shear have been presented. Based on the results of the tested slab specimens, the following conclusions and recommendations can be drawn:

1. Solid slab and LSRC slabs, without shear reinforcement, exhibit similar behaviour under shear.
2. LSRC slabs generally have a reduced shear capacity when compared to a solid slab having identical height; however the difference is not significant when compared with the predicted shear capacity based on standard design codes.
3. In the tested slabs, varying the amount of AAC blocks did not have any impact on the shear capacity of the LSRC slabs. This result is inconclusive for general use. Further investigation is required to determine the consistency of this outcome and any factors that might be affecting the results. For instance, the ratio between the depth of the inserted AAC blocks to the overall depth of the solid section could be a factor contributing to the effect.
4. All the LSRC slabs demonstrated very brittle failure and failed mainly by shear compression. However, the inserted AAC blocks were found to bond very well to the concrete and the shear crack propagation through them suggested that they contribute to the overall shear capacity both in terms of their tensile strength and ability to carry shear through interface friction.
5. Post-cracking behaviour was observed and the slabs could sustain further load increment after shear crack was developed. This was due to the combined contribution of the uncracked concrete, dowel action of the longitudinal reinforcement and aggregate interlocking in the middle region of the section.
6. The shape of the inserted AAC blocks has a significant effect on the shear capacity. When the inserted AAC blocks have been altered in shape to have a more curved profile, the capacity of the tested LSRC slab with curved bricks is almost identical to the capacity of the solid slab.

7. The test results on the solid slab show that the predicted shear capacity of a reinforced concrete slab based on the selected design codes is quite conservative. The design formulas for calculating the shear capacity of a solid slab can safely predict the shear capacity of an LSRC slab.
8. The Finite element model experienced the stiffer stiffness in comparison with the actual slabs. This is because the data plotted for the actual beam were from the second tests. The crack which is already available in the slabs due to the first test will contribute to stiffness reduction of the slabs.

8.4 Recommendation for Further Research

1. Further investigation is required to determine the consistency of this outcome and any factors that might be affecting the results. For instance, the ratio between the depth of the inserted AAC blocks to the overall depth of the solid section could be a factor contributing to the effect.
2. The limitation of the present study are that the beam cross section and the reinforcement are kept constant so more work are needed to study the effect of varying these parameters.
3. The punching shear behavior should be investigated to determine if the current design concepts regarding punching shear in a solid slab are transferrable to an LSRC slabs.
4. Further investigation is required to test the impact of The LSRC beams and slabs under reversal loading. This test is important to determine whether the effective compression zone of the LSRC beams is sufficient to such loading. The blocks might not have much impact on the slab because the neutral axis of the section subjected to reversal loading could be well within the bottom reinforcement layer.

REFERENCES

Abbadi, A., Koutsawa, Y., Carmasol, A., Belouettar, S., Azari, Z. "Experimental and Numerical Characterization of Honeycomb Sandwich Composite Panels". *Simulation Modelling Practice and Theory*. 2009; 17, 1533-1547.

Ahmad, S.H., Xie, Y., and Yu, T. "Shear Strength of Reinforced Lightweight Concrete Beams of Normal and High Strength Concrete". Magazine of Concrete Research. 1994; vol 46, no 166.

Aldejohann,Markus.; Schnellenbach-Held, Martina. Investigation on the Shear Capacity of Biaxial Hollow Slabs –Test Results and Evaluation-, Darmstadt Concrete 18 .2003. http://www.darmstadt-concrete.de/2003/slabs.html

Al-Khaiat, H., and Haque, M,N. "Effect of initial curing on early strength and physical properties of a lightweight concrete". *Cement and Concrete Research*. . 1997; 28 (6) : 859-866.

Alnuaimi, A,S., Al-Jabri, K,S., Hago, A ."Comparison Between Solid And Hollow Reinforced Concrete Beams". *Materials and Structures* .2008; 41: 269-286.

ANSYS Theory Reference, version 12.1 .

ASCE-ACI Committee 445. "Recent approach to shear design of structural concrete". *Journal of Structural Engineering ASCE*.1998; 124 (12): 1375 -417.

AS1012.9. Method of testing concrete – Determination of the compressive strength of concrete specimens. *Standards Australia*. 1999.

AS1012.10. Method of testing concrete – Determination of indirect tensile strength of concrete cylinder (Brasil or splitting test). *Standards Australia*. 2000.

AS1012.17. Method of testing concrete – Determination of the static chord modulus of elasticity and Poisson's ratio of concrete. *Standards Australia*.1997.

AS3600. Committee BD-002, Concrete Structures. *Standards Australia*.2009.

AS3700. Committee BD-004. *Masonry Structures*. Standards Australia.2001.

Arnesen, A., Sørensen, S.I., Bergan, P.G .“ Nonlinear Analysis of Reinforced Concrete”. *Computers and Structures.* 1980; Vol 12, pp 571-579.

Autoclaved Cellular Concrete .2009. http://www.cement.org/basics/concreteproducts_acc.acp (accessed April 15th 2009).

Barbosa, A.F., Ribeiro ,G.O., “Analysis of Reinforced Concrete Structures Using ANSYS Nonlinear Concrete Model”. *Computational Mechanics*. 1998; pp.1-7.

Bažant, Z.P. and Kim, J.K. “Size effect in Shear Failure of Longitudinally Reinforced Beams”. *ACI Journal, Proceedings*.1984; 81(5), 456-468.

Bobrowski, J. “Outstanding Applications of Lightweight Concrete and an Appreciation of Likely Future Development”. *The International Journal of Lightweight Concrete*.1980; 2, 5-20.

BubbleDeck technology .2008. http://www.bubbledeck.com (accessed April 23rd 2009).

Bungey, J.H. & Madandoust, R, “Shear strength variation in lightweight concrete beams” *Cement & Concrete Composites*. 1994;vol. 16, pp. 49-55.

Büyükkaragöz, A.” Finite Element Analysis of the Beam Strengthened with Prefabricated Reinforced Concrete Plate” .*Scientific Research and Essay*. 2010; 5(6), 533-544.

Choi, K.K., Park, H.G. and Wight, J.K. “Unified Shear Strength Model for Reinforced Concrete Beams-Part I: Development”. *ACI Structural Journal*.2007; 104(2), 142-152.

Choi, K.K. and Park, H.G. “Unified Shear Strength Model for Reinforced Concrete Beams-Part II: Verification and Simplified Method”. *ACI Structural Journal*.2007; 104(2), 153-167.

Dahmani, L., Khennane, A., Kaci, S.” Crack Identification in Reinforced Concrete Beams Using ANSYS Software” *Strength of Material* 2010; 42(2).

Desayi, P. and Krishnan, S. "Equation for the Stress- Strain Curve of Concrete", *Journal of American Concrete Institute*.1964; 61, 345-350.

Ezeldin, A.S and Balaguru, P.N "Characterization of Bond Between Fiber Concrete and Reinforcing Bars Using Nonlinear Finite Element Analysis ".*Computers and Stuctures*.1990; Vol 37 no 4 pp 569 – 584.

Gere, J.M. and Timoshenko, S.P. *Mechanics of Materials*, PWS Publishing Company,Boston Massachusetts.1997.

Hearne, E.J., Brettell, R. and Bright, N.J. "The Behaviour of Autoclaved Aerated Concrete Blockwork Subjected to Concentrated Loading". *The International Journal of Lightweight Concrete*. 1980; 2, 49-55.

Hollowcore Floor Overview Report .2007. www.dbh.govt.nz/UserFiles/File/Publications/Building/Technical-reports/hollowcore-floor-overview-report.doc (accessed April 21st 2009).

Horler, D.B . "An Update of Lightweight Aggregate Production in UK" Proceeding 2nd International Congress on Lightweight Concrete, London, April 1980; pp 11-22.

Ibrahim, A.M., Mubarak H.M. " Finite Element Modeling of Continuous Reinforced Concrete Beam with External Pre-stressed". *European Journal of Scientific Research*. 2009; Vol 30 No1 pp 177-186.

Jones, M.R. & McCarthy, "A. Behaviour and assessment of foamed concrete for construction applications" In: Dhir RK, Newlands MD, McCarthy A, (eds.). *Use of foamed concrete in construction*, London: Thomas Telford. 2005;pp. 61–88.

Kachlakef, D., Miller, T.,Yim,S.,Chansawat, K.,Potisuk, T., *FE Modeling of Reinforced Concrete Structures Strengthened with FRP Laminates*, Final Report SPR 316. Oregon State University.2001,

Kara, Ilker Fatih., Dundar, Cengiz.," Effect of Loading Types and Reinforcement Ratio on an Effective Moment of Inertia and Deflection of a Reinforced Concrete Beam". *Advances in Engineering Software*. 2009; 40, 836-846.

Kayali, O., Haque, M.N. & Zhu, B, "Some characteristics of high strength fiber reinforced lightweight aggregate concrete", *Cement & Concrete Composites*.2003; vol. 25, pp. 207–213.

Kong, P.Y.L." *Shear Strength of High Performance Concrete Beams"*, PhD Thesis, Curtin University of Technology, Perth, Western Australia. 1996.

Lai, K.L., Ravindrarajah, R.Sri., Pasalich, W., Hall, " Deformation Behaviour of Reinforced Polystyrene Concrete Beam". 1996 http://services.eng.uts.edu.au/ (accessed July 5, 2009).

Lihua, XU.,Yin, CHI., Jie, SU., Dongtao, XIA." Nonlinear Finite Element Analysis of Steel Fiber Reinforced Concrete Deep Beams". *Wuhan University Journal of Natural Sciences*. 2008;13 (2), 201-206.

Manalo, A.C., Aravinthan, T., Karunasena, W. and Islam, M.M. "Flexural Behaviour of Structural Fibre Composite Sandwich Beams in Flatwise and Edgewise Positions". *Composite Structures*. 2010; 92, 984 – 995.

Manalo, A.C., Aravinthan, T., Karunasena, W. and Islam, M.M). "In-Plane Shear Behaviour of Fibre Composite Sandwich Beams Using Asymmetrical Beam Shear Test", *Construction and Building Materials*. 2010; 24, 1952-1960.

Marti, P. "Basic Tools of Reinforced Concrete Beam Design," *ACI Journal, Proceedings*. 1985; 82(1), 46-56.

Matthew, P.W. and Bennett, D.F.H. "Economic long span concrete floors", British Cement Association. 1990; 2-6.

Meidell, A. "Minimum Weight Design of Sandwich Beams With Honeycomb Core of Arbitrary Density".*Composites Part B: Engineering*. 2009; 40, 284-291.

Memon, N.A., Sumadi, S.R. and Ramli, M. "Ferrocement Encased Lightweight Aerated Concrete: A Novel Approach to Produce Sandwich Composite", *Materials Letters* .2007; 61, 4035-4038.

Mindess, S. and Young, J. F. "*Concrete"* Prentice-Hall, Inc., Englewood Cliffs, New Jersey, USA.1981.

Mirmiran, Amir., Zagers, Kenneth., Yuan, Wenqing."Nonlinear Finite Element Modeling of Concrete Confined by Fiber Composites", *Finite Element in Analysis and Design* .2000; 35 79-96.

Moulia, M. & Khelafi, H. "Strength of short composite rectangular hollow section columns filled with lightweight aggregate concrete". *Engineering Structures*. 2007; vol. 29, pp. 1791–1797.

Mounanga, P., Gbongbon, W.,Poullain, P., Turcry,P "Proportioning and characterization of lightweight concrete mixtures made with rigid polyurethane foam wastes" *Cement and Concrete Composites*.2008; 30, 806-814.

Mousa, M.A. and Uddin, N. "Experimental and Analytical Study of Carbon Fiber-Reinforced Polymer (FRP)/ Autoclaved Aerated Concrete (AAC) Sandwich Panel". *Engineering Structures*. 2009;31, 2337-2344.

Narayanan, N., Ramamurthy, K" Structure and Properties of Aerated Concrete : a Review" *Cement and Concrete Composites*. 2000;22, 321 – 329.

Ngo,D., and Scordelis, A.C." Finite Element Analysis of Reinforced Concrete Beams", *Journal of the American Concrete Institute*. 1967; 64 (3), pp.152-163.

Nie, Jianguo., Qin, Kai., Cai, C.S. "Seismic Behavior of connections composed of CFSSTCs and steel-concrete composite beams - finite element analysis",*Journal of Construction Steel Research* .2008; 64 680 -688.

Nilson A.H. " Nonlinear Analysis and Reinforced Concrete by the Finite Element Method" *ACI Journal*.1968 ;65 (9), pp.757-766.

Özcan, D.M.,Bayraktar, Alemdar., Şahin, Abdurrahman., Haktanir, Tefaruk., Türker Temel,"Experimental and Finite Element Analysis on the Steel Fiber – Reinforced Concrete (SFRC) Beams Ultimate Behavior" *Construction and Building Materials* . 2009; 23 1064-1077.

Padmarajaiah, S.K., Ramaswamy, A. " A Finite Element Assessment of Flexural Strength of Prestressed Concrete Beam with Fiber Reinforcement" *Cement and Concrete Composites*. May 2001; 24, 229-241.

Prestressed Hollow-core Concrete Slabs .2001. http://www.cma.org.za/UploadedMedia/CMA%20Prestress%20(Multi%20Purpose)2(1) (accessed April 20th 2009).

Ramamurthy, K., Kunhanandan Nambiar, E.K., Indu Siva Ranjani, G,"A classification of studies on properties of foam concrete". *Cement & Concrete Composites*. 2009; vol. 31, pp. 388–396.

Russo, A. and Zuccarello, B. "Experimental and Numerical Investigation of The Mechanical Behaviour of GFRP Sandwich Panels", *Composite Structures*. 2007; 81, 575-586.

Schnellenbach-Held, M. and Pfeffer, K). "Punching Behavior of Biaxial Hollow Slabs", *Cement and Concrete Composite*. 2002; 24, 551-556.

Schaumann, E., Vallee, T. and Keller, T. "Modeling of Direct Load Transmission in Lightweight Concrete-Core Sandwich Beams", *ACI Structural Journal*. 2009; 106, 435-445.

Sengupta, A. & Menon, D. "Analysis and design for shear and torsion", Prestressed Concrete Structures, Section 5.1, p 6, Available: http://nptel.iitm.ac.in/courses/IIT-MADRAS/PreStressed_Concrete_Structures/index.php. accessed 12 May 2009.

Shah, S. P., Swartz, S. E. and Ouyang, C." *Fracture Mechanics of Concrete"*, John Wiley & Sons, Inc. New York, USA. 1995.

Sumajouw, M.D.J, and Rangan, B.V. "Low-Calcium Fly Ash – Based Geopolymer Concrete: Reinforced Beams and Columns" Research Report GC3, Faculty of Engineering, Curtin University of Technology. Perth. 2006.

Taylor, H. "The Fundamental Behaviour of Reinforced Concrete Beams in Bending and Shear", *ACI Special Publication*. 1974; 42(1), 43-77.

Walraven, J. and Lehwalter, N. "Size Effect in Short Beams Loaded in Shear," *ACI Structural Journal*. 1994: 91(5), 585-593.

Warner, R.F., Rangan, B.V., Hall, A.S. and Faulkes, K.A." *Concrete Structures*" Longman, Melbourne, Australia. 1998.

William, K.J.and Warnke ,E.P. “Constitutive Model for the Triaxial Behavior of Concrete”, *Proceeding IABSE* 1975; 19 1-30.

Wolanski, A.J.” *Flexural Behaviour of Reinforced and Prestressed Concrete Beams Using Finite Element Analysis*” Master Thesis, Marquette University, Wisconsin, USA. 2004.

PUBLISHED PAPERS

Advances in Structural Engineering

Dr. Vanissorn Vimonsatit
Department of Civil Engineering
Curtin University
Western Australia
Australia

7 FEB 2012

Dear Dr. Vimonsatit,

Paper No. **11-1400**
Paper Title : **Shear Behavior of Lightweight Sandwich Reinforced Concrete Slabs**
Authors : **Ade S. Wahyuni, Vanissorn Vimonsatit and Hamid Nikraz**

Thank you very much for returning the final version of the above paper to us. The paper has been found to be satisfactory and has been accepted for publication. You will hear from the publisher regarding the proofs of your paper in due course.

Yours sincerely,

Dr. Jian-Guo Dai
Associate Editor
Advances in Structural Engineering

Modern Methods and Advances in Structural Engineering and Construction
Cheung, S. O., Yazdani, S., Ghafoori, N., and Singh, A. (eds.)
ISEC-6, Zürich, June 21–26, 2011

BEHAVIOR AND STRENGTH OF LIGHTWEIGHT SANDWICH REINFORCED CONCRETE BEAMS

VANISSORN VIMONSATIT[1], ADE WAHYUNI[2] and HAMID NIKRAZ[3]

[1]*Department of Civil Engineering, Curtin University*
GPO Box U 1987, Bentley, Perth, Australia.
E-mail: v.vimonsatit@curtin.edu.au
[2]*Department of Civil Engineering, Curtin University*
GPO Box U 1987, Bentley, Perth, Australia.
E-mail: ade.wahyuni@postgrad.curtin.edu.au
[3]*Department of Civil Engineering, Curtin University*
GPO Box U 1987, Bentley, Perth, Australia.
E-mail: h.nikraz@curtin.edu.au

A lightweight concrete section has been developed with a novel use of prefabricated autoclaved aerated concrete (AAC). This section, namely LSRC section, is a reinforced concrete section in which AAC bricks are used as infill material. An experimental investigation into the strength of LSRC beams has shown promising results under both flexural and shears tests. Based on the test results, the flexural capacity was found to be almost identical to the capacity of the equivalent solid beam, while the shear capacity was reduced. The shear strength reduction was as expected due to the reduction in the compressive strength of AAC infill material. This paper focuses on a numerical investigation into the behavior and strength of LSRC beams using ANSYS finite element method of analysis. A numerical model is developed and the analytical results are comparable with the experiment.

Keywords: lightweight concrete, composite section, sandwich section, ANSYS.

1 Introduction

A newly developed lightweight reinforced concrete (LSRC) section has been experimentally investigated (Vimonsatit et al. 2010). The section is made up of a reinforced concrete with lightweight block infill. LSRC section can be used either as beams or slabs. The developed LSRC members are suitable for large span construction due to the weight saving benefits and ease of construction. This paper focuses on a numerical investigation to predict the behavior and strength of LSRC beams. The primary intent of the paper is to develop a numerical model that can be used to further investigate the behavior of LSRC beams under different loading conditions and constraints.

Finite element method (FEM) is a powerful tool commonly used for analyzing a broad range of engineering problems in different environments. FEM is employed extensively in the analysis of solids and structures and of heat transfer and fluids. A nonlinear FEM computer program ANSYS has been widely used for academic research as well for solving practical problems.

Buyukkaragoz (2010) used ANSYS to study on the subject of strengthening the weaker part of the beam by bonding it with prefabricated reinforced concrete plate. Single load was applied in the middle of the beam. solid65 and link8 were employed to

model the reinforced concrete with discrete reinforcement, while solid46 was used for modeling the epoxy which is used to bond the prefabricated plate to the beam. The result from experiment in the laboratory is quite similar to the finite element finding.

Barbosa and Riberio (1998) used ANSYS to compare the nonlinear modeling of reinforced concrete members with discrete and smeared reinforcement. Two different modeling were made for the same beam. Concrete was defined with solid65. In the first model, link8 bar was used as discrete reinforcement element. In the second model, steel reinforcement was modeled as smeared concrete element, defined according to the volumetric proportions of steel and concrete. Each model was analyzed four times according to four different material models. Based on their analysis, the results of the load-displacement curves were very similar for both discrete and smeared reinforcement. The differences exhibited at the load greater than the service load when the effects of material modeling led to the difference in the nonlinear behavior and ultimate load capacity.

Ibrahim and Mubarak (2009) used ANSYS to predict the ultimate load and maximum deflection at mid-span of continuous concrete beams, which were pre-stressed using external tendons. This model accounts for the influence of the second-order effects in externally pre-stressed members. The results predicted by the model were in good agreement with experimental data.

Padmarajaiah and Ramaswamy (2001) investigated the prestressed concrete with fiber reinforcement. They used COMBIN14 (spring) elements to model the interface behavior between the concrete and reinforcement. They found that the crack pattern predicted by ANSYS is in close agreement with the experimental results. Dahmani et al (2010), found that discrete reinforcement approach give better results than the smeared one. Kachlakev et al., (2001) studied beams externally strengthened with reinforced plastic carbon fiber (CFRC) with no stirrups being used in the experiment.

In the present study, ANSYS version 12.1 is employed for the numerically modeling of the LSRC beam because of its proven useful 3-D reinforced concrete element provided in the element library. In the following sections, beam details used in the experiment will be briefly described, followed by the description of the developed finite element modeling of concrete and steel reinforcement. The analytical results will be presented to compare with the experimental results. Some similarities and differences will be highlighted for the future improvement of the proposed numerical model.

2 Beam Details

The tested beam had a rectangular cross section, with a constant width and depth of 200 mm by 300 mm. The beam length was 3000 mm, with 2800 mm clear span when set up. Five beams were manufactured for two series of four-point test – the flexural test and the shear test. The distance between the two point loads was 800 mm and 1680 mm for the flexural and shears tests, respectively. The flexural test was to compare the flexural strength of solid beam and LSRC beams. Three beams were prepared, one solid (SB1F) and two with AAC blocks (LB1F and LB2F). In the shear test, two beams were prepared, one solid (SB1S) and one with AAC blocks (LB1S). The standard dimensions of the AAC blocks used were 180 mm x 75 mm x 300 mm. Figure 1 shows a typical LSRC beam with AAC blocks infill.

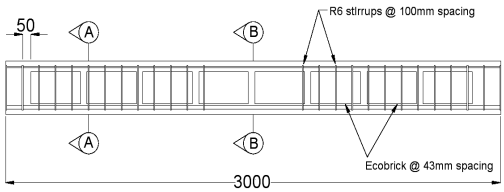

Figure 1. LSRC beam and section

3 Finite Element Model

The concrete was modeled with solid65, which has eight nodes with three degrees of freedom at each node, i.e., translation in the nodal x, y, and z directions. The element is capable of plastic deformation, cracking in three orthogonal directions, and crushing.

A link8 element was used to model the steel reinforcement. This element is also capable of plastic deformation. Two nodes are required for this element which has three degree of freedom, as in the case of the concrete element. Discrete method was applied in the modeling of the reinforcement and stirrups used in the tested specimen. The two elements were connecting at the adjacent nodes of the concrete solid element, such that the two materials shared the same nodes. By taking advantage of the symmetry of the beam layout, only half of the beam in longitudinal direction has been modeled in the finite element analysis.

3.1 *Concrete*

For concrete, ANSYS requires an input data for material properties, which are Elastic modulus (E_c), ultimate uniaxial compressive strength (f_c'), ultimate uniaxial tensile strength (modulus of rupture, f_r), Poisson's ratio (ν), shear transfer coefficient (β_t). The modulus of elasticity of concrete was 26500 MPa which was determined in accordance with AS 1012.17 (1997). Poisson's ratio for concrete was assumed to be 0.2 for all the beams.

The shear transfer coefficient, β_t, represents the conditions of the crack face. The value of β_t, ranges from 0 to 1 with 0 representing a smooth crack (complete loss of shear transfer) and 1 representing a rough crack (i.e., no loss of shear transfer) as described in ANSYS. The value of β_t specified in this study is 0.2, which is recommended as the lower limit to avoid having convergence problems (Dahmani et al 2010).

The numerical expressions by Desayi and Krisnan (1964), Eqs. (1) and (2), were used along with Eq. (3) (Gere and Timoshenko 1997) to construct the multi-linear isotropic stress-strain curve for concrete in this study.

$$f = \frac{E_c \varepsilon}{1 + (\frac{\varepsilon}{\varepsilon_0})^2} \quad (1)$$

$$\varepsilon_0 = \frac{2 f_c'}{E_c} \quad (2)$$

$$E = \frac{f}{\varepsilon} \quad (3)$$

where :

f = stress at any strain ε
ε = strain at stress f
ε_o = strain at the ultimate compressive strength f_c'

The concrete used was grade 40, having the compressive strength of 43.3 MPa at 28 days. The strength value of AAC blocks used in the model was 3.5 MPa. The compressive stress at 0.3 of the compressive strength was used as the first point of the multi-linear stress-strain curve.

The crushing capability of the concrete was turned off to avoid any premature failure (Barbosa and Riberio 1998).

3.2 *Steel Reinforcement*

All beams were provided with top and bottom longitudinal bars, N20 bars were used as the bottom steel in all beams with tensile strength at yield was 560 MPa while the yield strength of R-bars which was used as the top bar and the stirrup was 300 MPa.

The steel for the finite element models was assumed to be an elastic-perfectly plastic

material and identical in tension and compression. Poisson ratio of 0.3 was used for the steel. Elastic modulus, E_s = 200,000 MPa.

4. Results and Discussion

The typical finite element model of the beam and the result at failure are illustrated in Figure 2.

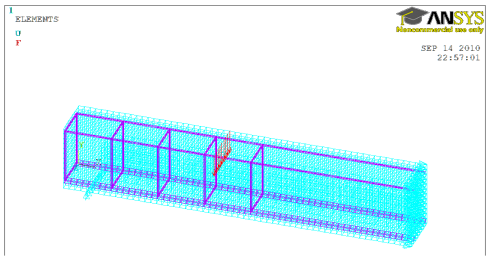

(a)Beam and reinforcement

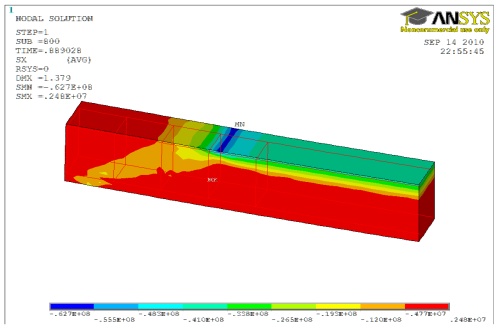

(b) Stress contour at shear failure

Figure 2. FEM model of LSRC beam and results

The load deflection characteristics from the finite element analysis (SB1F, LB1F and LB2F) are plotted to compare with the flexural test results in Figure 3. All results show similar trend of the linear and nonlinear behavior of the beam. In the linear range, the load-deflection relation from the finite element analysis agrees well with the experimental results when the applied load is below 40kN. After the first cracking, the finite element model shows greater stiffness than the tested beam. The final load for the model is also greater than the ultimate load of the actual beam by 16%. Based on these results, the concrete replacement by AAC blocks, as tested on LB1F and LB2F, has virtually no effect on the flexural strength of the section, which is as expected.

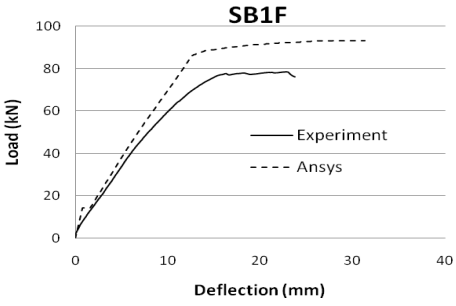

(a) Solid beam

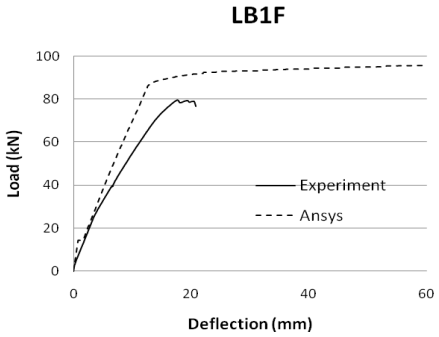

(b) Beam with maximum AAC blocks

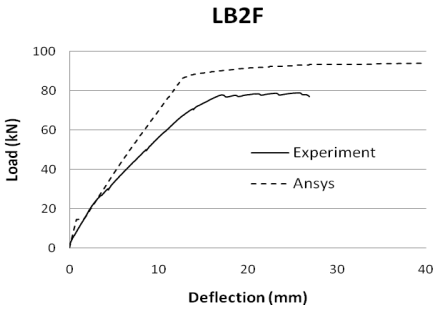

(c) Beam with half number of AAC blocks

Figure 3. Load deflection relation of beams failed in flexure: (a) solid beam, (b) beam with maximum AAC blocks, (c) beam with half number of AAC blocks

Under the shear (SB1S and LB1S), the results also show the similar trend between the experiment and the numerical results, as shown in Figure 4. The shear strength reduction was as expected due to the reduction in the compressive strength of AAC infill material. The comparison of analytical and experimental results is reported in Table 1.

There are several factors that may cause the greater stiffness in the finite element models. Microcracks produced by drying shrinkage and handling are present in the concrete to some degree. These would reduce the stiffness of the actual beams, however, the finite element models do not include micro cracks during the analysis.

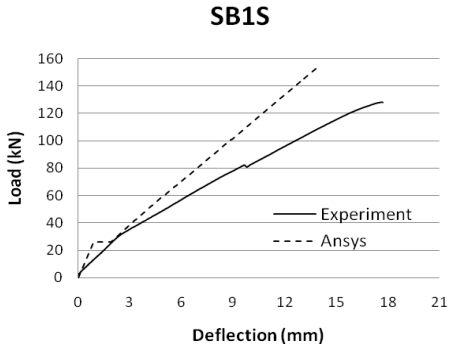

(a) Solid beam

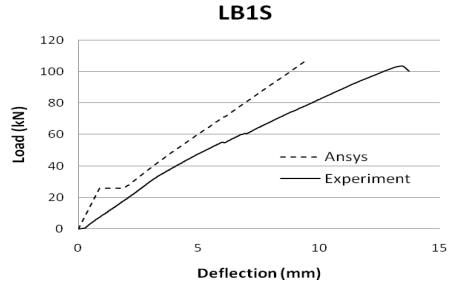

(b) Beam with maximum AAC blocks

Figure 4. Load deflection relation of beams failed in shear: (a) solid beam, (b) beam with maximum AAC blocks

Table 1. Load at failure from the experiment and numerical results.

Specimen	Ultimate load		
	Experiment (kN)	FEM (kN)	Ratio
SB1F	78.5	93.1	1.18
LB1F	78.9	94.0	1.19
LB1F	78.0	93.9	1.20
SB1S	128.2	153.0	1.19
LB1S	103.5	107.6	1.04

Perfect bond between the concrete and reinforcing steel elements was assumed in the finite element analysis but the assumption would not be true for the actual beams. As bond slip occurs, the composite action between the concrete and steel reinforcing is lost. Thus, as also pointed out by (Kachklakef et al. 2001), the overall stiffness of the actual beams could be lower than what the finite element models would predict, due to the factors that have not been incorporated into the models.

5. Conclusion

Finite element model based on computer program ANSYS (12.1) has been developed to predict the behavior and strength of lightweight sandwich reinforced concrete beams. The model is verified against the experimental results. Based on the presented investigation, the developed model compares well in the low loading range. In the high loading range the model is less conservative. The model and the analysis method can be further improved by incorporating the factors affecting the stiffness and the nonlinear behavior of the beam such as micro cracking and bonding between the concrete and the steel. A simple adjustment can be made to the value of the modulus of elasticity in the analysis based on an empirical-based technique. Further investigations are required

to investigate the consistency of the results and the factors affecting the results.

Based on the developed FEM model, the behavior and strength of the newly developed LSRC beams under different load patterns and support constraints can be further predicted. This investigation is necessary as the first step for interested practitioners to gain an understanding of LSRC performance and its use as an alternative lightweight concrete option.

Reference

ANSYS *Theory Reference*, version 12.1, Swanson Analysis System, available at Curtin University, 2010.

Bangash, M.Y.H., *Concrete and Concrete Structures: Numerical Modeling and Applications*, Elsevier Science Publishers Ltd, London, 1989.

Barbosa, A.F., Ribeiro ,G.O., Analysis of Reinforced Concrete Structures Using ANSYS Nonlinear Concrete Model, *Computational Mechanics*, pp.1-7, 1998.

Büyükkaragöz, A., Finite Element Analysis of the Beam Strengthened with Prefabricated Reinforced Concrete Plate, *Scientific Research and Essay*, 5(6), 533-544, 2010.

Dahmani, L., Khennane, A., Kaci, S .,Crack Identification in Reinforced Concrete Beams Using ANSYS Software, *Strength of Material*, 42(2), 2010.

Desayi, P and Krishnan, S., Equation for the Stress-Strain Curve of Concrete, *Journal of American Concrete Institute*, 61, 345-350, 1964.

Gere, J.M. and Timoshenko, S.P., Mechanics of Materials, PWS Publishing Company,Boston Massachusetts, 1997

Ibrahim, AM., Mubarak, HM., Finite Element Modeling of Continuous Reinforced Concrete Beam with External Pre-stressed, European *Journal of Scientific Research*, 30 (1), 177-186, 2009.

Kachlakef, D., Miller, T, Yim, S., Chansawat, K., and Potisuk, T., FE Modeling of Reinforced Concrete Structures Strengthened with FRP Laminates, *Final Report SPR 316*. Oregon State University, 2001.

Padmarajaiah, S.K., Ramaswamy, A., A Finite Element Assessment of Flexural Strength of Prestressed Concrete Beam with Fiber Reinforcement, *Cement and Concrete Composites*, 24, 229-241, May 2001

Vimonsatit, V., Wahyuni, A.S., Mazlan, M.A., and Nikraz, H., Use of Lightweight Concrete as Infill of Reinforced Concrete Sections, Proceedings, *ACMSM 21*, December 7-10, 2010.

Modern Methods and Advances in Structural Engineering and Construction
Cheung, S. O., Yazdani, S., Ghafoori, N., and Singh, A. (eds.)
ISEC-6, Zürich, June 21–26, 2011

SHEAR BEHAVIOR OF LIGHTWEIGHT SANDWICH REINFORCED CONCRETE SLABS

VANISSORN VIMONSATIT[1], ADE S WAHYUNI[2] and HAMID NIKRAZ[3]

[1]*Department of Civil Engineering, Curtin University*
GPO Box U 1987, Bentley, Perth, Australia.
E-mail: v.vimonsatit@curtin.edu.au
[2]*Department of Civil Engineering, Curtin University*
GPO Box U 1987, Bentley, Perth, Australia.
E-mail: ade.wahyuni@postgrad.curtin.edu.au
[3]*Department of Civil Engineering, Curtin University*
GPO Box U 1987, Bentley, Perth, Australia.
E-mail: h.nikraz@curtin.edu.au

A new lightweight sandwich reinforced concrete (LSRC) section has been developed which is suitable to be used for slab members in reinforced concrete structures. Prefabricated autoclaved aerated concrete (AAC) blocks are used as infill in the slab section where the concrete is considered ineffective under bending. As a result, the flexural capacity of an LSRC section is expected to be the same as equivalent solid section having identical height. The ability to resist shear is however in question as the AAC infill generally has lower strength grade than that of the normal dense concrete. This paper presents a numerical investigation into the behavior of LSRC slabs when shear is critical and the slabs will failure in shear. ANSYS version 12.1 is employed to develop three dimensional nonlinear finite element models of LSRC slabs. The numerical study will be compared with the test results. Some differences in the results were found due to the support modeling. The hinge-hinge support over predicted both the strength and stiffness of the modeled slabs when compared with the tested slabs, while the hinge-roller support condition led to underestimated outcomes. Recommendations for the modeling improvement are made.

Keywords: lightweight concrete, reinforced concrete, composite section, sandwich section.

1 Introduction

Concrete is one of the most common construction materials. A challenge for engineers when using concrete is to overcome its heavy weight particularly in large span construction (Matthew and Bennett 1990). Basic concept in dealing with the weight is by minimizing the use of concrete while maintaining the desired strength and stiffness of the section. Technologies such as prestressed hollow planks, pre-tensioned, post-tensioned and bubbledeck have been commonly used in the industry. Schnellenbach-Held and Pfeffer (2002) investigated the structural behavior of biaxial hollow slab, known as bubbledeck slab. This technology combines the advantages of material-saving and extreme load-carrying capacity due to its optimized cross-section. Girhammar and Pajari (2008) studied the effect of concrete topping for improving the shear capacity of hollowcore units. The idea is to reduce the thickness of the precast unit while increasing the thickness of the concrete topping, without compromising the load-

carrying capacity of the whole composite section.

Autoclaved aerated concrete (AAC) was invented in Sweden in the mid 1920s and has been used worldwide. The basic raw materials in producing AAC are Portland cement, limestone, aluminum powder, and sand. In the process aluminum powder reacts chemically to create million of tiny hydrogen gas bubbles that give AAC its light weight. It is about one fourth of the weight normal concrete, provides excellent thermal and sound insulation, and fire resistance. AAC products include blocks, wall panels, floor and roof panels and lintels.

A novel use of AAC as infill of a reinforced concrete section has been proposed (Vimonsatit et al. 2010a). The section is called, in short, LSRC section. The section is made up of a reinforced concrete with prefabricated AAC blocks used as infill in the section where the concrete is considered ineffective under bending. The developed LSRC section can be used either as structural or non-structural elements. LSRC members are particularly suitable for large span construction due to the weight saving benefits and ease of construction.

Based on the test results, LSRC members performed well under bending. The flexural capacity of LSRC beams and slabs are found to be comparable with the solid concrete section having identical height. However, the shear capacity is of concern. An experimental investigation into the shear capacity of LSRC slabs found that the shear reduction of the tested slabs could be up to 25% of the capacity of the equivalent solid slab (Vimonsatit et al. 2010b). The primary intent of the paper is to develop a finite element model to numerically investigate the behavior of LSRC slabs when fail in shear.

ANSYS is chosen for the numerical modeling of the LSRC slabs because of its very useful 3-D reinforced concrete element provided in the element library. In the following sections, slab details used in the experiment will be briefly described. This will be followed by the description of the finite element modeling of concrete and steel reinforcement of the slab using ANSYS. The analytical results will be presented to compare with the experimental results. Some similarities and differences will be highlighted for the improvement of the proposed numerical model.

2 Slab Details

Four slabs were manufactured, one solid (SS1), and three LSRC sections. All slabs had the same dimensions and reinforcement details. Slabs were 3000 mm long, 1000 mm wide, and had the total depth of 250 mm. The shear span-to-depth ratio was equal to 2. The standard dimension of an AAC block used was 300 mm long, 180 mm wide, and 75 mm thick. Two blocks were put together to create the total block thickness of 150 mm. LS1 contained 64 standard blocks, which were the maximum number of blocks that could be placed within the specimen. LS2 contained 32 blocks, half of that contained in LS1, while LS3 had the same amount of blocks as in LS1 but the corners of the blocks were cut off to investigate the shape effect on the slab. In all LSRC slabs, blocks were placed evenly in both directions. The minimum gaps between the blocks in LS1 were 50 mm and 43 mm in the cross-section and the longitudinal directions of the slab, respectively. The applied loads and displacements were measured using load cells and LVDT's and were measured continuously by the data acquisition system. During loading, the formation of the cracks on the sides of the beams were also marked and recorded.

3 Finite Element Model

The concrete was modeled with solid65, which has eight nodes with three degrees of freedom at each node, i.e., translation in the nodal x, y, and z directions. The element is

capable of plastic deformation, cracking in three orthogonal directions, and crushing.

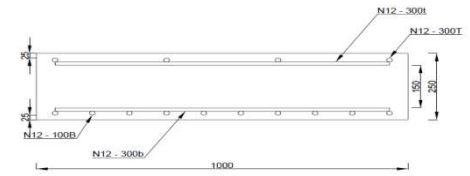

SS1

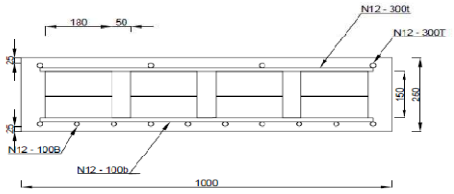

LS1

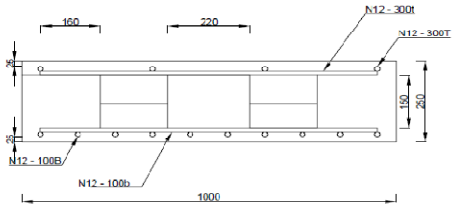

LS2

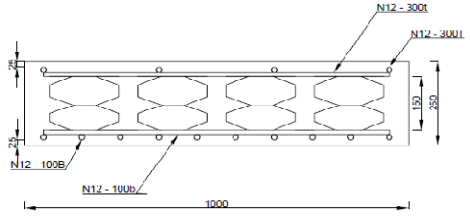

LS3

A link8 element was used to model the steel reinforcement. This element is also capable of plastic deformation. Two nodes are required for this element which has three degree of freedom, as in the case of the concrete element. Discrete method was applied in the modeling of the grid reinforcement in the slab specimen. The two elements were connecting at the adjacent nodes of the concrete solid element, such that the two materials shared the same nodes

3.1 *Concrete*

For concrete, ANSYS requires an input data for material properties, which are Elastic modulus (E_c), ultimate uniaxial compressive strength (f_c'), ultimate uniaxial tensile strength (modulus of rupture, f_r), Poisson's ratio (ν), shear transfer coefficient (β_t). f_c' and f_r used in this study is 43 MPa and 3.5 MPa respectively, The modulus of elasticity of concrete was 26500 MPa which was determined in accordance with AS 1012.17-1997. Poisson's ratio for concrete was assumed to be 0.2 for all the beams. The modulus of elasticity for AAC is 8000 MPa, with f_c' = 3.5 MPa.

The shear transfer coefficient, β_t, represents the conditions of the crack face. The value of β_t, ranges from 0 to 1 with 0 representing a smooth crack (complete loss of shear transfer) and 1 representing a rough crack (i.e., no loss of shear transfer) as described in ANSYS. The value of β_t specified in this study is 0.4. The shear transfer coefficient for a closed crack β_c was taken as 1.

Numerical expression by Desayi and Krisnan (1964), Eqs. (1) and (2), were used along with Eq. (3) (Gere and Timoshenko 1997) to construct the uniaxial compressive stress-strain curve for concrete in this study.

$$f = \frac{\mathrm{E}_c \varepsilon}{1 + \left(\frac{\varepsilon}{\varepsilon_0}\right)^2} \tag{1}$$

$$\varepsilon_o = \frac{2 f'_c}{\mathrm{E}_c} \tag{2}$$

$$\mathrm{E}_c = \frac{f}{\varepsilon} \tag{3}$$

where f and ε are the stress and the corresponding strain, respectively. The strain at the ultimate compressive strength is denoted by ε_o. The compressive stress at 0.3 of the compressive strength was used as the first point of the multi-linear stress-strain curve.

The crushing capability of the concrete was turned off to avoid any premature failure.

3.2 *Steel Reinforcement*

Steel grade N12 bars were used for top and bottom steel reinforcement grid in all slabs. The tensile strength at yield was 500 MPa. In the finite element models, steel bars were assumed to be made of an elastic-perfectly plastic material and the behavior in tension and compression was identical. Poisson's ratio of 0.3 was used, and the elastic modulus, Es = 200,000 MPa.

4. Results and Discussion

Analyses were made of the developed numerical model for the solid slab and LSRC slabs. The typical finite element model of the slabs and the results at failure are illustrated in Figure 2.

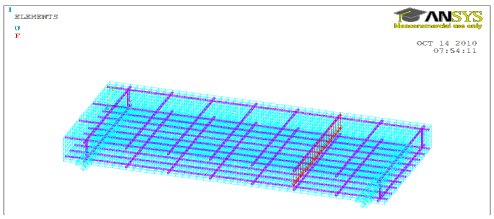

(a) Slab and reinforcement

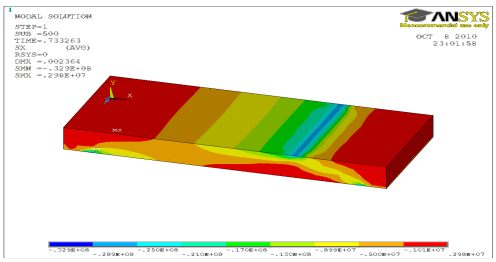

(b) Stress contour at shear failure

Figure 2. FEM model of LSRC slab and results

Each model was analyzed twice to investigate the effect of the support condition on the results. The support conditions were assumed either as hinge-hinge or hinge-roller. The load deflection characteristics from the analytical results are plotted to compare with the experimented results in Figure 3. The four graphs show similar results in both linear and nonlinear behavior of the slabs. Based on these graphs, the numerical models exhibit greater stiffness than the experiment ones when the support condition is hinge-hinge (hinge support). The hinge-roller condition (simple support) better represented the elastic stiffness of the slab in the low loading range, however underestimated it as the load increased until failure. This finding is similar to the results by Song et al. (2002) who demonstrated that the numerical result of reinforced concrete T-girder bridge is greatly dependent on the support modeling in a nonlinear finite element analysis. It was proposed in the same paper when a spring was laterally attached to a roller support, the results improved and compared well with the experimental results.

There are several other factors that could cause the differences in the results of the finite element analysis and the experiment. The greater stiffness in the finite element model of the slabs with hinge support could be due to the lack of the proper modeling of microcracks in concrete produced, for example, by drying shrinkage. Another factor was the bond between the concrete and reinforcing steel elements, as also pointed out by Kachklakef et al. (2001), the overall stiffness of the actual members could be lower than what the finite element models would predict, due to the factors that have not been incorporated into the models.

The hinge-roller support appeared to predict well in the loading range but not in the increased loading range. It is clear that at the

high loading, the frictional factor between the slab and the supporting elements would be increased in the actual test set up. This factor could be the main contributing factor to the differences.

Comparing the failure loads of LSRC slabs with the solid slab in Table 1, the failure load of LS3 was almost equal to the failure load of the solid slab. These results are consistent from both experimental and numerical investigations indicating that creating curved shape of AAC blocks by cutting of the four corners increased the resistance to shear of the tested LSRC slab.

Table 1. Load at failure from the experiment and numerical (hinge support) results.

Specimen	Ultimate load		
	Experiment (kN)	FEM (kN)	Ratio
SS1	180.9	230.9	1.28
LS1	179.9	224.9	1.25
LS2	172.3	227.7	1.32
LS3	186.6	233.5	1.25

5. Conclusion

A numerical model has been developed to predict the behavior and strength of lightweight sandwich reinforced concrete slabs. Two types of support conditions were considered, a hinge support and a simple support. The model is verified against the experimental results. Based on the presented investigation, the developed model has some differences in the stiffness and strength when compared with the experimental results. The hinge-hinge support model over predicted both the strength and stiffness of the slabs when compared with the tested slabs. The hinge-roller support condition could better represent the stiffness in the low loading range but as the load increased, the stiffness was significantly underestimated.

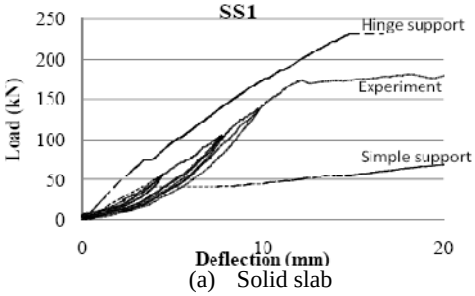

(a) Solid slab

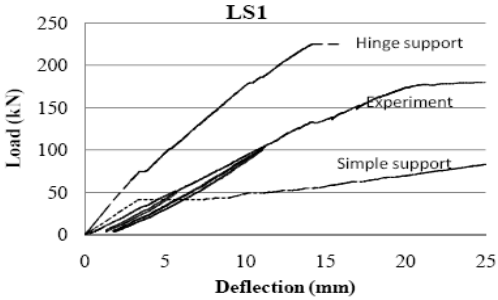

(b) slab with maximum AAC blocks

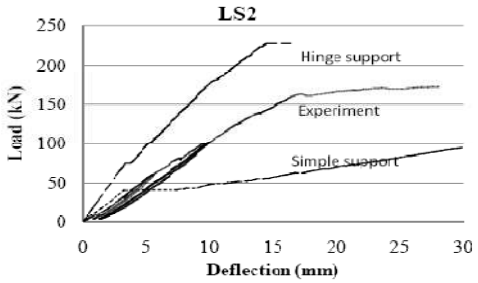

(c) Slab with half number of AAC blocks

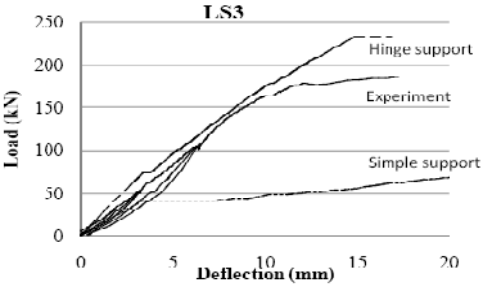

(d) Slab with curved AAC blocks

Figure 3. Load deflection relation of slabs

Further investigations are required to investigate the consistency of the results and the factors affecting the results. The model can be further improved by attaching a spring to the roller support to account for any lateral resistance between the slabs and the supporting elements in the actual tests. A sensitivity analysis on the design parameters used in the finite element modeling would also be a good indication of the differences in the results.

Reference

ANSYS Theory Reference, version 12.1, available at Curtin University, 2010.

AS 1012.17, Method of testing concrete – Determination of the static chord modulus of elasticity and Poisson's ratio of concrete, *Standards Australia*, 1997.

Bangash, M.Y.H., *Concrete and Concrete Structures: Numerical Modeling and Applications*, Elsevier Science Publishers Ltd, London, 1989.

Desayi, P and Krishnan, S., Equation for the Stress-Strain Curve of Concrete, *Journal of American Concrete Institute*, 61, 345-350, 1964.

Gere, J.M. and Timoshenko, S.P., Mechanics of Materials, PWS Publishing Company,Boston Massachusetts, 1997

Kachlakef, D., Miller, T, Yim, S., Chansawat, K., and Potisuk, T., FE Modeling of Reinforced Concrete Structures Strengthened with FRP Laminates, *Final Report SPR 316*. Oregon State University, 2001.

Girhammar, U.A., Pajari, M., Test and Analysis on Shear Strength of Composite Slabs of Hollow Core Units and Concrete Topping, *Construction and Building Materials* , 22, 1708-1722, 2008.

Matthew, P.W. & Bennett, D.F.H.. Economic long span concrete floors, *British Cement Association*, 2-6, 1990.

Schnellenbach-Held, M., Pfeffer, K., Punching Behavior of Biaxial Hollow Slabs, *Cement and Concrete Composites*, 24, 551-556, 2002

Song, H-W., You, D-W., Byun, K-J.,Maekawa, K. Finite Element Failure analysis of Reinforced Concrete T-Girder Bridges, *Engineering Structures*, 24, 151-162, 2002

Vimonsatit, V., Wahyuni, A.S., Mazlan, M.A., and Nikraz, H., Use of Lightweight Concrete as Infill of Reinforced Concrete Sections, Proceedings, *ACMSM 21*, December 7-10, 2010a.

Vimonsatit, V., Wahyuni, A.S., Macri, P.J., and Nikraz, H., Experimental Investigation of Behaviour and Shear Strength Capacity of Lightweight Sandwich Reinforced Concrete Slab, Proceedings, *ACMSM 21*, December 7-10, 2010b.

Incorporating Sustainable Practice in Mechanics of Structures and Materials-
Fragomeni, Venkatesan, Lam and Setunge (eds
© 2011 Taylor and Francis Group, London, ISBN 978-0-415-61657-7

Use of Lightweight Concrete as Infill of Reinforced Concrete Sections

V.Vimonsatit, A. S. Wahyuni*, M.A. Mazlan and H. Nikraz
Department of Civil Engineering, Curtin University of Technology, Perth, Australia
**Bengkulu University, Indonesia, currently PhD student at Curtin University of Technology*

ABSTRACT: In structural design, an ideal situation in material saving is to reduce the weight of the structure without having to compromise on its strength and serviceability. This paper presents a novel use of lightweight concrete to create a lightweight sandwich reinforced concrete (LSRC) section. The developed LSRC section can be used as beams or slabs in concrete structures. An experimental program has been conducted to explore the potential use of the developed LSRC section as beam members. Based on the tested beams, the flexural and shear strengths of LSRC beams are found to be comparable with the strengths of the solid beams having identical height. Details on the development of LSRC sections, experimental testing and results are presented. Benefits of using the developed LSRC beams will be highlighted.

1 INTRODUCTION

Lighter weight of concrete members is desirable particularly when designers or contractors have to deal with large open floor plans and especially in highrise construction. Several options are available using well developed technologies such as post-tensioned concrete (StrongForce 2009), prestressed precast planks (Hegger & Roggendrof 2008), and Bubbledeck technology (Aldejohann & Schnellenbach 2003). These technologies are usually available as commercial products thereby the main project contractor needs to engage the technology specialist/supplier to deliver their respective products in both design and construction phases.

Alternative to the specialist products is the use of lightweight material. Lightweight concrete can either be made with lightweight aggregate, foamed technology, or autoclaved aerated technology. The benefits of lightweight concrete are numerous and have been well recognised. Lightweight aggregate is commonly used in structural application, for example, in reinforced concrete beams (Bungey & Madandoust 1994, Ahmad et al. 1995), with high strength fiber (Kayali et al. 2003, Mousa & Uddin 2009), and as an infill in reinforced concrete columns (Moulia & Khelafi 2007). Foamed concrete, or cellular concrete, is either cement or mortar in which foaming agent is added to create air-voids within it. The density of foamed concrete varies in a wide range of 400 to 1600 kg/m3 depending on the foam dosage. Literature classification on the properties of foamed concrete (Ramamurthy et al. 2009) and its historical use in construction application (Jones & Mcarthy 2005) is published recently.

Autoclaved aerated concrete (AAC) was invented in Sweden in the mid 1920s and has been used worldwide. It is about one-fourth of the weight of normal concrete, provides excellent thermal and sound insulation, and fire resistance. AAC products include blocks, wall panels, floor and roof panels, and lintels.

Use of AAC in structural application is still very limited due to its low compressive strength compared to normal concrete. For domestic construction, AAC can be used as load-bearing walls when integral with reinforcing frame (Moulia & Khelafi 2007). The Masonry Structures Code of Australia (AS3700-2001) includes provisions for AAC block design.

This paper presents a novel use of AAC blocks in developing an LSRC section which is suitable for use as beams or slabs. The LSRC members have weight saving benefits and are easy to construct due to the lighter weight. The construction method of LSRC members can either be fully precast, semi-precast, or cast in-situ. In addition to the weight saving benefit of the developed LSRC section, the semi-precast construction of LSRC members has additional cost and time saving benefits.

An experimental program has been conducted to explore the feasibility of using LSRC section as a beam member. Of primary concern is the flexural and shear strength of the LSRC beam when compared with the solid beam of identical height. In the fol-

lowing sections, the detailed development of LSRC section will be presented. This is followed by the experimental arrangement and results. Test results are compared with the calculation based on the design provision in AS3600 (2009).

2 DEVELOPMENT OF LSRC SECTION

Concrete is the most used construction material; it has been pointed out (Sumajouw & Rangan 2006) that the overall use of concrete in the world is only second to water. The main advantages of concrete material are that it is cost-effective, made from locally available material, and can be readily moulded into any required shape. Concrete is very good in compression but poor in tension, therefore steel is provided as reinforcement in concrete structures. A reinforced concrete beam, or slab, is normally designed for its strength to carry the load transferred in flexure and shear. Under the elastic bending theory, the flexural strength of a reinforced concrete section is calculated from the coupling between compression in concrete and tension in the reinforcing steel. In calculating the moment capacity of the section, the effective concrete in compression above the neutral axis can be further simplified using a uniform stress block (AS3600-2009). This is the basis of the developed LSRC section in which prefabricated lightweight blocks are used to replace the ineffective concrete portion of the reinforced concrete section.

2.1 *LSRC Section*

In reinforced concrete, the structural properties of the component materials are put to efficient use. The concrete carries compression and the steel reinforcement carries tension. The relationship between stress and strain in a normal concrete cross-section is almost linear at small values of stress. However, at stresses higher than about 40 percent of the compressive concrete strength the stress-strain relation becomes increasingly affected by the formation and development of microcracks at the interfaces between the mortar and coarse aggregate (Warner et al. 1998). A typical stress and strain diagram of a reinforced concrete beam in bending can be seen in Fig. 1(a).

Concrete has low tensile strength, therefore when a concrete member is subjected to flexure, the concrete area under the neutral axis of the cross-section is considered ineffective when it is in tension. In creating an LSRC section, prefabricated lightweight blocks are used to replace the concrete within this ineffective region. The developed LSRC section can be used for beams or slabs. Typical LSRC beam and slab sections are as shown in Fig. 1(b) and 1(c), respectively.

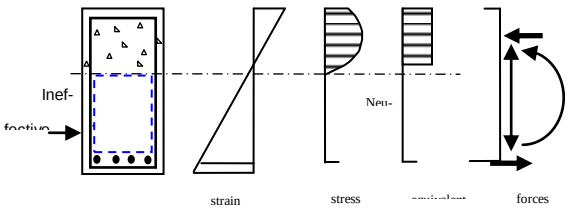

(a) Stress-strain diagram of a reinforced concrete section

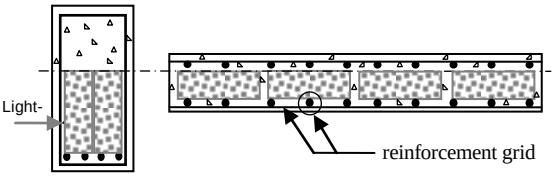

(b) LSRC beam (c) LSRC slab

Figure 1. Reinforced Concrete Section with Lightweight Blocks

2.2 *Construction of LSRC members*

As per any reinforced concrete members, LSRC members can be fully precast, semi-precast, or cast in-situ. Lightweight blocks can be technically placed between the lower and upper reinforcements of the section. In a beam member, the encasing shear stirrups can be installed before or after the placement of the blocks. When preparing for the experiment, the casting bed and steel mould were prepared and secured, lower and upper reinforcing steels and shear stirrups were pre-fabricated. Lightweight blocks were inserted within the encasing stirrups through the side of the beam. This method is typical for either precast or cast in-situ construction. Fig. 2(a) shows a ready-to-cast LSRC beam in a steel mould at the Concrete Lab of Civil Engineering Department, Curtin University of Technology at Bentley, where the experiment was conducted.

When dealing with a large concrete member such as a long span beam or a large floor construction, it is of advantage for constructors to consider semi-precast construction method. The semi-precast construction helps resolve, to a certain extent, the complication due to the heavy weight. LSRC members are also suitable for semi-precast construction. The lower part of concrete section can be cast with the lower reinforcing steels in which the shear stirrups and lightweight blocks are already put in place. The semi-precast LSRC members can be depicted in Fig. 2(b). Alternatively, the precast can be done with the portion below the underside of the blocks, which means that the concrete can be cast prior to the placement of the blocks. If this is the case, side formworks will be required when prepare the upper part of the section for concreting. It is necessary to ensure that the section is monolithic by making sure during casting that the concrete can flow in properly through to the sides of the beam and in the gaps between the lightweight blocks.

(a) Placement of AAC blocks

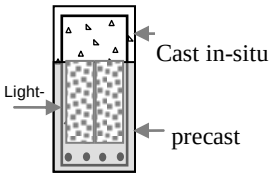

(b) semi-precast section

Figure 2. Construction of LSRC member

2.3 *Benefits of LSRC members*

The developed LSRC members have several benefits.

1 It provides a novel use of lightweight AAC blocks to create structural members
2 LSRC section can be used as beam or slab subjected to one-way or two-way actions
3 It can achieve a weight reduction of up to 20-30%, or more, resulting not only in using less concrete material in the members, but also in demanding less supporting structure and foundation
4 The construction method is simple and can be precast, semi-precast, or cast in-situ, which does not require engaging any specialist contractor.
5 Based on point 4, the main constructor can cut down on the administrative cost and time due to unnecessary outsourced activities.
6 The semi-precast construction has an additional benefit as the precast portion can be used as the formwork of the cast in-situ portion on site. Therefore, installation of heavy formwork and falsework is not required.

3 EXPERIMENTAL ARRANGEMENT

An experimental program has been set up to investigate the behaviour of the developed LSRC members under loading condition. Several tests have been conducted on LSRC beams and slabs. In this paper the test set-up and results of LSRC beams are presented. Testing of LSRC slabs to investigate the shear capacity is presented in the companion paper (Vimonsatit et al. 2010).

3.1 *Beam details*

The tested beams had rectangular section, with a constant width and depth of 200 mm and 300 mm. The beam length was 3000 mm, with 2800 mm clear span when set up. Five beams were manufactured for two series of tests – the flexural test and the shear test. The flexural test was to compare the flexural strength of the solid beam and LSRC beams. The aim was to investigate the effect of using different amount of AAC blocks infill on the performance of the beam. Three beams were prepared, one solid (SB1F) and two with AAC blocks (LB1F and LB2F). In the shear test, two beams were prepared, one solid (SB1S) and one with AAC blocks (LB1S). The details of beam LB1F is as shown in Fig. 3.

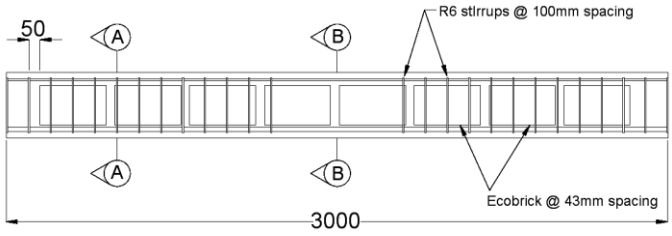

(a) Beam LB1F

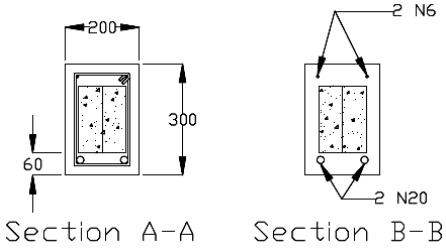

(b) Cross-section of LB1F

Figure 3. Beam details

The standard dimensions of the Ecobricks used were 180 mm x 75 mm x 300 mm. The control beams SB1F and SB1S were solid beams with the self weight of 405.4 kg and an average concrete density of 2413 kg/m3. Beams LB1F and LB1S had eight AAC blocks placed within the beam, which was the maximum possible amount of bricks based on the gap size between each block to ensure smooth concrete flow without any restrictions during pouring. The gap specified between one block to the other was 40 mm. The reduction of self weight due to incorporating AAC blocks within the beam was found to be 20% weight reduction compared to the solid beam. Beam LB2F contained four AAC blocks within the beam, each was spacing evenly along the beam span. The weight reduction of LB2F was half of LB1F, which was about 10% reduction of SB1F. The details of the tested beams are summarized in Table 1.

3.2 *Material*

Concrete used was grade 40, having the compressive strength of 43.4 MPa at 28 days. Tensile steel reinforcement was N-grade, having the yield strength of 500 MPa. Superplasticiser was added to the con-

crete mix to increase the workability of the concrete to ensure the concrete filled all the gaps for beam specimens with AAC blocks in it. The maximum size of aggregate was 10 mm.

Table 1 Details of Tested Beams

ID	Section	Testing
SB1F	Solid - no blocks	Flexure
LB1F	with 8 blocks	Flexure
LB2F	with 4 blocks	Flexure
SB1S	Solid - no blocks	Shear
LB1S	with 8 blocks	Shear

3.3 *Test set-up*

Three beams were designed to fail in flexure, in the flexure test, and two beams were designed to fail by shear, in the shear test. The beams were simply supported and were subjected to two point loads. In the flexure test, the distance between the two point loads was 800 mm. The distance between the two point loads for shear test was 1680 m. The typical test set up for the flexure and shear tests is as shown in Fig. 4. The beams were loaded to failure using two 50 tonne capacity hydraulic jacks which acted as the two point load. The jacks were attached to a reaction frame. Two supporting frames with 200 mm long x 150 mm diameter steel rollers were used as the end support.

To ensure a uniform dispersion of force during loading and to eliminate any torsion effects on the beam due to slight irregularities in the dimension of the beams, plaster of paris (POP) and 100 mm wide x 250mm long x 20mm thick distribution plates were placed on the rollers and also under the jacks.

3.4 *Instrumentation*

The vertical deflections of the test beams were measured using Linear Variable Differential Transformers (LVDTs). LVDTs were placed at 200 mm spacing within 2.8 metres span. LVDT were also attached on each loading jack to capture the vertical deflection at the loading point. The LVDTs were attached to a truss frame as seen in Fig. 4. With this arrangement, the curvature of the beam can be identified in relation to the loading increment. During the initial set up of the LVDTs, the instruments were calibrated before the test commenced. An automated data acquisition system with a Nicolet data logger system was used to record the load-deformation from the jacks and the LVDTs.

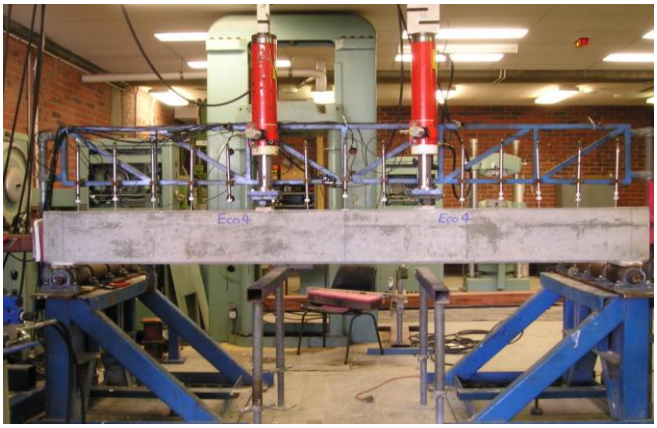

Figure 4. Typical test set-up

4 RESULTS AND DISCUSSIONS

Five beams were tested, three tests were to determine the flexural strength and load-deformation behaviour of the solid beam and the LSRC beams. Additional two tests were conducted to compare the shear capacity between the solid and the LSRC beam. Note that the load values described in the following sections refer to the average value of the two applied point loads.

4.1 *Flexural and Shear Strength*

The failure loads of the solid and LSRC beams under the flexure test were found to be of insignificantly different. It was found that beam LB1F, which had the maximum AAC blocks, failed at an average load of 78.9 kN, LB2F and SB1F beams failed at 78.6 kN and 78.5 kN, respectively.

When a beam is more critical in shear, rather than in flexure, an LSRC beam is expected to exhibit lower shear resistance than the equivalent solid beam. This is because the inserted AAC blocks in an LSRC beam have lower compressive strength than the normal concrete. As a result, an LSRC beam has less effective concrete area to resist the shear when compared to the solid beam of identical height. Based on the two beam tests, the failure loads of SB1S and LB1S were 128 kN and 102 kN, respectively. A significant 20% reduction in the shear capacity of LSRC beam compared to the equivalent solid beam.

4.2 *Load-deformation behaviour*

The load-deformation behaviour of all the tested beams was found to be similar and followed the same trend. The loads versus deflections at the mid-span of all the beams under flexure and shear are plotted in Fig. 5. The effect of using LSRC section on the member stiffness is further discussed in Wahyuni, et al. (Wahyuni et al. in prep.).

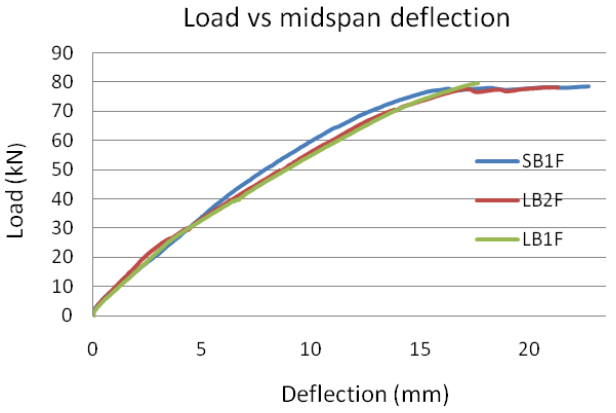

(a) Flexure Tests

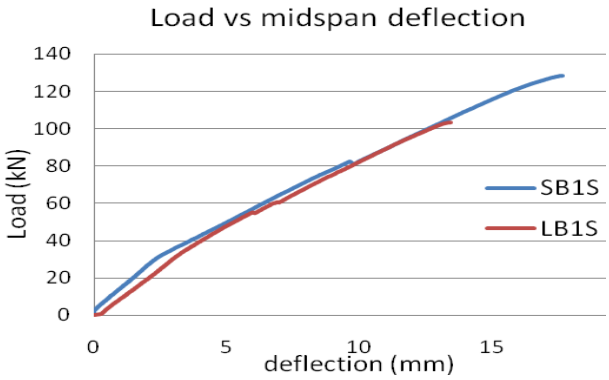

(b) Shear Test

Figure 5. Load versus mid-span deflection

4.3 *Crack*

Under the flexural test, the main flexure cracks were developed within the two loading points and widen up as load increased. At failure, the concrete in the compression region ruptured. It was seen that the exposed reinforcing steel in this region buckled. Typical crack patterns and failure modes of the tested beams under the flexural test are shown in Fig 6.

For beams tested in shear, the behaviours of the two tested beams were similar. Small flexure cracks occurred first at the midspan region of the beam. Subsequently, the flexure cracks extended as flexure-shear cracks were developed between the support and the loading point. At the load approaching the failure load, critical web shears crack were developed diagonally within the shear span. The cracks continued to widen as the load increased, and failure occurred soon after depicting a typical sudden type of shear failure. The typical progressions of the cracks and the failure modes of the beam tested in shear are shown in Fig. 7.

After the test, it was of concern to determine whether the inclination of the critical shear crack was influenced by the position of the AAC blocks within the crack region. After the beam failed, the beam was cut using concrete saw to examine the actual position of the blocks. It was found that the cracks propagated right through the blocks as if the section was monolithic. This behaviour indicates good bonding between the concrete and the blocks.

Figure 6. Typical crack formations of the flexural test

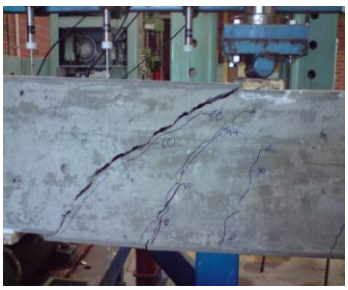

Figure 7. Typical crack formations of the shear test

4.4 *Correlation of test results with analytical prediction*

The test results on the failure loads of the beams are compared to the analytical predictions based on Australian standard for concrete design (AS3600-2009). The predicted flexural strength is calculated from the solid beam section. The result shows good correlation with all the experimental values. The ratio between the experiment and the predicted flexure strength is about 0.97; all are within 3% difference. Based on these results, the concrete replacement by AAC blocks, as tested on LB1F and LB2F, has virtually no effect on the flexural strength of the section, which is as expected.

The predicted shear strength obtained from the design calculation based on AS3600 (2009) shows good correlation with the LSRC beam. The design value of the shear capacity appears to be conservative for the solid beam. The test/predicted shear strength ratios for the solid and LSRC beams were 1.27 and 1.01, respectively. Therefore, design adjustment needs to be made should the designer maintain the same level of conservativeness in predicting the shear capacity of an LSRC beam, as that of an equivalent solid beam.

5 CONCLUSION

Experimental results of the flexural and shear tests of solid beams and the developed LSRC beams are presented. The following conclusions are drawn based on the test results. These findings are specific to the tested beams and the parameters used only. Further investigations are required for more general conclusions.

1. Under the flexure test, there was insignificant difference of less than one percent in the flexural strength between the solid beam and the beams filled with AAC blocks. The predicted load at failure (AS3600-2009) matched very well with the failure loads obtained from all the tests. This shows that the proposed LSRC sections performed well under flexure.
2. The results show that the flexural strength of the two LSRC beams is actually greater than the solid beam. This is due to the selfweight reduction of the tested beam, which was about 10 - 20% of the equivalent solid beam. At failure load, the bending moments caused by the applied load and the selfweight of the solid beam and of the LSRC beams, taken into account the weight reduction by AAC blocks infill, were almost equal in all the tested beams under flexure.
3. Based on the shear tests, the LSRC beam had lower shear strength than the equivalent solid beam. The reduction of the shear strength is 22%, which is quite significant in design. This result deserves more attention to determine the influence of the shear capacity in an LSRC beam.
4. Due to the conservativeness of the shear design provision in AS3600 (2009), it can safely predict the shear capacity of the tested LSRC beam.

In the companion paper (Vimonsatit et al. 2010), more experiments have been conducted to further investigate the shear strength and behaviour of LSRC slabs.

6 ACKNOWLEDGMENT

The authors wish to thank the reviewers for the comments provided on the earlier draft of this paper. The authors appreciated the comments provided by Prof B.V. Rangan on this topic. Lightweight concrete blocks used in the experiment sponsored by Ecobrick, Australia were gratefully acknowledged.

7 REFERENCES

Ahmad, S.H., Xie, Y. and Yu, T. 1995. Shear ductility of reinforced concrete beams with normal strength and high strength concrete, *Cement & Concrete Composites*, vol. 17, pp. 147- 159.

Aldejohann, M. & Schnellenbach, M. 2003. Investigation on the shear capacity of biaxial hollow slabs-Test results and evaluation, *Darmstadt Concrete*, vol. 18, pp. 532-545.

AS3700 Committee BD-004, 2001. *Masonry Structures*, Standards Australia.

AS3600 Committee BD-002, 2009. *Concrete Structures*, Standards Australia.

Bungey, J.H. & Madandoust, R, 1994. Shear strength variation in lightweight concrete beams, *Cement & Concrete Composites*, vol. 16, pp. 49-55.

Jones, M.R. & McCarthy, A. 2005 Behaviour and assessment of foamed concrete for construction applications. In: Dhir RK, Newlands MD, McCarthy A, (eds.). *Use of foamed concrete in construction*, London: Thomas Telford, pp. 61–88.

Hegger, J. & Roggendorf, T. 2008. Shear capacity of prestressed hollowcore slabs in slim floor constructions, *Engineering Structures*, vol. 31 (2), pp. 551-559.

Kayali, O., Haque, M.N. & Zhu, B. 2003. Some characteristics of high strength fiber reinforced lightweight aggregate concrete, *Cement & Concrete Composites*, vol. 25, pp. 207–213.

Matthew, P. W. & Bennett, D.F.H. 1990. Economic long span concrete floors, *British Cement Association* Available: http://www.brmca.org.uk/downloads/ECONOMIC_ LONG_SPAN.pdf, accessed 4 Sept 2009

Moulia, M. & Khelafi, H. 2007. Strength of short composite rectangular hollow section columns filled with lightweight aggregate concrete, *Engineering Structures*, vol. 29, pp. 1791–1797.

Mousa, M.A. & Uddin, N. 2009. Experimental and analytical study of carbon fiber-reinforced polymer (FRP)/autoclaved aerated concrete (AAC) sandwich panels, *Engineering Structures*, vol. 31, pp. 2337-2344.

Ramamurthy, K., Kunhanandan Nambiar, E.K., Indu Siva Ranjani, G. 2009. A classification of studies on properties of foam concrete, *Cement & Concrete Composites*, vol. 31, pp. 388–396.

StrongForce 2010. The economics of post tensioning *http://www.infolink.com.au/c/StrongForce/The-economics-of-post-tensioning-n756144*, accessed 5 May 2010.

Sumajouw, M.D.J. & Rangan, B.V. 2006. Low-calcium fly ash-based Geopolymer concrete: reinforced Beams and columns, *Research Report GC 3*, Faculty of Engineering, Curtin University of Technology, Perth, Australia.

Vimonsatit, V., Wahyuni, A. S., Macri, P. & Nikraz, H. 2010. Experimental investigation of shear strength and behaviour of lightweight sandwich reinforced concrete slab, *ACMSM21*, 7-10 December 2010, Melbourne.

Wahyuni, A. S.,Vimonsatit, V. & Nikraz, H. 2010. Stiffness of LSRC members subjected to flexure and shear, in preparation.

Warner, R.F., Rangan, B.V., Hall, A.S. & Faulkes, K.A. 1998. *Concrete Structures*, Longman, Melbourne, Austraia.

Incorporating Sustainable Practice in Mechanics of Structures and Materials-
Fragomeni, Venkatesan, Lam and Setunge (eds
© 2011 Taylor and Francis Group, London, ISBN 978-0-415-61657-7

Experimental Investigation of Behaviour and Shear Strength Capacity of Lightweight Sandwich Reinforced Concrete Slab

V.Vimonsatit, A. S. Wahyuni *, P. Macri and H. Nikraz
Department of Civil Engineering, Curtin University of Technology, Perth, Australia
**Bengkulu University, Indonesia, currently PhD student at Curtin University of Technology*

ABSTRACT: This paper presents an experimental investigation of the shear strength and behaviour of lightweight sandwich reinforced concrete (LSRC) slabs. Eight tests were conducted on four slabs, one solid and three LSRC slabs. Based on the tests, LSRC slabs exhibited similar behaviour to the equivalent solid slab. There was a 15% reduction in the shear capacity of LSRC slab compared to the solid slab of identical height. When compared against the predicted shear capacity based on current design codes, the reduction in the shear capacity of LSRC slabs was greater than the code-based design capacity of the solid slab.

1 INTRODUCTION

With an increasing demand for large span structures due to economic and aesthetic reasons (Matthew & Bennet 1990), practitioners are facing even more challenges in providing cost effective solutions to fulfil this demand. Sustainability is another essential area in the construction industry. A way to depict sustainability is by minimising resources used. As a result there has been a vast interest in research and development of lightweight concrete as alternatives to normal weight concrete (Ramamurthy et al. 2009, Jones & McCarthy 2005). The lightweight option, if feasible, leads to several benefits in the construction process. Clearly, the main benefits are the cost and time savings due to the weight reduction and the less of supporting structure and foundation.

A lightweight sandwich reinforced concrete (LSRC) section has been developed and an experiment program on LSRC beams has been conducted (Vimonsatit et al. 2010). An LSRC section is a reinforced concrete section that contains lightweight concrete in the form of prefabricated concrete blocks. This development is based on the elastic bending theory that when a reinforced concrete member is subjected to bending there is an ineffective concrete portion which does not contribute to the flexural strength of the section. This ineffective portion could therefore be replaced by lightweight concrete to reduce weight. Other technologies currently used, particularly to overcome the large span design and construction (Matthew & Bennet 1990) are post-tensioned solid slab, ribbed slab, waffle slab, precast hollowcore, double-T and Bubbledeck slabs (Aldejohann & Schnellenbach 2003).

The proposed development of LSRC sections offers an alternative lightweight option to the construction industry. Based on the tested LSRC beams (Vimonsatit et al. 2010), the flexural capacity of the LSRC beams was found to be almost identical to the capacity of the solid beam of identical height. However, when the member is predominantly subjected to shear, the LSRC beam exhibited lower resistance to shear than the equivalent solid beam. It is therefore of interest to further investigating the performance of LSRC members under shear. This paper presents the experimental investigation into the capacity and behaviour of LSRC slabs under one-way shear. In the next sections, the details of the tested slabs will be described. The predicted shear capacity of the solid slab will be calculated based on Australian concrete design code (AS3600-2009). Test results on the shear strength, modes of failure, and load-deflection characteristics of the tested slabs will be presented and discussed. The shear capacity will be compared with the predicted capacity based on current design codes (ACI318-02, Eurocode 2).

2 SPECIMEN DETAILS

Eight tests have been conducted from four slabs, one solid and three LSRC sections. Slabs were designed according to AS3600 (2009) such that the shear failure would occur prior to the flexural failure of the slab. All slabs had the same dimensions and reinforcement details. Slabs were 3000 mm long, 1000

mm wide, and had the total depth of 250 mm.

2.1 *Shear capacity*

In determining the shear capacity, current design methods for shear are based on empirical approach. According to AS3600 (2009) the ultimate shear strength, V_{uc}, of a reinforced concrete member without shear reinforcement and not subjected to any axial force is given by:

$$V_{uc} = \beta_1 b_v d_0 [\frac{A_{st} f_c^{'}}{b_v d_0}]^{1/3} \quad (1)$$

$$\beta_1 = 1.1[1.6 - \frac{d_0}{1000}] \geq 1.1 \quad (2)$$

where b_v is the minimum effective web width in mm, d_0 is the distance of the extreme compression fibre of the concrete to the centroid of the outermost layer of tensile reinforcement in mm, and A_{st} is the area of fully anchored longitudinal steel provided in the tension zone of the cross-section under consideration. An increase in the shear strength of a shallow beam is accounted for by the factor β_1. The primary factors affecting the shear capacity, as seen in (1), are the size of the member, the ratio of tensile steel reinforcement and the concrete strength $f_c^{'}$. Other factors affecting the shear capacity of a reinforced concrete section are the axial force and the location of concentrated load points with reference to the support point (the shear span-to-depth ratio *a/d*), but these factors are not present in this study. There was no axial force and the span-to-depth ratio was kept constant (*a/d* = 2) in all the tests.

In the web-shear crack region, which is usually uncracked in flexure, the load causing web-shear cracks can be estimated by equating the principle tensile stress at a critical point in the web to the tensile strength of the concrete(Warner et al. 1998). Using Mohr's circle, the principal tensile stress σ_1 caused by the longitudinal stress, σ, and shear stresses, τ, acting on an element is given by:

$$\sigma_1 = \sqrt{(0.5\sigma)^2 + \tau^2} + 0.5\sigma \quad (3)$$

$$\tau = \frac{VQ}{Ib_w} \quad (4)$$

where Q = is the first moment about the centroidal axis of the top (or bottom) portion of the member's cross-sectional area, defined from the level at which τ is being calculated. I is the moment of inertia of the entire cross-sectional area computed about the neutral axis, and b_w is the width of the cross-sectional area, measured at the point where τ is being calculated. The recommended value of the maximum principal tensile stress sufficient to cause diagonal cracking is $0.33\sqrt{f_c^{'}}$ in both Australian and American codes. In design, the exact location of the principal tensile stress is usually not known depending on the distribution of longitudinal and shear stresses across the section. However, at a region nearer to support where the bending moment is close to zero, the maximum principle tensile stress occurs at the neutral axis of the cross section. Thus, for a rectangular section without any bending moment and where the maximum principal tensile stress is at the neutral axis of the cross-sectional area. The shear formula (4) is based on the assumption that the shear stress is constant across the width of the section. In a wider section, such as in the present case, shear stresses are not necessarily constant and the maximum shear stress occurred at the edges could be significantly greater than the maximum shear stress based on (4).

In the present case, concrete grade was 40 MPa, having the cylinder strength at 28 days of 43.4 MPa. The slab specimen was reinforced with N-grade steel with the steel yield strength of 500 MPa. The primary reinforcement in the bottom layer was N12-100, i.e., bar diameter of 12 mm and spacing of 100 mm. Other reinforcements were N12-300, provided based on minimum reinforcement requirement for crack control (AS3600-2009). Concrete cover was 25 mm to the outer face of the steel bars. Based on (1) and (2), the flexural-shear cracking capacity of this reinforced concrete section is calculated as V_{uc} = 195 kN. The shear force corresponding to the web-shear crack calculated from (3) and (4) is significantly greater than this force. Therefore, the shear capacity of the tested slab is governed by the flexural-shear cracking force.

2.2 *Solid and LSRC Sections*

Based on the design for shear capacity, the details of the tested slabs are as shown in Fig. 1. Four slabs were constructed, one solid slab SS1 and three LSRC slabs, LS1, LS2 and LS3. Prefabricated autoclaved aerated concrete (AAC) blocks were used as the lightweight concrete material in the LSRC slabs. In each LSRC slab, the amount of AAC blocks infill was varied in order to investigate the effect on the capacity and behaviour of the slab.

The standard dimension of an AAC block used was 200 mm long, 180 mm wide, and 75 mm thick. Two blocks were put together to create the total block thickness of 150 mm. LS1 contained 64 standard blocks, which were the maximum number of blocks that could be placed within the specimen. LS2 contained 32 blocks, half of that contained in LS1, while LS3 had the same amount of blocks as in LS1 but the corners of the blocks were cut off to investigate the shape effect on the slab. In all LSRC slabs, blocks were placed evenly in both directions. The minimum gaps between the blocks in LS1 were 50 mm and 43 mm in the cross-section and the longitudinal directions of the slab, respectively.

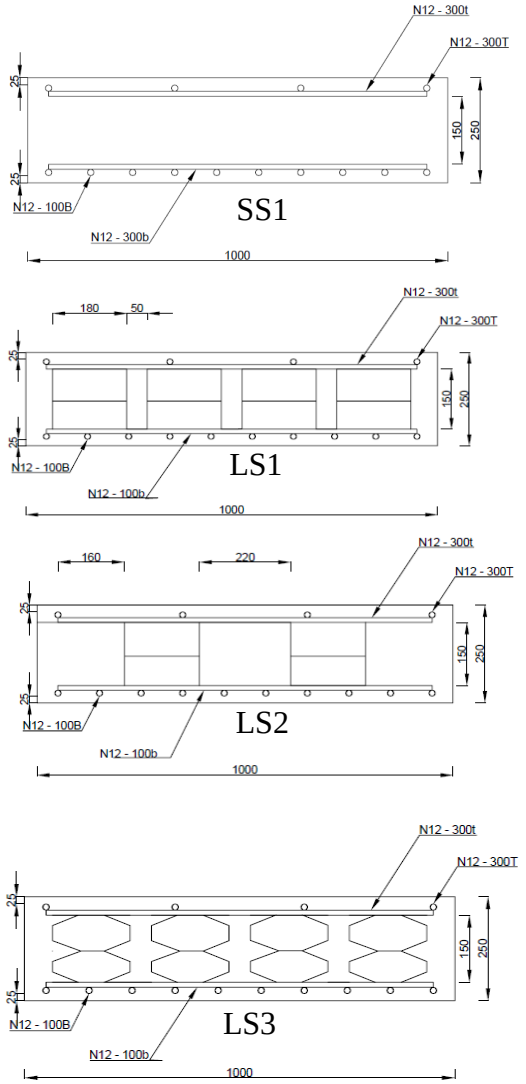

Figure 1. Sectional details of the tested slabs

2.3 *Construction of LSRC Slabs*

The construction of LSRC slabs can be done in as much the same way as of the LSRC beams. The construction can either be fully precast, semi-precast, or cast in-situ. The difference between slab and beam members is that a slab does not usually contain encasing steel stirrups as in the beam. The AAC blocks infill can either be prefabricated together with the reinforcement bars off site, or manually placed at the casting area.

In preparing the slab specimens, prefabricated AAC blocks were first shaped into the desired dimensions for use in LSRC slabs. Casting beds and side formworks were prepared and cleaned. The bottom reinforcement grid was placed on the casting bed, followed by the placement of AAC blocks. The top reinforcement grid was then placed on top of the blocks. It should be noted that the blocks were tied between the top and bottom reinforcement layers in order to avoid any displacement of the blocks during pouring and setting of concrete. Fig. 2 shows LS1 and LS3 prior to casting.

All the four tested slabs were cast at the same time with the same batch of concrete. Immediately after casting, the slabs and the control cylinders were covered with plastic sheets to avoid moisture loss and routinely watered daily for 5 days when the cylinders and the external sides of the formwork were stripped. The slabs were removed from the formwork 7 days after casting.


(a) LS1 (b) LS3

Figure 2. Construction of LSRC slabs

2.4 *Weight of Slabs*

In the tested LSRC slabs, Ecobricks (2007) were used as AAC blocks infill. The density of Ecobricks was 550 kg/m3 and the total weight reductions for each type of slab were between 14-27% of the equivalent solid slab. Table 1 presents a detailed breakdown of each slab. The maximum weight reduction was in LS1 which contained the maximum amount of Ecobricks.

Table 1. Details of Tested slabs

ID	No of Blocks	Vol Blocks (m3)	Vol Concrete (m3)	% Concrete	% wt reduction
SS1	-	-	0.75	100.0	-
LS1	64	0.26	0.49	65.3	27
LS2	32	0.13	0.62	82.6	14
LS3	64	0.16	0.59	78.6	17

3 EXPERIMENTAL ARRANGEMENT

The Heavy Loading Frame located in the concrete lab at Curtin University was used for the tests. The slabs were supported on roller supports and two hydraulic jacks were used to apply the load with a combined maximum loading capacity of 400 kN under force control. The applied load limitation had restricted the setup on the spanning arrangement of the slabs. Slabs were to be tested in shear, therefore, the bending moment induced by the load tests should not be more critical than the corresponding shear. As a result, the slab specimen was set with the span as shown in Fig. 3(a), the two locations of the jacks are as depicted in Fig. 3(b). The shear span-to-depth ratio (*a/d*) was equal to 2 at the testing end of the slab where critical shear failure was expected.

The applied load when the slab reached the predicted shear capacity was expected at 232 kN. Hinges were used at the top of the jacks to allow the jacks to move with the slab during testing. A trans-

verse spreader steel beam was used to transform the two-point loadings to a uniform one-way action across the slab width. Plaster was applied to the underside of the bearing plate which was located directly under the spreader beam above the slab. This plaster ensured that the load applied to the slab was distributed evenly. With this setup, one individual test on each end of each slab was able to be conducted as failure of the slab only occurred at the end being tested. The cantilevering end of the slab was not affected. For safety during load test, the slab was restricted from moving at one end by a rubber pad which did not prohibit the vertical deflection of any part of the slab when under load.

During load test, an Linear Variable Differential Transformer (LVDT) was attached to each load cell. Both LVDTs were calibrated and setup to measure the displacement of the slabs associated with the applied loads. The load and deformation were recorded by LDS Nicolet data acquisition system. During loading, the formation of the cracks on the sides of the beams were also manually marked and recorded.

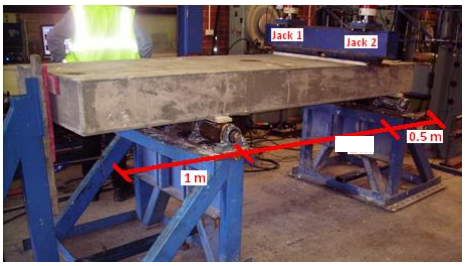

(a) Loading Span

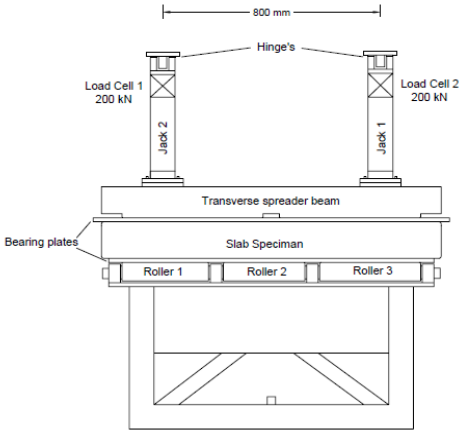

(b) Uniform one-way action

Figure 3. Test Setup

4 RESULTS AND DISCUSSIONS

4.1 *Shear Strength*

Many shear strength models have been developed according to experimental results. Recently, Choi et al. (2007a, 2007b) developed a theoretical model to predict the shear strength of reinforced concrete beams that is applicable for slender and deep beams. In general, as well established by ASCE-ACI Committee 445 (1998), shear resistance in a reinforced concrete slab with no shear reinforcement can be assessed from three main components: the area of uncracked concrete in compression, the interface shear action, often called "aggregate interlock" or "crack friction", and the dowel action of the longitudinal tensile reinforcement bars intersecting the shear cracks. The contribution of the uncracked concrete depends mainly on the concrete strength and the depth of the uncracked zone, which is a function of the longitudinal reinforcement properties. The mechanical interlock allows shear transfer across a crack in the tensile zone, depending on crack roughness, crack width and concrete strength. The dowel action depends on the amount and size of the longitudinal reinforcement.

In a previous investigation by Taylor (1974) into the contribution of each component in carrying shear in reinforced concrete beams, it was found that the compression zone carried 20-40%, aggregate interlock carried 33-50% and dowel action 15-25% of the shear. For beams without shear reinforcement, and with a single layer of reinforcing bars, the dowel action can be neglected (Choi et al. 2007a).

The overall results from the experiment demonstrate that there is a difference in the ultimate failure loads of the solid slab and the LSRC slabs. The maximum reduction in the shear capacity of the LSRC slabs is 15% of the equivalent solid slab. Based on the three main components of the shear resistance, as described above, this difference could be due to the reduction in the interface shear action component. It has been observed after the test that the inserted AAC blocks in the LSRC slab bonded very well to the concrete. As a result, the inclined shear crack continued to propagate directly through the blocks at the same angle as the concrete. This had the effect on the interface shear action component of the shear capacity as the associated interface friction of the crack consisted of both a normal-strength concrete component and a lower-strength AAC block component.

Table 2 summarises the experimental results for all tested slabs. Presented in Column (3) of the table is the load at which the flexural crack was visible. The loads at which the first and second inclined shear cracks became visible were presented on Columns (4) and (5), respectively. The ultimate load at collapse is presented in Column (6).

All slabs were tested both ends, described as Test 1 and Test 2 in Column (2) of the table. The solid slab SS1 failed at 400 kN in the first Test and 358 kN in the second Test. The lower capacity obtained in the Test 2 was as expected as there were some initial flexural cracks caused by Test 1 of the slab.

Table 2. Summary of the load results, unit in kN.

Slab (1)	Test (2)	1st Flex Crack (3)	1st Shear Crack (4)	2nd Shear Crack (5)	Ult Load (6)	Ult Shear (7)
SS1	1	100	340	340	400	300
SS1	2	100	340	340	358	268
LS1	1	100	290	304	376	282
LS1	2	100	270	300	360	270
LS2	1	100	290	340	350	262
LS2	2	70	290	340	340	255
LS3	1	80	320	330	402	301
LS3	2	100	320	370	373	278

In both LS1 and LS2 slabs, the longitudinal reinforcement was the same, the only varying parameter between the two slabs was the amount of AAC blocks. LS1, which had more numbers of the blocks in it, failed unexpectedly at a slightly greater load than LS2, in both tests. The failure loads from Test 1 and Test 2 of LS1 are 376 kN and 360 kN, and of LS2 are 350 kN and 340 kN, respectively.

In slab LS3, the shape of the inserted Ecobricks was altered by trimming of the four corners of the bricks in order to investigate the shape effect. The test results show that the failure loads of LS3 were almost equal to the failure loads of the solid slab. These results indicate that cutting off the four corners increased the resistance to shear of the tested LSRC slab. This finding deserves attention as it means that it is possible to develop an LSRC section that has the same flexural and shear strength as that of the solid section. The trade off for this is the less weight reduction of the slab. In order to increase the weight reduction, it is recommended that the shape of the AAC blocks infill can be altered only at the region where shear is known to be critical.

4.2 *Load-deflection behaviour*

The load versus deflection behaviours of all the tested slabs are plotted together in Fig. 4 for comparison. The responses of all the slabs to the applied load were similar. The initial slope of the load-deflection relationship is constant until the first flexural crack develops. After the initiation of the first crack, the slope of the graph becomes shallower with a decrease in stiffness of the slab.

During testing, two cycles of loading were applied. The first was when the load reached at 100 kN and the second at 200 kN. During loading and reloading, some flexural cracks were observed resulting in a small residual deflection of less than 1 - 2 mm when the slab was unloaded. Upon reloading, the relationship between load and deflection remained linear until the magnitude of the applied load reached to 300 - 330 kN. Further from these loads, all slabs exhibited rapid increase in deflection with the increase in loading. At failure, the ultimate loads varied between 340 - 402 kN, (cf. Table 1). The corresponding deflections at maximum loadings were 21 - 25 mm in all slabs.

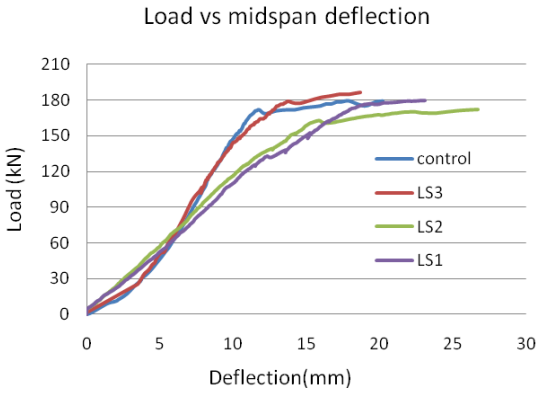

Fig. 4 Load versus deflection of tested slabs

4.3 *Mode of failure*

The stresses in a typical cross-section of a reinforced concrete member are the combination of longitudinal and shear stresses. When the member is subjected to bending, transverse tensile cracks form when the tensile strength of the concrete is reached. Flexural tensile cracks occur as vertical lines, which are originated in the region where the bending moment is large and the shear small. The typical flexural crack patterns will be disturbed whenever there are changes in the member geometry and loading (Warner et al. 1998). Cracks that form in the region where both the bending moment and the shear force are significant are inclined cracks, which are called flexural-shear cracks. If shear becomes large in any region of the member, inclined tensile cracks form and can lead to a premature 'shear' failure. This type of cracks is referred to as web-shear cracks, or diagonal tension cracks. Formation of inclined cracks as well as post-cracking behaviour depends on the relative magnitudes of the bending moment and shear force. Sengupta and Menon (2009) describes five possible modes of shear failure, namely diagonal tension failure, shear compression failure, shear tension failure, web crushing failure and arch rib failure.

All four slabs tested in this experiment have been designed to have a low span-to-depth ratio and adequate flexural reinforcement so that they fail in shear. Based on the test results, the slabs exhibited diagonal tension failure and shear compression failures. When the ultimate shear at failure was reaching, inclined crack propagated rapidly and there was crushing of the concrete at the compression edge of the slab above the tip of the inclined crack.

For the purpose of discussing the modes of failure of the tested slabs, jack 1 was applied to the left hand

side of the beam and jack 2 the right hand side of the beam (cf. Fig. 3). The main shear cracks appeared on both the left and right hand side of the slab at a loading when the first shear crack occurred as identified in Column (4) of Table 1. The crack then extended diagonally on both sides from the loading point to about 80 - 100 mm in front of the support point. The slab then continued to take slightly increased load and failed suddenly in a shear compression failure at the ultimate load.

In all the tested slabs, just prior to failure, a secondary main flexural shear crack occurred on either one side or both sides of the slab. This was the result of the redistribution of the load once the main shear cracks on both sides were widening up. At the point of failure, in all tests except Test 2 of slab LS1, the concrete in the top of the slab crushed while the slab was split up by the diagonal shear crack as shown in Fig. 5(a). In LS1 Test 2, a tensile splitting failure was observed within the shear span at the level of the top longitudinal reinforcement. The crack then extended along the level of the top reinforcement for about 400 mm before extending diagonally downwards above the support. This resulted in the spalling of the concrete above the top reinforcement when failure occurred as shown in Fig. 5(b).

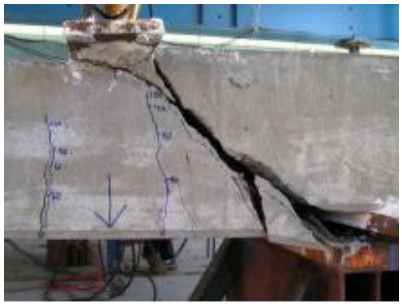

(a) Typical shear compression failure

(b) Spalling of the concrete above the top reinforcement

Fig. 5 Shear crack at failure

5 CORRELATIONS OF TEST RESULT WITH DESIGN CODES

As described in the previous section, there are a number of mechanisms that contribute to shear transfer in concrete. Opinions vary around the world on the relative importance of each of these mechanisms in the total shear resistance. As a result, various different models and formulas have been developed to predict the shear capacity of a reinforced concrete member with and without shear reinforcement.

Current concrete design codes provide empirical shear strength equations that are simple to use. The tested slabs were designed based on AS3600-2009, the shear capacity was expected at 195 kN. A comparison with other design codes has been made. The predicted shear capacity of the slabs, which are governed by the flexural shear capacity, is equal to 245 kN and 147 kN based on ACI 318M-02 and Eurocode 2, respectively. Table 3 shows the ratio of the shear capacity between the test values and the design values based on codes.

Table 3. Ratio between test results and predicted shear capacity

Slab (1)	Test (2)	AS3600 (3)	ACI318-02 (4)	Eurocode 2 (5)
SS1	1	1.54	1.22	2.04
SS1	2	1.37	1.09	1.82
LS1	1	1.45	1.15	1.92
LS1	2	1.38	1.10	1.84
LS2	1	1.34	1.07	1.79
LS2	2	1.30	1.04	1.73
LS3	1	1.54	1.23	2.05
LS3	2	1.43	1.14	1.90

It is clearly evident from this table that all the codes conservatively estimate the shear capacity of the slabs. Both the Australian and US design codes give the same value for the web shear capacity as this value is less than the flexural shear capacity. Due to the conservatism of the design codes, based on these results, the design formulas provided in the codes can be safely used to predict the shear capacity of LSRC slabs.

6 CONCLUSION AND RECOMMENDATION

Experimental results of the strength and behaviour of LSRC slabs subjected to shear have been presented. Based on the results of the tested slab specimens, the following conclusions and recommendations can be drawn:

1. Solid slab and LSRC slabs, without shear reinforcement, exhibit similar behaviour under shear.
2. LSRC slabs generally have a reduced shear capacity when compared to a solid slab having identical height; however the difference is not significant when compared with the predicted shear capacity based on standard design codes.
3. In the tested slabs, varying the amount of AAC blocks did not have any impact on the shear capacity of the LSRC slabs. This result is inconclusive for general use. Further investigation is required to determine the consistency of this outcome and any factors that might be affecting the

results. For instance, the ratio between the depth of the inserted AAC blocks to the overall depth of the solid section could be a factor contributing to the effect.

4. All the LSRC slabs demonstrated very brittle failure and failed mainly by shear compression. However, the inserted AAC blocks were found to bond very well to the concrete and the shear crack propagation through them suggested that they contribute to the overall shear capacity both in terms of their tensile strength and ability to carry shear through interface friction.
5. Post-cracking behaviour was observed and the slabs could sustain further load increment after shear crack was developed. This was due to the combined contribution of the uncracked concrete, dowel action of the longitudinal reinforcement and aggregate interlocking in the middle region of the section.
6. The shape of the inserted AAC blocks has a significant effect on the shear capacity. When the inserted AAC blocks have been altered in shape to have a more curved profile, the capacity of the tested LSRC slab with curved bricks is almost identical to the capacity of the solid slab.
7. The test results on the solid slab show that the predicted shear capacity of a reinforced concrete slab based on the selected design codes is quite conservative. The design formulas for calculating the shear capacity of a solid slab can safely predict the shear capacity of an LSRC slab.
8. Further studies are underway to determine the consistency of the results. A numerical approach is being employed by the authors to model LSRC members in order to further investigate their strength and behaviour under varying parameters. Investigations shall include:
   a. Determination of design parameters affecting the shear capacity of LSRC section, such as the size effect, span-to-depth ratio, support condition, and shape and location of AAC blocks
   b. The contribution of AAC blocks on the shear capacity of LSRC member in both un-cracked and cracked states through interface friction and aggregate interlocking
9. Punching shear behaviour needs to be investigated to determine whether current design concepts regarding punching shear in a solid slab are adoptable to predict an LSRC slab.

7 ACKNOWLEDGMENT

The authors wish to thank the reviewers for the comments provided on the earlier draft of this paper. The authors appreciated the comments provided by Prof BV Rangan on this research topic. Lightweight concrete blocks used in the experiment sponsored by Ecobrick, Australia were gratefully acknowledged.

8 REFERENCES

ACI Committee 318, 2002. Building Code Requirements for Structural Concrete (ACI 318M-02) and Commentary (318M-02), *American Concrete Institute*, Farmington Hills, Mich. 443 pp.

Aldejohann, M. & Schnellenbach, M. 2003. Investigation on the shear capacity of biaxial hollow slabs-Test results and evaluation", *Darmstadt Concrete*, vol. 18, pp. 532-545.

AS3600 Committee BD-002, 2009. Concrete Structures, Standards Australia.

ASCE-ACI Committee 445, 1998. Recent approaches to shear design of concrete structures, *J. Structural Engineering, ASCE*, vol. 124 (12), pp. 1375-1417.

Choi, K., Park, H.G. & Wight, J.W. 2007. Unified shear strength model for reinforced concrete beams – Part I: Development, *ACI Structural Journal*, March-April, pp. 142-152.

Choi, K., Park, H.G. & Wight, J.W. 2007. Unified shear strength model for reinforced concrete beams – Part II: Verification and Simplified Method, *ACI Structural Journal*, March-April, pp. 153-161.

Ecobricks - The new brick wall (2007), Available: http://www.ecobrick.com.au/html/about/what-is-ecobrick/, accessed 21 March 2009.

Eurocode 2, Concrete, BS EN 1992-1-1, *European Standards*

Fico, R., Prota, A. & Manfredi, G. 2008. Assessment of Eurocode-like design equations for the shear capacity of FRP RC members. *Composites*: Part B 39, 792–806.

Jones, M. R. & McCarthy A. 2005. Behaviour and assessment of foamed concrete for construction applications. In: Dhir RK, Newlands MD, McCarthy A, editors. *Use of foamed concrete in construction*, London: Thomas Telford, pp. 61–88.

Matthew, P.W. & Bennett, D.F.H. 1990. Economic long span concrete floors, *British Cement Association*, pp. 2-6.

Ramamurthy, K. Kunhanandan Nambiar, E.K., Indu Siva Ranjani, G. 2009. A classification of studies on properties of foam concrete, *Cement & Concrete Composites* vol. 31, pp. 388–396.

Sengupta, A. & Menon, D. 2009. Analysis and design for shear and torsion, *Prestressed Concrete Structures*, Section 5.1, p 6, Available: http://nptel.iitm.ac.in/courses/IIT-MADRAS/PreStressed_Concrete_Structures/index.php. accessed 12 May 2009.

Taylor, H. 1974. The Fundamental Behavior of Reinforced Concrete Beams in Bending and Shear, *ACI*, vol. 42(1), pp. 43-77.

Vimonsatit, V., Wahyuni, A. S., Mazlan, M. A. & Nikraz, H. 2010. Use of lightweight concrete as infill of reinforced concrete section, ASMCM 21, 7-10 December 2010, Melbourne.

Warner, R.F., Rangan, B.V., Hall, A.S. & Faulkes, K.A. 1998. *Concrete Structures*, Longman, Melbourne, Australia.

APPENDICES

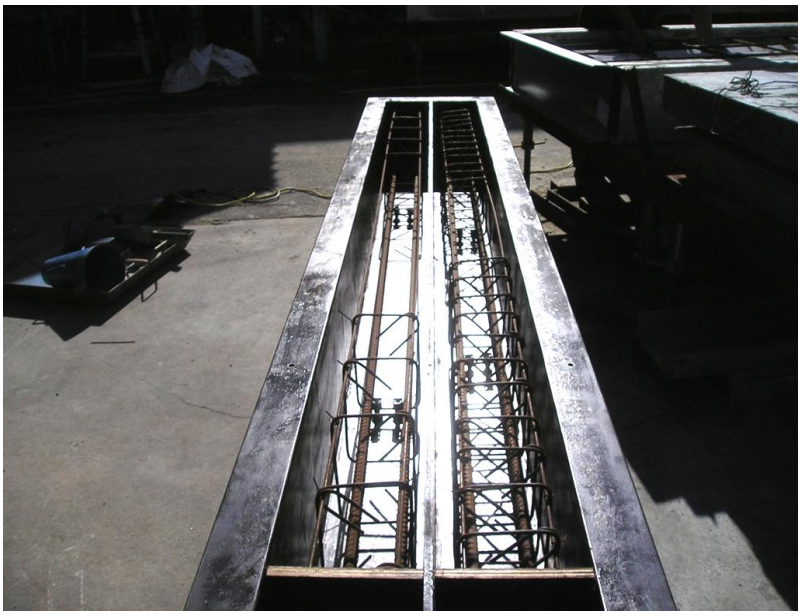

Reinforcement cage in steel mould for control beams

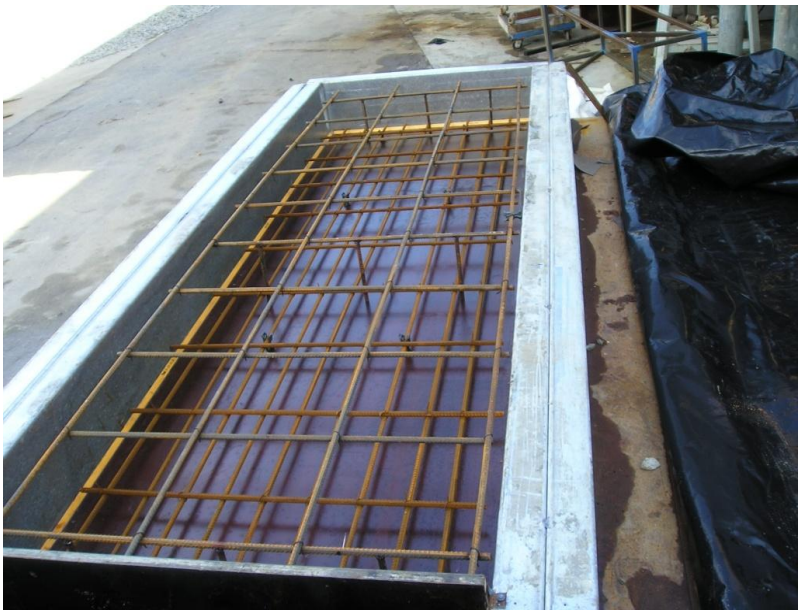

Slab reinforcement for control

The beam specimen was taken out of the mould

The slab specimen was taken out of the mould

Beam SB1F fails in flexure

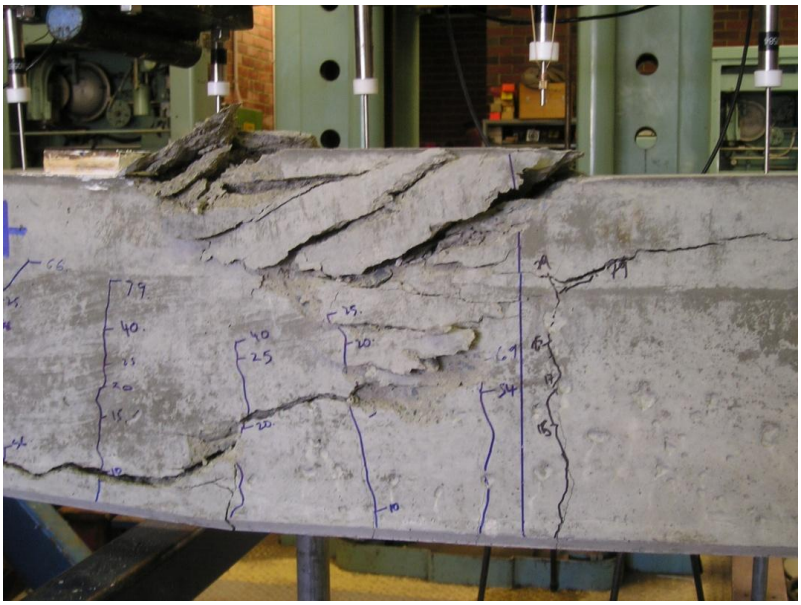

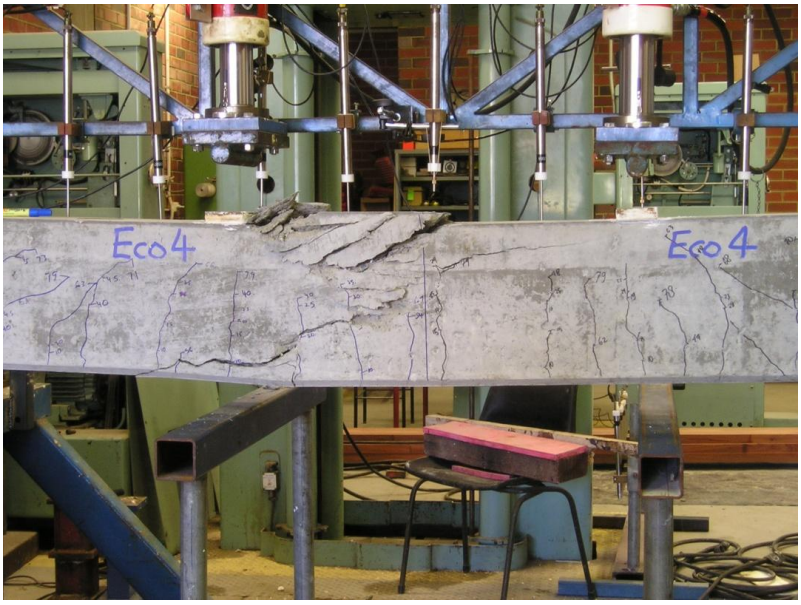

Beam LB1F fails in flexure

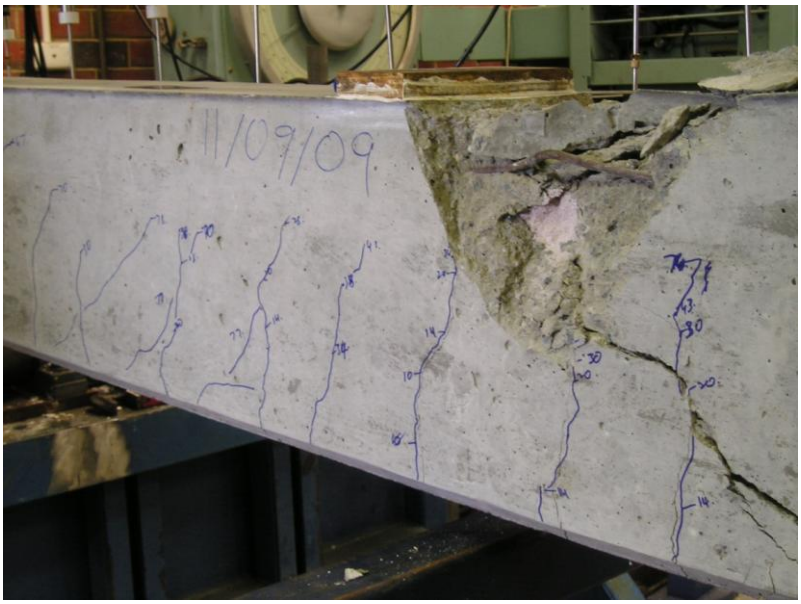

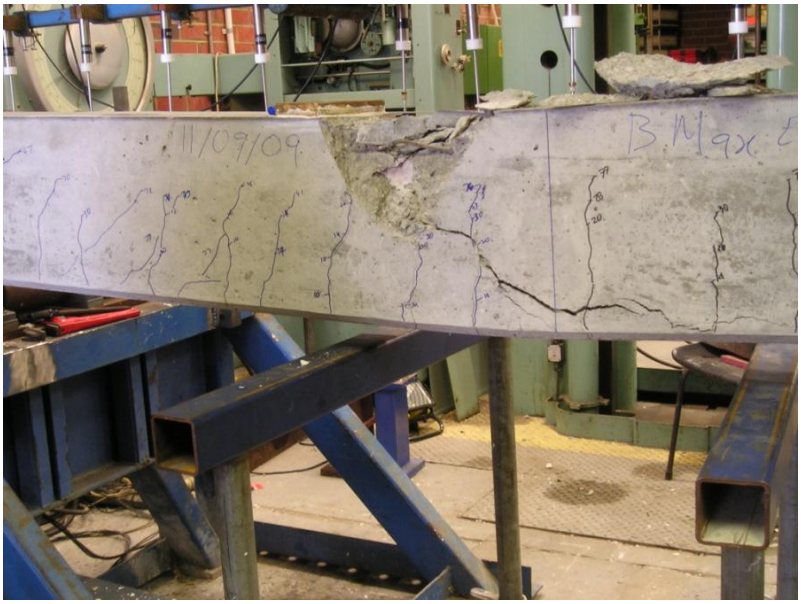

Beam LB2F fails in flexure

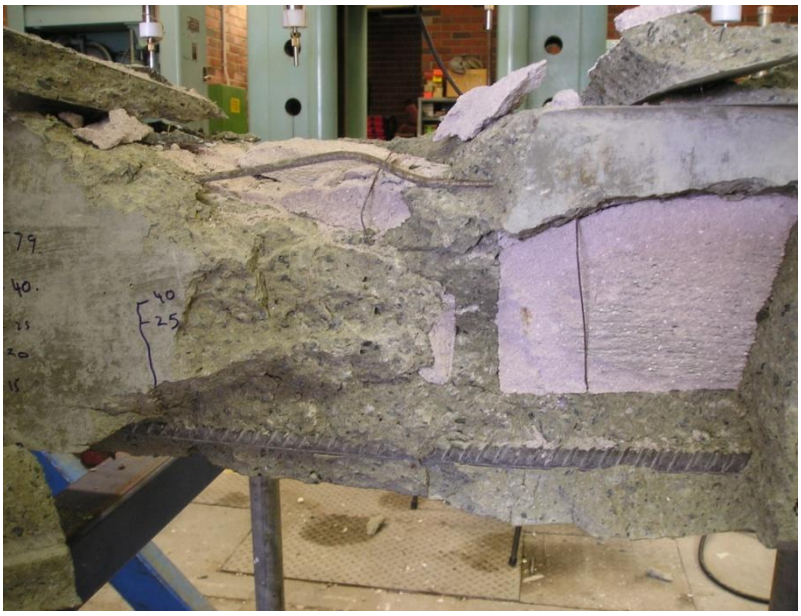

Good bonding between concrete and AAC blocks

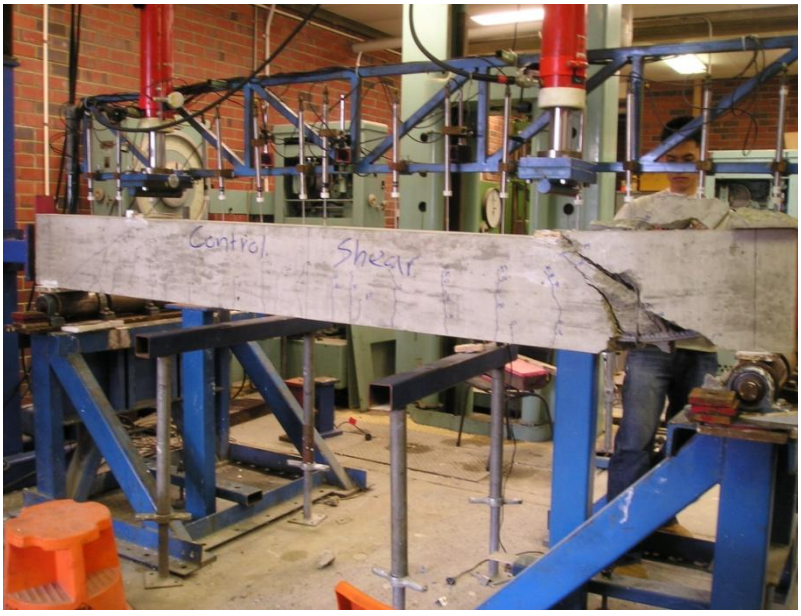

Beam SB1S fails in Shear

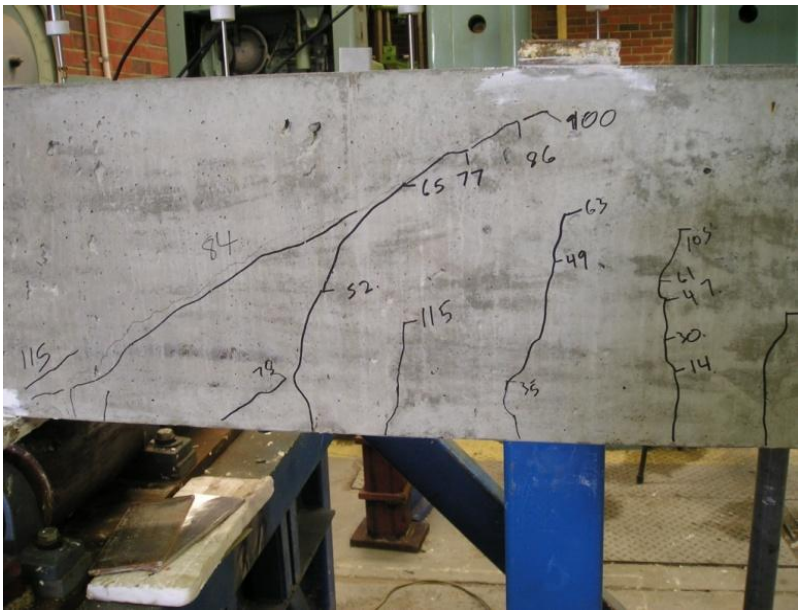

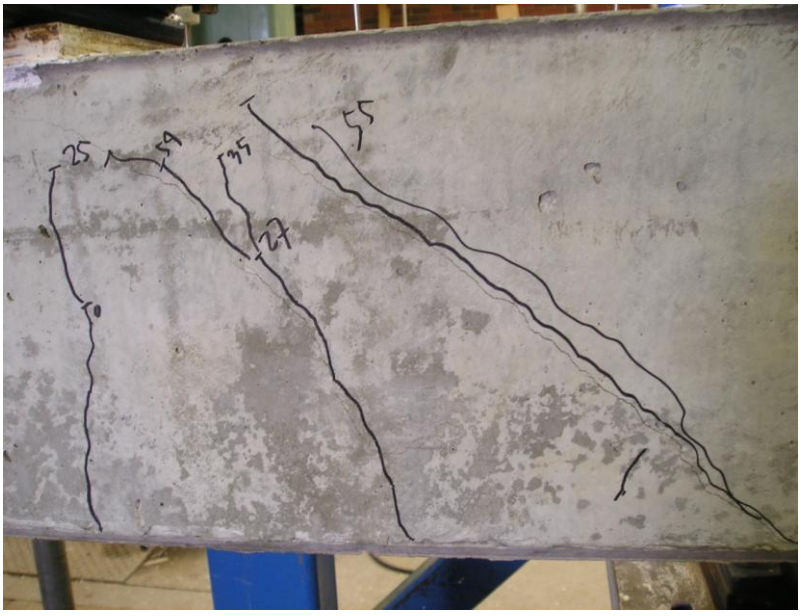

Beam LB1S fails in Shear

The failure of SS1

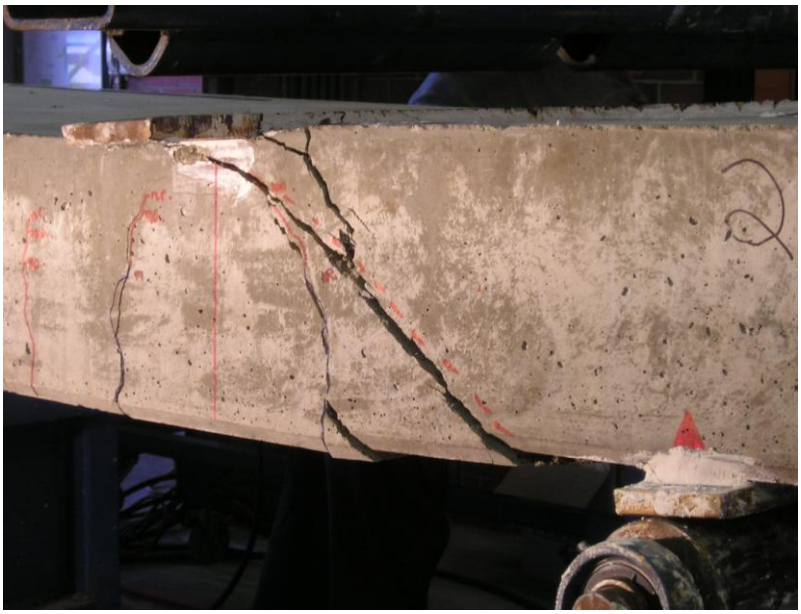

The left hand side of LS1 slab at failure (test 1)

Right hand side of slab LS1 at failure (test 1)

Crack propagated underneath the slab

The Right hand side of slab LS1 at failure (test 2)

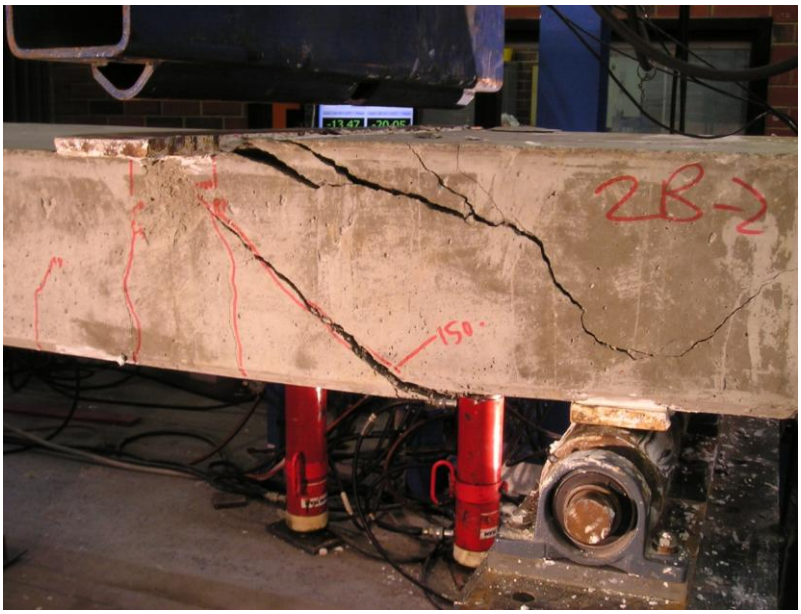

The Left hand side of slab LS1 at failure (test 2)

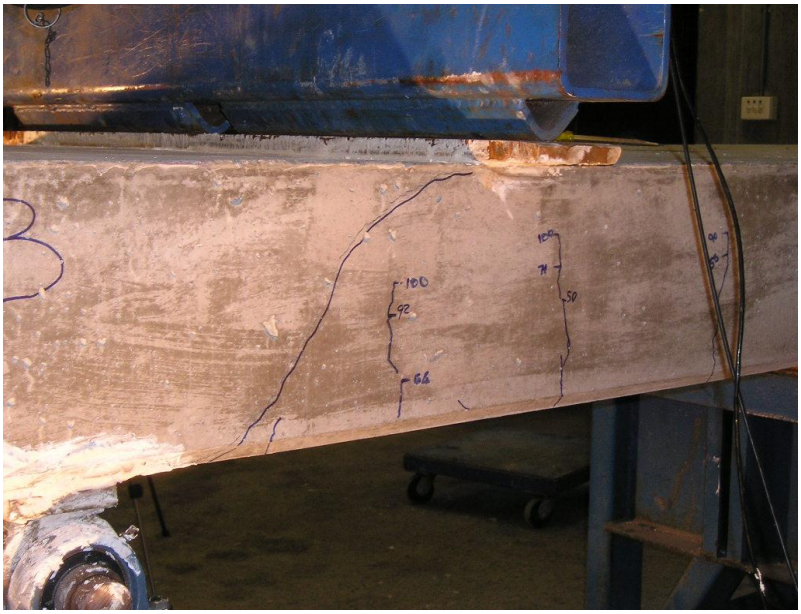

The shear crack of LS2

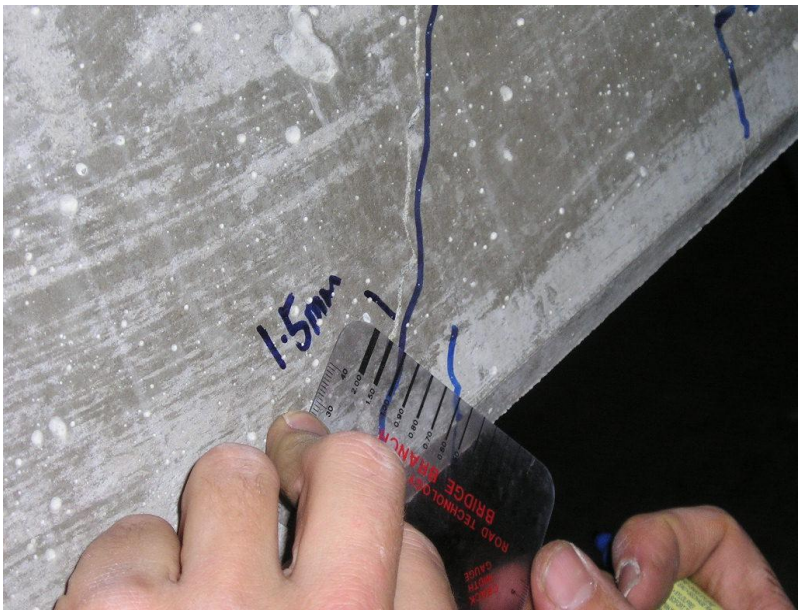

The crack width of LS2

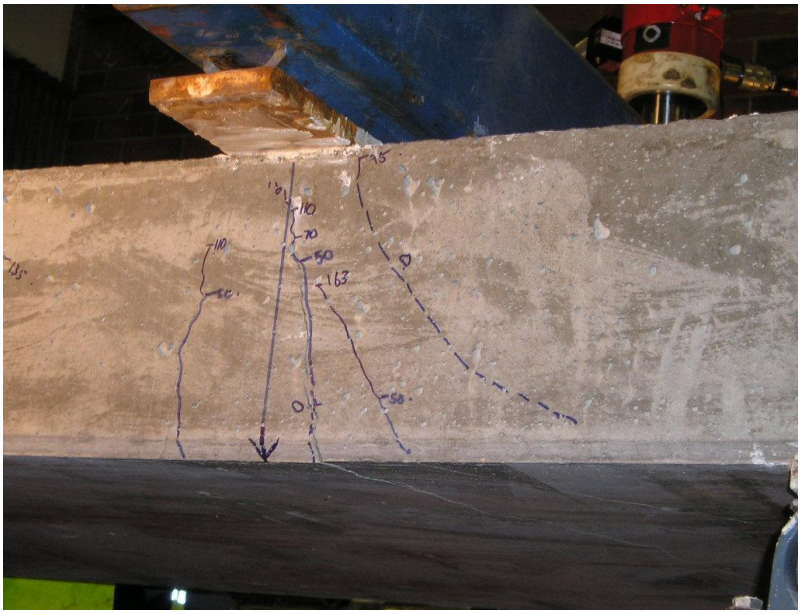

The shear crack of LS2

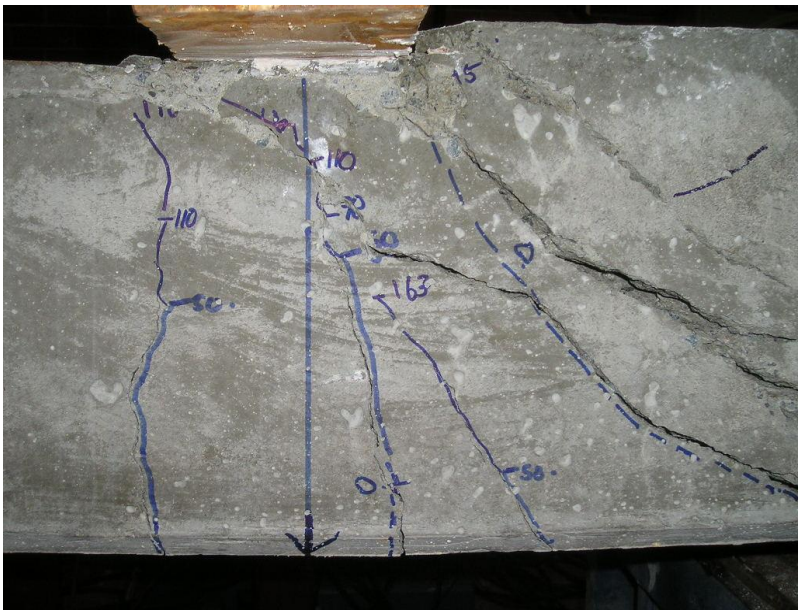

The shear crack of LS2

Crack propagated through the opposite site of the slab

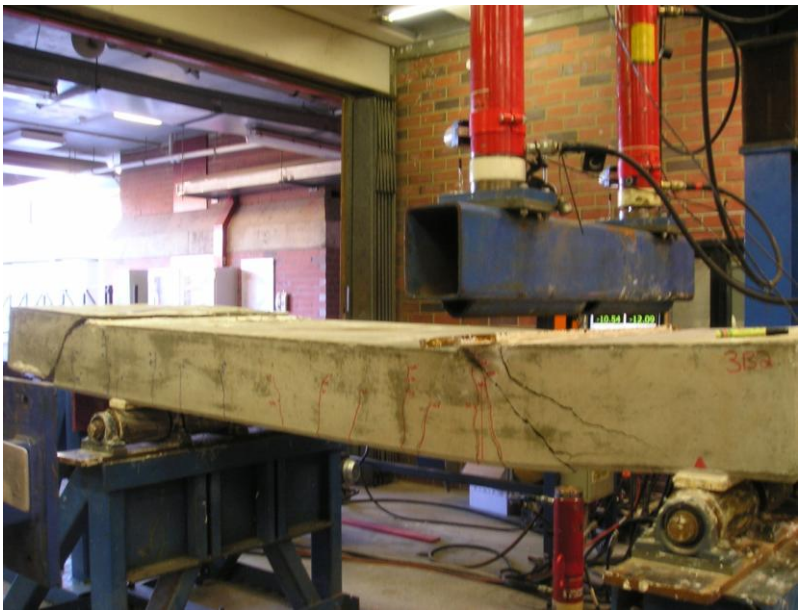

Slab LS2 after failure for both side

The crushed concrete in the top of the slab

Left hand side of LS3

The crushed concrete in the top of the slab

The failure of LS3